NOVA SCHOOL OF
SCIENCE & TECHNOLOGY

DEPARTAMENTO DE QUÍMICA

JOÃO RICARDO MARQUES LOPES
Licenciado em Bioquímica

BIOTRANSFORMATION OF ENVIRONMENTAL TOXICANTS BY DIFFERENT ENZYMES

MESTRADO EM BIOQUÍMICA

Universidade NOVA de Lisboa
(Março), (2022)

NOVA SCHOOL OF
SCIENCE & TECHNOLOGY

DEPARTAMENTO DE QUÍMICA

BIOTRANSFORMATION OF ENVIRONMENTAL TOXICANTS BY DIFFERENT ENZYMES

JOÃO RICARDO MARQUES LOPES
Licenciado em Bioquímica

Orientador: Ricardo José Lucas Lagoa, Adjunct Professor,
Polytechnic Institute of Leiria

Coorientadores: Paula Alexandra Quintela Videira, Assistant
Professor,
NOVA University Lisbon

Júri:

Presidente: Pedro António de Brito Tavares
Arguentes: Luísa Bernardina Lopes Maia
Vogais: Ricardo José Lucas Lagoa

MESTRADO EM BIOQUÍMICA

Universidade NOVA de Lisboa
(Março), (2022)

Biotranformation Of Environmental Toxicants By Different Enzymes

Copyright © JOÃO RICARDO MARQUES LOPES, Faculdade de Ciências e Tecnologia, Universidade NOVA de Lisboa.
A Faculdade de Ciências e Tecnologia e a Universidade NOVA de Lisboa têm o direito, perpétuo e sem limites geográficos, de arquivar e publicar esta dissertação através de exemplares impressos reproduzidos em papel ou de forma digital, ou por qualquer outro meio conhecido ou que venha a ser inventado, e de a divulgar através de repositórios científicos e de admitir a sua cópia e distribuição com objetivos educacionais ou de investigação, não comerciais, desde que seja dado crédito ao autor e editor.

The work developed until the present date has originated:

- **Poster Presentation:** Dorinda Marques-da-Silva, **João Lopes**, Ricardo Lagoa (2021). *"Methanol increases the efficiency of Anthracene degradation by Laccase"*. Conference of the European Federation of Biotechnology. May 10th -14th, Online conference.

- **Oral Presentation: João Lopes**, Dorinda Marques-da-Silva, Joaquim Rui Rodrigues, Paula Videira, Ricardo Lagoa (2021). *"Differential effect of ABTS on the laccase and peroxidase-catalyzed degradation of organic pollutants"*. XXI National Congress of Biochemistry. October 14th – 16th, Évora, Portugal.

- **Manuscript submitted for publication: João Lopes**, et al. *"Comparison of laccases and hemeproteins systems in bioremediation of organic pollutants"*.

AKNOWLEDGEMENTS

I am grateful to the MBStox project for taking me in and allowing me to develop this thesis. I am also grateful for the work opportunities granted to me to grow professionally and for supporting me in them.

I am grateful to the Foundation for Science and Technology (FCT –Portugal) for funding this reseach project and my scholarship.

I am grateful to the ESTG - Polytechnic Institute of Leiria for allowing me to use the facilities that I required to develop my work.

I would like to thank Professor Ricardo Lagoa for all of the time and attention invested in guiding my work, for the countless revisions and corrections, and for pushing me forward towards new goals.

I would like to thank Dr^{a} Dorinda Marques-da-Silva for all of the cooperation in the laboratory and moral support.

I would like to thank my friends and colleagues for supporting me at a professional and personal level. Thank you for accompanying me along this journey through all of these years.

Finally, a very special thanks to my family for all of their encouragement and unwavering support. Thank you for always believing in me, for always being available to help me, for supporting me through the countless hardships that I faced in these troublesome times, and for celebrating with me in my achievements.

ABSTRACT

Pollution is currently one of the greatest global problems. Oxidoreductase enzymes have shown the capacity to transform hazardous chemical compounds. Investigating the ability of enzymes to transform environmentally concerning pollutants is essential to understand the toxicological role of those enzymes and for the development of novel bioremediation technologies. The present work studied the capacity of laccase, horseradish peroxidase (HRP), hemoglobin, and cytochrome *c* (Cc) to transform the azo dye methyl orange (MO), polycyclic aromatic hydrocarbons (PAHs), such as anthracene and benzo[a]pyrene (BaP), and the organophosphate pesticide chlorpyrifos.

The use of the redox mediator ABTS in low concentrations (10 µM) increased MO decolorization by laccase over 10 fold, while the hemeproteins efficiently decolorized MO directly and the presence of ABTS afforded no benefit in these cases. Hemoglobin-catalyzed MO decolorization was followed by rapid inactivation of the hemeprotein. The presence of ABTS (50 µM) enabled laccase-catalyzed transformation of PAHs, for example, the oxidation of anthracene reaching 69 ± 4% in 24 h, and also enhanced anthracene transformation catalyzed by HRP. Cc exhibited the capacity to degrade various PAHs (77 ± 10% of anthracene and 70 ± 4% of BaP) without requiring mediator and the presence of ABTS (50 µM) was clearly disadvantageuos (5 ± 5% oxidation of anthracene). Despite the capacities shown by the enzymatic systems studied, none was able to transform chlorpyrifos.

Further studies of the laccase-ABTS system showed that it was inhibited by the presence of Fe^{3+} ions and by humic acid, issues that can be problematic in the implementation of bioremediation processes.

The results in this work indicate that hemoglobin and Cc potentially have a role in the metabolism of environmental toxicants by being able to transform PAHs and MO at neutral pH. Moreover, the presence of cardiolipin-containing membranes enhanced the peroxidase activity of Cc, including towards PAHs and the azo dye. These results support the hypothesis that Cc participates in the transformation of toxicants at the inner mitochondria membrane, where cardiolipin and Cc are located.

Keywords: biotransformation; enzymatic remediation; metalloproteins; organic pollutants.

RESUMO

Poluição é atualmente um dos maiores problemas mundiais. Enzimas oxidoredutases demonstraram a capacidade de transformar compostos químicos nocivos. Investigar a competência de enzimas em transformar poluentes ambientalmente preocupantes é essencial para compreender o papel toxicológico dessas enzimas e para o desenvolvimento de novas tecnologias de biorremediação.

O presente trabalho estudou a capacidade de lacase, peroxidase de rábano (HRP), hemoglobina e citocromo *c* (Cc) em transformar o corante azo alaranjado de metilo (MO), hidrocarbonetos policíclicos aromáticos (PAHs), como antraceno e benzo[a]pireno (BaP), e o pesticida organofosfato clorpirifós.

O uso do mediador redox ABTS em concentrações baixas (10 µM) aumentou a descolorização de MO por lacase em 10 vezes, enquanto as hemoproteínas descolorizaram eficientemente MO diretamente e a presença de ABTS não proporcionou nenhum benefício nestes casos. Descolorização de MO catalisada por hemoglobina foi seguida por inativação rápida da hemoproteína. A presença de ABTS (50 µM) possibilitou a transformação de PAHs catalisada por lacase, por exemplo a oxidação de antraceno alcançando 69 ± 4% em 24 h, e também possibilitou a transformação de antraceno catalisada por HRP. Cc demonstrou a capacidade em degradar vários PAHs (77 ± 10% de antraceno e 70 ± 4% de BaP) sem necessitar de mediador e a presença de ABTS (50 µM) foi evidentemente desvantajosa (5 ± 5% oxidação de antraceno). Apesar das capacidades demonstradas pelos sistemas enzimáticos estudados, nenhum foi capaz de transformar clorpirifós.

Estudos adicionais do sistema lacase-ABTS demonstraram que o sistema foi inibido pela presença de iões de Fe^{3+} e por ácido húmico, aspetos que podem ser problemáticos na implementação de processos de biorremediação.

Os resultados deste trabalho indicam que a hemoglobina e Cc potencialmente possuem um papel no metabolismo de tóxicos ambientais por serem capazes de transformar PAHs e MO a pH neutro. Além disso, a presença de membranas contendo cardiolipina aumentou a atividade peroxidase do Cc, incluindo relativamente a PAHs e ao corante azo. Estes resultados apoiam a hipótese que Cc participa na transformação de compostos tóxicos na membrana interna da mitocôndria, onde cardiolipina e Cc se encontram.

Palavas-chave: Biotransformação; remediação enzimatica; metaloproteínas; poluentes orgânicos.

TABLE OF CONTENTS

AKNOWLEDGEMENTS IX

ABSTRACT........ XI

RESUMO........ XIII

TABLE OF CONTENTS XV

LIST OF FIGURES........ XVII

LIST OF TABLES........ XXIII

ABBREVIATIONS XXV

1. INTRODUCTION........ 1

1.1. Polycyclic aromatic hydrocarbons and other organic pollutants in the environment 1
1.2. Human toxicology of polycyclic aromatic hydrocarbons and other organic pollutants 4
1.3. Bioremediation 5
1.4. Enzymes in remediation of organic pollutants 6
1.4.1. Laccase 6
1.4.2. Peroxidases 8
1.5. Aims of the Thesis........ 12

2. MATERIALS AND METHODS........ 13

2.1. Chemicals, buffers, humic acid, and liposomes 13
2.1.1. Chemicals 13
2.1.2. Preparation of buffers 15
2.1.3. Preparation of humic acid solutions........ 15
2.1.4. Preparation of liposomes........ 16
2.2. Proteins and their stock solutions........ 16
2.2.1. Protein stock solutions and determination of concentration 17
2.3. Stock solutions of PAHs and chlorpyrifos 17
2.4. Methods of analysis of the target pollutants........ 17
2.4.1. Hexane extraction of target pollutants 18
2.4.2. UV-Vis spectra of PAHs and chlorpyrifos........ 18
2.4.3. High-Performance Liquid Chromatography 19
2.5. Studies of enzyme activity using ABTS as substrate 19
2.5.1. Determination of enzymatic activity........ 19
2.5.2. Effect of humic acid on enzyme-catalyzed ABTS oxidation 20
2.5.3. Effect of pH and liposomes on enzyme-catalyzed ABTS oxidation........ 20
2.6. Decolorization of methyl orange........ 21

2.6.1. Decolorization of methyl orange by laccase 21
2.6.2. Decolorization of methyl orange by peroxidase-type proteins 21
2.6.3. Influence of metal ions on methyl orange decolorization by laccase-ABTS system 22
2.6.4. Effect of humic acid on enzyme-catalyzed methyl orange decolorization......22
2.7. Degradation of PAHs and chlorpyrifos 23
2.7.1. Enzyme-catalyzed degradation of PAHs and chlorpyrifos 23
2.7.2. Effect of humic acid on anthracene degradation by laccase-ABTS system 24
2.7.3. Anthraquinone degradation by laccase-ABTS system......24
2.8. Quenching of radicals by humic acid 25

3. RESULTS AND DISCUSSION 27

3.1. Environmental toxicants in this work and their analysis 27
3.1.1. Basic physico-chemical properties......28
3.1.2. UV-Vis absorption spectra of the PAHs and chlorpyrifos 31
3.1.3. Analytical methods 37
3.2. Activity of laccase and peroxidase-type proteins using ABTS as substrate 39
3.2.1. Activity of laccase using ABTS as substrate 39
3.2.2. Oxidation of ABTS catalyzed by horseradish peroxidase......41
3.2.4. Peroxidase activity of cytochrome c using ABTS as substrate 43
3.2.5. Comparison of ABTS oxidation efficiencies of the enzymes and enzyme-like proteins at different pH 45
3.3. Studies of methyl orange decolorization by laccase......49
3.3.1. Methyl orange decolorization by laccase alone and with ABTS mediation......50
3.3.2. Influence of metal ions in laccase-ABTS system......51
3.4. Studies of anthracene degradation by laccase 54
3.5. Influence of humic acid in laccase catalytic systems 60
3.5.1. Humic acid solutions and spectra......60
3.5.2. Influence of humic acid in laccase activity with ABTS as substrate 61
3.5.3. Influence of humic acid in laccase decolorization of methyl orange 63
3.5.4. Influence of humic acid in laccase-catalyzed degradation of anthracene 66
3.6. Methyl orange and anthracene degradation studies with peroxidase-type proteins......68
3.6.1. Methyl orange decolorization 68
3.6.2. Peroxidase-catalyzed anthracene degradation......77
3.7. Quenching of radicals in the inhibition of laccase catalysis by humic acid 80
3.7.1. Quenching of ABTS radicals 80
3.7.2. Scavenging of methyl orange decolorization products 82
3.8. Effect of lipid membranes in the peroxidase activity of heme proteins......83
3.8.1. Oxidation of ABTS and dye decolorization 84
3.8.2. Degradation of benzo[b]fluoranthene 86
3.9. Studies of transformation of other PAHs and chlorpyrifos 87
3.9.1. Transformation of benzo[a]pyrene......87
3.9.2. Transformation of chlorpyrifos......90
3.9.3. Transformation of different PAHs by cytochrome c......91

4. CONCLUSIONS 95

REFERENCES......99

LIST OF FIGURES

Figure 1.1 – Molecular structure of the model organic pollutants anthracene (a), benzo[a]pyrene (b), chlorpyrifos (c) and azo dye methyl orange (d). 2

Figure 1.2 – A representative scheme of an enzymatic remediation process. Adapted from (Mousavi *et al*. 2021; Arca-Ramos *et al*. 2015) 5

Figure 1.3 – Copper centers in typical fungal laccases and their role in the catalytic process. Type 1 copper captures the electrons from the reducing substrate that are, after, transferred to the trinuclear copper cluster where molecular oxygen is reduced to water. The trinuclear cluster (T2/T3 site) is composed of one binuclear type 3 site and one type 2 site. Laccase PDB entry: 1GYC. 6

Figure 1.4 – (A) The catalytic cycle of a laccase-mediator system in the oxidation of a non-phenolic substrate and possible undesired side-reactions of the mediator. (B) Oxidation of ABTS to ABTS radical. Retrieved from (D'Acunzo and Galli 2003). 7

Figure 1.5 – Catalytic mechanism of (A) HRP and (B) MnP. Adapted from (Abdel-Hamid *et al*. 2013). 9

Figure 3.1 – UV-Vis spectra of anthracene (1 mg/L) in (A) acetonitrile; (B) water with 1% (v/v) acetonitrile; and (C) mixtures of acetonitrile:water (% v/v is indicated). 33

Figure 3.2 – UV-Vis spectra of benz[a]anthracene (1 mg/L) in (A) acetonitrile; (B) water with 1% (v/v) acetonitrile. 33

Figure 3.3 – UV-Vis spectra of benzo[b]fluoranthene (1 mg/L) in (A) acetonitrile; (B) water with 1% (v/v) acetonitrile. 34

Figure 3.4 – UV-Vis spectra of benzo[a]pyrene (1 mg/L) in (A) acetonitrile; (B) water with 1% (v/v) acetonitrile. 34

Figure 3.5 – UV-Vis spectra of chlorpyrifos (25 mg/L) in (A) acetonitrile; (B) water with 1%(v/v) acetonitrile. 35

Figure 3.6 – Changes in the UV-Vis spectra of 0.5 mM ABTS during the oxidation catalyzed by laccase (1 µg/mL) in 100 mM acetate buffer pH 5.0, at 25 ºC. 39

Figure 3.7 – Enzymatic activity of laccase (0.5 µg/mL and 1 µg/mL) with 0.5 mM ABTS measured in 100 mM acetate buffer pH 5.0 and 25 ºC. The oxidation of ABTS was followed at 420 nm, 436 nm, 600 nm, and 734 nm. The observed ΔAbs/Δt (min^{-1}) are indicated for each wavelength after the addition of laccase, first to a final concentration of 0.5 µg/mL and then 1.0 µg/mL to check the response of the assay. Experimental traces from blank assays (ABTS without addition of enzyme) are shown in the lateral graphic. 40

Figure 3.8 – Enzymatic activity of HRP (1×10^{-3} µg/mL) with 100 µM of H_2O_2 and 0.5 mM ABTS measured in 100 mM acetate buffer pH 5.0, at 25 ºC. In the assay A, ABTS was incubated with the enzyme before addition of H_2O_2. In the assay B, ABTS was incubated with H_2O_2 before addition of HRP. The ΔAbs/Δt (min^{-1}) observed in each assay are indicated. 42

Figure 3.9 – Enzymatic activity of hemoglobin (10 µg/mL) with 100 µM of H_2O_2 and 0.5 mM ABTS measured in 100 mM acetate buffer pH 5.0 and 25 ºC. In the assay A, ABTS was incubated with the protein before addition of H_2O_2. In the assay B, ABTS was incubated with H_2O_2 before addition of hemoglobin. The initial ΔAbs/Δt (min^{-1}) observed in each assay are indicated. 43

Figure 3.10 – Enzymatic activity of Cc (100 µg/mL) with 100 µM of H_2O_2 and 0.5 mM ABTS measured in 100 mM acetate buffer pH 5.0 and 25 ºC. This assay was carried with Sigma C7752 product of Cc. In the assay A, ABTS was incubated with the protein before addition of H_2O_2. In the assay B, ABTS was incubated with H_2O_2 before addition of Cc. The ΔAbs/Δt (min^{-1}) observed in each assay are indicated. 44

Figure 3.11 – Effect of H_2O_2 concentration on the enzymatic activity of Cc measured in 100 mM acetate buffer pH 5.0 and 25 ºC. Enzymatic reaction was initiated with the addition of 100 µM of H_2O_2. Reactional mixture contained Cc (100 µg/mL), 0.5 mM ABTS and H_2O_2 concentrations ranging between 10 µM and 200 µM. The assay was carried with Sigma C7752 product of Cc. The ΔAbs/Δt (min^{-1}) observed after each addition of H_2O_2 are indicated. 45

Figure 3.12 – Effect of pH in enzymatic activity of (A) laccase (1 µg/mL), (B) HRP (1 × 10^{-3} µg/mL) with 100 µM of H_2O_2 and (C) Cc (100 µg/mL) with 100 µM of H_2O_2, using 0.5 mM ABTS as substrate. Reactional mixtures were prepared in 100 mM acetate buffer pH 5.0 or 5.5, or 100 mM phosphate buffer pH 6.0, 7.0 or 8.0. In all the assays, the reaction was triggered by addition of the protein, and the ABTS oxidation was monitored at 420 nm. Sigma C7752 Cc was used in these assays. 47

Figure 3.13 – Comparison of the ABTS oxidation rate catalyzed by laccase, HRP, and Cc at different pH. Assays were carried with ABTS initial concentration 0.5mM, at 25 ºC. Acetate buffer (100 mM) was used for pH 5.0 and 5.5, while phosphate buffer (100 mM) was used for pH 6.0, 7.0, and 8.0. Enzymatic assays were performed using a final concentration of 1 µg/mL of laccase, 1 × 10^{-3} µg/mL of HRP, or 100 µg/mL of Cc in the presence of 100 µM of H_2O_2. The measurements with Cc (Sigma C7752) were triplicated and the mean ± SE is represented. 48

Figure 3.14 – UV-Vis spectrum of 10 mg/L (30.6 µM) of methyl orange at pH 5.0 in acetate buffer (100 mM) and at pH 7.0 in phosphate buffer (100 mM) at 25 ºC. At the wavelength used to monitor the decolorization in this work (477 nm), methyl orange shows an absorbance close to that at the maximum (463 nm). 49

Figure 3.15 – Representative assay of methyl orange decolorization by laccase and the effect of ABTS. The absorbance of methyl orange, initial concentration 10 mg/L (30.6 µM), in 100 mM acetate buffer pH 5.0, was followed at 477 nm, at 25 ºC. The concentration of the enzyme was 100 µg/mL. The decolorization rates in $\Delta Abs/\Delta t$ (min^{-1}) are indicated for each reactional condition, in the absence and after additions of ABTS to reach a final concentration of 5 and 10 µM. 50

Figure 3.16 – Effect of ABTS on laccase-catalyzed decolorization of methyl orange. Assay conditions indicated in Figure 3.15 caption. The decolorization rates in the presence of ABTS were normalized to the rate observed in the corresponding control in the absence of ABTS, which was taken as 100%. The control decolorization rates in $\Delta Abs/\Delta t$ (min^{-1}) in absence of ABTS were -0.002 ± 0.001 min^{-1}. 51

Figure 3.17 – Assays of methyl orange decolorization by laccase and 5 µM ABTS in the presence of 0.1- and 1-mM concentrations of (A) Fe^{3+}, (B) $Cu^{2+}$and (C) Ca^{2+} ions. Methyl orange decolorization in 100 mM acetate buffer pH 5.0 was monitored at 477 nm, at 25 ºC. The dye initial concentration was 10 mg/L (30.6 µM) and the enzyme concentration was 100 µg/mL. The decolorization rates in $\Delta Abs/\Delta t$ (min^{-1}) are indicated for each reactional condition. 53

Figure 3.18 – Effect of Fe^{3+}, Cu^{2+}, and Ca^{2+} ions on methyl orange decolorization rate by laccase-ABTS system. Assay conditions indicated in Figure 3.17 caption. The decolorization rates in the presence of the metal cations were normalized to the rate observed in the corresponding control in the absence of the metal, which was taken as 100%. The control decolorization rates in $\Delta Abs/\Delta t$ (min^{-1}) in absence of added metal cations were -0.010 ± 0.003 min^{-1}. 54

Figure 3.19 – Effect of ABTS on laccase-catalyzed degradation of anthracene. Assays were carried with an anthracene initial concentration of 1 mg/L (5.6 µM) and laccase 100 µg/mL. Incubation assays were carried in 100 mM acetate buffer pH 5.0, in the absence of light, at 20 ºC. After 24 h incubation, the remaining anthracene concentration in the presence of ABTS was compared to the control without enzyme, which was taken as 0% degradation. Results from duplicate assays are shown as Mean ± SE. 55

Figure 3.20 – HPLC chromatograms of anthracene and degradation products generated by the laccase-ABTS system. Chromatograms are shown for an anthracene (1 mg/L) control incubation in the absence of enzyme, and anthracene after 24 h incubation with laccase (100 µg/mL) without and with ABTS 50 µM. A chromatogram of an anthraquinone (1 mg/L) standard is also shown, and anthraquinone peaks (t_R=4.5min) are highlighted by dashed lines. The unidentified oxidation product P1 (t_R=4.8min) is indicated in the red chromatogram. Incubation assays were carried in 100 mM acetate buffer pH 5.0, in the absence of light, at 20 ºC. The chromatograms are displaced in the vertical and horizontal axis for better observation. The chromatograms shown are representative results of at least triplicate assays for each reaction condition. 56

Figure 3.21 – Effect of ABTS on anthraquinone and P1 formation during laccase-catalyzed degradation of anthracene. Assay conditions indicated in Figure 3.19 caption. Results from triplicate assays are shown as Mean ± SE. 57

Figure 3.22 – HPLC chromatograms of anthraquinone after incubation with the laccase-ABTS system. Chromatograms are shown for a 24h incubation of anthraquinone (1 mg/L) with ABTS but without the enzyme (Control) and with the laccase-ABTS system. A 100 µg/mL concentration of laccase and 50 µM ABTS was used. Incubation assays were carried in acetate buffer (100 mM, pH 5.0), in the absence of light, at 20 ºC. The chromatograms are displaced in the vertical and horizontal axis for better observation. The chromatograms shown are representative results of triplicate assays for each reaction condition. 59

Figure 3.23 – Hypothetical pathway of anthracene oxidation. Compounds between brackets were not identified in the present work. 59

Figure 3.24 – UV-Vis spectra of representative humic acid solutions prepared in the work. The stock solutions were diluted in water to a final concentration of humic acid of 10 mg/L. 61

Figure 3.25 – Representative assays of the effect of humic acid on ABTS oxidation by laccase. The ABTS initial concentrations was 50 µM and laccase 1 µg/mL, in 100 mM acetate buffer pH 5.0 at 25 ºC. Small volumes of humic acid stock solution were added to the spectrophotometer cuvette to reach the final concentrations indicated. In the assay with the Blank solution (buffer without humic acid), a volume equivalent to the 50 mg/L humic acid was added to the cuvette. The oxidation rates in ΔAbs/Δt (min^{-1}) are indicated for each reactional condition. The experimental traces shown are representative of at least triplicate assays. 62

Figure 3.26 – Effect of humic acid on laccase oxidation of ABTS. Assay conditions indicated in Figure 3.25 caption. The control oxidation rates in ΔAbs/Δt (min^{-1}) in absence of humic acid were 0.012 ± 0.003 min^{-1}. The data plotted is the Mean ± SE from three independent experiments. 62

Figure 3.27 – Effect of humic acid on methyl orange decolorization by laccase. Decolorization assays were carried with 300 µg/mL laccase and an initial dye concentration of 10 mg/L (30.6 µM), in 100 mM acetate buffer pH 5.0. Dye decolorization was followed at 477 nm at 25 ºC in the absence and in the presence of different humic acid concentrations from 0.5 to 100 mg/L. The decolorization rates in the presence of humic acid were normalized to the rate observed in the corresponding controls carried using equivalent volumes of Blank solution (buffer without humic acid), which were taken as 0% inhibition. The control decolorization rates in ΔAbs/Δt (min^{-1}) in absence of humic acid were -0.003 ± 0.001 min^{-1}. The data plotted is the Mean ± SE from three independent experiments. 64

Figure 3.28 – Representative assays of the effect of humic acid on methyl orange decolorization by laccase. The absorbance of methyl orange, initial concentration 10 mg/L (30.6 µM), in 100 mM acetate buffer pH 5.0, was followed at 477 nm, at 25 ºC. The concentration of the enzyme was 900 µg/mL. In the humic acid assay shown, volumes of humic acid stock solution were added to reach the final concentrations indicated, whereas in the Control assay equivalent volumes of blank solution (buffer without humic acid) were added to the spectrophotometer cuvette. The Control assay trace is displaced vertically and horizontally for better visualization. 64

Figure 3.29 – Effect of humic acid on methyl orange decolorization by laccase-ABTS system in the presence of ABTS. Decolorization assays were carried with 100 µg/mL laccase, an initial dye concentration of 10 mg/L (30.6 µM) and ABTS 5 µM or 50 µM, in 100 mM acetate buffer pH 5.0. Dye decolorization was followed at 477 nm, at 25 ºC, in the absence and in the presence of different humic acid concentrations from 0.5 to 100 mg/L. The decolorization rates in the presence of humic acid were normalized to the rate observed in the corresponding controls carried using equivalent volumes of Blank solution (buffer without humic acid), which was taken as 0% inhibition. The control decolorization rates in ΔAbs/Δt (min^{-1}) in absence of humic acid were -0.009 ± 0.002 min^{-1} for assays with 5 µM ABTS and -0.029 ± 0.005 min^{-1} for assays with 50 µM ABTS. The data plotted is the Mean ± SE are representative of at least triplicate assays. 65

Figure 3.30 – Effect of humic acid on anthracene degradation by laccase-ABTS system. Degradation assays were carried with 100 µg/mL laccase, an initial anthracene concentration of 1 mg/L (5.6 µM), and 50 µM ABTS, in 100 mM acetate buffer pH 5.0. After 24 h incubation, the remaining anthracene concentration was compared to the control without enzyme, which was taken as 0% degradation. Results from at least triplicate assays are shown as Mean ± SE. 66

Figure 3.31 – Effect of humic acid on anthraquinone formation by laccase-catalyzed degradation of anthracene. Assay conditions indicated in Figure 3.30 caption. Results from triplicate assays are shown as Mean ± SE. 67

Figure 3.32 – HPLC chromatograms of anthracene degradation by the laccase-ABTS system. Chromatograms are shown for standard humic acid (500 mg/L), an anthracene (1 mg/L) control incubation in the absence of enzyme, and anthracene after 24 h incubation with the laccase-ABTS system without humic acid and with humic acid (500 mg/L). Incubation assays were carried in acetate buffer (100 mM, pH 5.0), in the absence of light, at 20 ºC. The chromatograms are displaced in the vertical and horizontal axis for better observation. The chromatograms shown are representative results of at least triplicate assays for each reaction condition. 68

Figure 3.33 – Representative assays of methyl orange decolorization by (A) HRP, (B) hemoglobin, and (C) Cc and the effect of ABTS. The concentration of the proteins used was 0.2 µg/mL of HRP, 10 µg/mL of hemoglobin and 100 µg/mL of Cc, and the concentration of H_2O_2 was 100 µM. The absorbance of methyl orange, initial concentration 10 mg/L (30.6 µM), in 100 mM acetate buffer pH 5.0, was followed at 477 nm at 25 ºC. Panel (D) shows the oxidation of ABTS by Cc in the same conditions as panel (C), but in the absence of methyl orange. The decolorization rates in ΔAbs/Δt (min^{-1}) are indicated for each reactional condition in the absence and after the additions of ABTS to reach a final concentration of 5 and 10 µM. . 70

Figure 3.34 – Monitoring of HRP-ABTS system in decolorization of methyl orange. The assay was carried in the same conditions as in Figure 3.33.A, except that with 50 µM of ABTS. The course of the reactions (methyl orange decolorization and ABTS oxidation) were followed at 477 and 734 nm. 71

Figure 3.35 – Influence of the methyl orange availability in the medium on the kinetics of decolorization by HRP and by Cc. Assay conditions indicated in Figure 3.33 caption. The kinetics of decolorization can be compared before and after the replenishment of methyl orange in the reactional mixture. 72

Figure 3.36 – Influence of H_2O_2 exhaustion in the medium on the kinetics of decolorization by HRP and by Cc. Assay conditions indicated in Figure 3.33 caption. The kinetics of decolorization can be compared before and after the replenishment of H_2O_2 in the reactional mixture. 73

Figure 3.37 – Representative assays of methyl orange decolorization by HRP, by hemoglobin, and by Cc. The concentration of the proteins used was 0.2 µg/mL of HRP, 10 µg/mL of hemoglobin and 100 µg/mL of Cc, and the concentration of H_2O_2 was 100 µM. The absorbance of methyl orange, initial concentration 10 mg/L (30.6 µM), in 100 mM phosphate buffer pH 7.0, was followed at 477 nm at 25 ºC. The decolorization rates in ΔAbs/Δt (min^{-1}) are indicated in Table 3.7 for each peroxidase and peroxidase-like proteins. 74

Figure 3.38 – Effect of humic acid in Cc-catalyzed ABTS oxidation. Assays were performed using 100 µg/mL of Cc, 100 µM H_2O_2, 500 µM ABTS and 50 mg/L of humic acid in 0.1 M acetate buffer (0.1 M pH 5.0 containing 0.1 mM DTPA) and 25 ºC. ABTS oxidation was monitored at 420 nm and at 734 nm. 76

Figure 3.39 – Effect of humic acid on methyl orange decolorization by (A) HRP and (B) Cc. The concentration of the proteins used was 0.2 µg/mL of HRP and 100 µg/mL of Cc, and the concentration of H_2O_2 was 100 µM. The absorbance of methyl orange, initial concentration 10 mg/L (30.6 µM), in 100 mM acetate buffer pH 5.0, was followed at 477 nm at 25 ºC. The decolorization rates in ΔAbs/Δt (min^{-1}) are indicated for each reactional condition in the absence and after addition of humic acid in a final concentration of 50 mg/L. . 76

Figure 3.40 – Effect of humic acid (50 mg/L) in HRP- and Cc-catalyzed oxidation of ABTS and MO. Assays were performed in acetate buffer (100 mM pH 5.0 containing 0.1 mM DTPA), at 25 ºC. The inhibitory effect in ABTS oxidation was assayed for HRP (1×10^{-3} µg/mL) and Cc (100 µg/mL for ABTS) with 100 µM of H_2O_2 and 500 µM of ABTS. Conditions of MO assay indicated in Figure 3.39 caption. Relative rates were calculated through the comparison of the ABTS oxidation and MO decolorization rates after the addition of humic acid with the rates obtained in the absence of humic acid, which were taken as 100%. 77

Figure 3.41 – HPLC chromatograms of anthracene and degradation products generated by HRP (A) and Cc (B) systems. Chromatograms are shown for (A) an anthracene (1 mg/L) without protein nor ABTS, anthracene with HRP 0.2 µg/mL in the presence of H_2O_2 100 µM without ABTS and with ABTS 50 µM, and (B) with Cc 100 µg/mL with H_2O_2 100 µM without ABTS and with ABTS 50 µM after 24 h incubation. The unidentified oxidation product P2 (t_R=5.6min) is indicated in the blue chromatogram, in addition to anthraquinone and P1. Incubation assays were carried in 100 mM acetate buffer pH 5.0, in the absence of light, at 20 ºC. Some chromatograms are displaced in the vertical and horizontal axis for better observation. The chromatograms shown are representative results of at least triplicate assays for each reaction condition. 79

Figure 3.42 – Effect of ABTS in HRP- and Cc-catalyzed degradation of anthracene. Assay conditions indicated in Figure 3.41 caption. Results from triplicate assays are shown as Mean ± SE. 79

Figure 3.43 – Decay of ABTS$^{\bullet+}$ in the presence of 75 mg/L and 150 mg/L of humic acid. The initial concentration of ABTS was 500 µM. ABTS oxidation was catalyzed by laccase (1 µg/mL) until absorbance approximated 0.5 (14 µM) and then, the enzyme was blocked with azide (0.1 mM) before addition of humic acid. An equivalent assay with non-inhibited enzyme is shown. Assays were performed in acetate buffer (100 mM, pH 5.0) at 20 ºC. The observed ΔAbs/Δt (min^{-1}) are indicated for each reactional condition in the absence and after addition of humic acid. 81

Figure 3.44 – Decay of ABTS$^{\bullet+}$ (14 µM) in the presence of 75 mg/L and 150 mg/L of humic acid. The ABTS$^{\bullet+}$ used was produced by oxidation of ABTS with persulfate. Assays were performed in acetate buffer (100 mM, pH 5.0) at 20 ºC. The steady ΔAbs/Δt (min^{-1}) observed several minutes after addition of humic acid is indicated in the plots. 82

Figure 3.45 – Representative assay of methyl orange decolorization products in the presence of 75 mg/L and 150 mg/L of humic acid. The absorbance of methyl orange, initial concentration 10 mg/L (30.6 µM), in 100 mM acetate buffer pH 5.0, was followed at 477 nm, at 25 ºC. Laccase was used at a concentration of 300 µg/mL and blocked with 0.2 mM of azide. 83

Figure 3.46 – Effect of phospholipid small unilamellar vesicles on (A) ABTS oxidation and (B) methyl orange decolorization by hemoglobin. Small unilamellar vesicles of phosphatidylcholine (PC) and PC/Cardiolipin (CL) were used at 200 µM. Assays were performed with 10 µg/mL of hemoglobin, 100 µM H_2O_2, and triggered with the addition of ABTS (100 µM) or methyl orange (30.6 µM), in phosphate buffer (20 mM, pH 7, supplemented with DTPA) at 25 ºC. The oxidation of ABTS was monitored at 734 nm and the decolorization of methyl orange was monitored at 477 nm. Control assays were performed in the absence of lipid vesicles. 84

Figure 3.47 – Effect of phospholipid small unilamellar vesicles on (A) ABTS oxidation and (B) methyl orange decolorization by Cc. Small unilamellar vesicles of phosphatidylcholine (PC) and PC/Cardiolipin (CL) were used at 200 µM. Assays were performed with 12.5 µg/mL of Cc, 100 µM H_2O_2, and triggered with the addition of ABTS (100 µM) or methyl orange (30.6 µM), in phosphate buffer (20 mM, pH 7, supplemented with DTPA) at 25 ºC. The oxidation of ABTS was monitored at 734 nm and the decolorization of methyl orange was monitored at 477 nm. Control assays were performed in the absence of lipid vesicles. 85

Figure 3.48 – HPLC chromatograms of BbF and degradation products generated by Cc in the absence and in the presence of CL-containing small unilamellar vesicles. Chromatograms are shown for a BbF control (1 mg/L) in the absence of Cc, BbF with Cc 12.5 µg/mL, and H_2O_2 100 µM with or without CL vesicles (200 µM). Incubation assays were carried in 20 mM phosphate buffer pH 7.0, in the absence of light, for 24h at 20 ºC. The chromatograms are displaced in the vertical and horizontal axis for better observation. The chromatograms shown are representative results of triplicate assays for each reaction condition. 86

Figure 3.49 – HPLC chromatograms of BaP and degradation products generated by laccase, HRP, and Cc systems. Chromatograms are shown for (A) BaP with laccase 100 µg/mL with and without ABTS 50 µM, (B) BaP with HRP 0.2 µg/mL in the presence of H_2O_2 100 µM with and without ABTS 50 µM (C) and BaP with Cc 100 µg/mL with H_2O_2 100 µM without ABTS. A chromatogram corresponding to a BaP (1 mg/L) control incubation in the absence of protein is shown in the three panels. Incubation assays were carried in 100 mM acetate buffer pH 5.0, for 24h, in the absence of light, at 20 ºC. The chromatograms are displaced in the vertical and horizontal axis for better observation. The chromatograms shown are representative results of triplicate assays for each reaction condition. 89

Figure 3.50 – HPLC chromatograms of a mixture of PAHs and degradation products generated by Cc. Chromatograms are shown for the PAH mixture incubated with and without Cc 100 µg/mL, in the presence of H_2O_2 100 µM, at pH 5.0 (A) and pH 7.0 (B). Incubations were carried in (A) 100 mM acetate buffer pH 5.0 and (B) 100 mM phosphate buffer pH 7.0, in the absence of light, at 20 ºC. A magnification of the chromatograms in the interval from 2 to 9 min is shown in the insets at each panel. The chromatograms (including in the magnification) are displaced in the vertical and horizontal axis for better observation. The chromatograms shown are representative results of triplicate assays for each reaction condition. 92

LIST OF TABLES

Table 2.1 – Specifications of the more important reagents used in this work. 13

Table 2.2 – Proteins used in this work and their specifications according to the commercial information. 16

Table 3.1 – Chemical structures and physico-chemical properties of the polycyclic aromatic hydrocarbons and the organophosphate pesticide chlorpyrifos used in this work. 29

Table 3.2 – HPLC parameters used for pollutant analysis. For all the analyses, a C18 column was used in an Agilent 1100 system. 37

Table 3.3 – Optimization of anthracene extraction with hexane. The recovery of 0.3 mg/L anthracene from 1 mL aqueous solutions (100 mM acetate buffer pH 5) achieved with each extraction protocol is presented as Mean ± SE. 37

Table 3.4 – Efficiency of extraction of target pollutants with the hexane extraction protocol. The recovery of anthracene, anthraquinone, benzo[a]pyrene, and chlorpyrifos from aqueous solutions (acetate buffer 100 mM, pH 5) is presented as Mean ± SE. Recovery of anthracene and anthraquinone was also measured in the presence of humic acid. 38

Table 3.5 – Molar extinction coefficients of $ABTS^{\bullet+}$ radical at pH 5.0. 39

Table 3.6 – Comparison of the specific ABTS oxidizing activity of laccase, HRP, hemoglobin, and Cc measured in 100 mM acetate buffer pH 5.0 at 25 ºC. Two commercial forms of Cc were studied. 46

Table 3.7 – Comparison of MO decolorization rates of peroxidase-type proteins measured in 100 mM acetate buffer pH 5.0 and in 100 mM phosphate buffer pH 7.0, at 25 ºC. 74

Table 3.8 – Anthracene reaction products generated by HRP- and Cc-catalyzed degradation, alone and in the presence of ABTS. Assay conditions indicated in Figure 3.41 caption. Results from triplicate assays are shown as Mean ± SE. 80

Table 3.9 – Results from transformation assays of chlorpyrifos by laccase, HRP, and Cc. Assays with 25 mg/L of chlorpyrifos were carried for laccase 100 µg/mL without ABTS and with ABTS 50 µM, HRP 0.2 µg/mL in the presence of H_2O_2 100 µM without ABTS and with ABTS 50 µM, and for Cc 100 µg/mL with H_2O_2 100 µM without ABTS. All assays were carried in 100 mM acetate buffer pH 5.0, in the absence of light, at 20 ºC. After 24 h incubation, the remaining chlorpyrifos concentration was compared to controls without protein, which were taken as 0% transformation. Results from triplicate assays are shown as Mean ± SE. 90

Table 3.10 – Summary of the retention times of the chromatographic peaks observed after incubations of polycyclic aromatic hydrocarbons with cytochrome *c*. The figures in the present work showing the chromatograms corresponding to incubations of each compound are indicated in the first column. 93

ABBREVIATIONS

ABTS - 2,2′-azino-bis-(3-ethylbenzothiazoline-6-sulphonate)
BaA – Benz[a]anthracene
BaP - Benzo[a]pyrene
BbF – Benzo[b]fluoranthene
Cc - Cytochrome c
CL – Cardiolipin
DTPA - Diethylenetriaminepentaacetic acid
HA – Humic Acid
HPLC - High-performance liquid chromatography
HRP - Horseradish peroxidase
LogP - Octanol/water partition coefficient
MnP - Manganese peroxidase
MO - Methyl Orange
PAH - Polycyclic aromatic hydrocarbons
PC – Phosphatidylcholine
POP - Persistent organic pollutant
ROS – Reactive oxygen species
SUV - Small unilamellar vesicle
t_R - Retention time

1.
Introduction

1.1. Polycyclic aromatic hydrocarbons and other organic pollutants in the environment

Persistent organic pollutants (POPs) are organic compounds that remain in the environment for long periods of time due to their resistance to degradation (Ritter *et al*. 1995; Jones and de Voogt 1999). The pollutants of the POP group include polycyclic aromatic hydrocarbons (PAHs) and halogenated hydrocarbons. PAHs constitute a class of hazardous chemicals, composed only by hydrogen and carbon atoms, consisting of three or more fused benzene rings in various structural configurations (Kim *et al*. 2013). Organophosphates are a class of hazardous compounds composed by a central phosphate atom and alkyl or aromatic substituents (Greaves and Letcher 2016).

Anthracene is a low molecular weight PAH composed by 3 fused benzene rings arranged linearly (Figure 1.1). This PAH is used often as a model PAH due to its environmental impact and because anthracene-like structures can be found in the chemical structures of other PAHs. Furthermore, the biodegradation and metabolism of anthracene by biological systems has been well studied (Ike *et al*. 2019; Alcalde *et al*. 2002; Johannes *et al*. 1996) and this well-established knowledge makes anthracene a valuable model for detoxification studies of PAHs. Benzo[a]pyrene (BaP) is a PAH that possesses an anthracene-like structure and is more toxic and persistent PAH than anthracene. The interest in the study of BaP arises from its high toxicological potential, more noticeably due to the carcinogenicity associated with this substance (Lee 2010; Baali and Yahyaoui 2020).

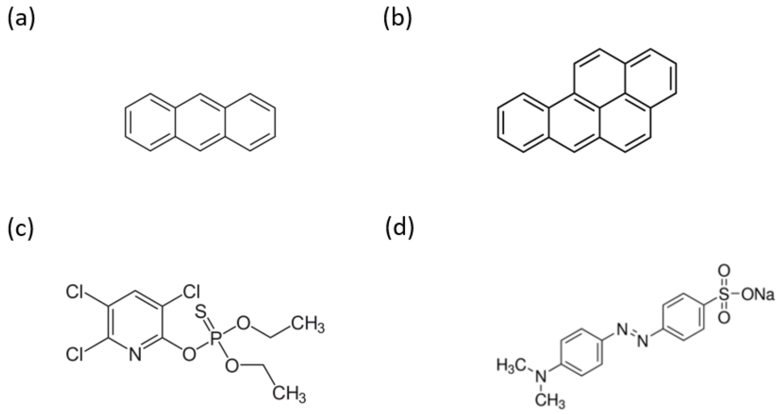

Figure 1.1 – Molecular structure of the model organic pollutants anthracene (a), benzo[a]pyrene (b), chlorpyrifos (c) and azo dye methyl orange (d).

Chlorpyrifos is one of the most globally used organophosphates in pesticides (Figure 1.1). Chlorpyrifos has been shown to be degradable by biological systems which, alongside its toxicity and environmental impact, makes this substance a suitable model of organophosphates for degradation studies (Eaton *et al*. 2008; John and Shaike 2015; Dar *et al*. 2019). Azo dyes are organic compounds widely used for multiple purposes (domestic use, pharmaceutical, and textile industry, etc.), and are hazardous to the environment despite not being persistent pollutants (Ambatkar and Mukundan 2015; Thomas and Brogat 2017). Bismarck brown, Methyl Red, and Methyl Orange (MO) (Figure 1.1) are commonly used as dye models for degradation or decolorization studies.

The vast majority of organic pollutants originate from anthropogenic activities for a variety of purposes such as agricultural, domestic, health, or industrial uses (Jones and de Voogt 1999; Patel *et al*. 2020; Speigth 2011). The increase in industrialization worldwide led to the production of alarming quantities of POPs which, due to its hazardous effects and recalcitrant character, raised important environmental concerns. These pollutants are introduced in the environment through various ways and be transported and distributed across the environment, making the presence of POPs in nature ubiquitous (Ritter *et al*. 1995).

Access to good quality drinking water is essential for the quality of life of a population. In Europe, access to high-quality drinking water has been achieved through a long tradition of drinking water management in many countries but also through the establishment of environmental legislation. It was established that the threshold level of BaP concentrations in water intended for human consumption was 0.010 μg/L, for other PAHs was 0.10 μg/L, for pesticides was 0.10 μg/L and the total pesticides (sum of individual pesticides) was 0.50 μg/L (EU 1998). In 2018, the European Environment Agency reported that the requirements to achieve a good chemical status were not being achieved for BaP in 1630 water bodies, for anthracene in 123 water bodies, and for pesticides in 621 water bodies

(Kristensen *et al*. 2018). Multi-annual measurements of PAHs in drinking water in France obtained from the French regulatory monitoring database, SISE'Eaux (Water Environmental Health Information System), between 2000 and 2012 revealed several municipalities with estimated BaP concentrations between 5 µg/L and 50 µg/L in water (Ioannidou *et al*. 2018). Rico *et al.* (2021) reported levels of chlorpyrifos exceeding the European water quality standards through the analysis of a database of surface water from the Iberian Peninsula between 2012 and 2017. From the 14600 surface water samples collected, chlorpyrifos was detected in 21% of the samples and 2% exceeded the concentration limit of chlorpyrifos for water quality with the highest measured concentration being 96 µg/L (Rico *et al*. 2021).

Global levels of PAHs in water and soils greatly variates between different locations and depending on local anthropologic activity. The majority of the environmental and public health concerns regarding PAHs can be attributed to the 16 PAHs that were designated as high priority pollutants by EPA which are acenaphthene, acenaphthylene, anthracene, BaP, benz[a]anthracene (BaA), benzo[b]fluoranthene (BbF), benzo[k]fluoranthene, benzo[g,h,i]perylene, chrysene, dibenz[a,h]anthracene, fluoranthene, fluorene, indeno[1,2,3-c,d]pyrene, naphthalene, phenanthrene, and pyrene. An overview of PAH global distribution by Adeniji *et al.* (2018) revealed worldwide occurrences and distribution of PAHs at greater concentrations in regions with higher anthropological activity and industrialization. Total mean concentrations ranged from 0.0003 to 42,350 µg/L in water and 0 to 1.266 × 109 µg/kg (dry weight) in the sediment from samples collected in African, American, Asian, and European regions. Lower molecular weight PAHs (4 or 5 rings) were the most predominantly found in water samples due to their higher water solubility while higher molecular weight PAHs were found more commonly in soil samples (Adeniji *et al*. 2018).

The fate of POPs is dependent on diverse environmental factors and on their physicochemical properties. The interaction between POPs and components of the environment may affect the permanence of the pollutants. Due to its hydrophobicity, POPs can adsorb to hydrophobic components (*e.g.,* humic acid) (Chianese *et al*. 2020; Baali and Yahyaoui 2020) and these may act as transport vectors for POPs. Their typical semi-volatility allows them to occur and be transported for long distances (Ritter *et al*. 1995). The high stability of POPs makes them recalcitrant to degradation and accumulate in the environment (Jones and de Voogt 1999; Ashraf 2017).

1.2. Human toxicology of polycyclic aromatic hydrocarbons and other organic pollutants

The high hydrophobicity of POPs facilitates their permeation through lipidic biological membranes and accumulation in fatty tissues of organisms, leading to biomagnification and contamination of the food chains in the polluted environment (Wenning and Martello 2014; Ritter *et al*. 1995). Contaminated organisms may suffer toxic effects depending on the type of exposure and substance toxicity.

Carcinogenicity is one of the most concerning health effects associated with PAH contamination (Abdel-Shafy and Mansour 2016; Baali and Yahyaoui 2020). The human metabolization of PAHs occurs mainly through cytochrome P450 family enzymes. PAHs are transformed through peroxidation into metabolites like phenols and quinones, but also into reactive species such as epoxides or radical cations or quinones (Moorthy *et al*. 2015). PAHs and their metabolites can react with DNA and result in abnormal gene expression and lead to mutagenesis and carcinogenesis (Kondraganti *et al*. 2003). As aforementioned, BaP is one of the PAHs that receives more focus in toxicological studies. The genotoxicity and carcinogenicity associated with BaP are attributed to an activated epoxide metabolite, BaP 7,8-diol-9,10-epoxide, produced through metabolic toxification (Lagoa *et al*. 2020). Toxicological information about anthracene in humans is still scarce but it is known that, if metabolically activated, anthracene can interact in photosensitization reactions and produce reactive oxygen species (ROS) (Pokora and Tukaj 2010).

Exposition to organophosphate compounds is commonly associated with neurological and immunological toxicity (Ubaid ur Rahman *et al*. 2021) however, organophosphates are capable of genotoxicity (John and Shaike 2015). The main toxicological mechanism of chlorpyrifos is through the inhibition of choline esterase, which affects the nervous system (Kousba *et al*. 2004). Chlorpyrifos also interferes with signal transduction, release, and uptake of neurotransmitters and impairs neuron differentiation (Burke *et al*. 2017; Ubaid ur Rahman *et al*. 2021; Eaton *et al*. 2008). The human metabolization of chlorpyrifos occurs mainly through cytochrome P450 mediated oxidation, transforming chlorpyrifos in its more toxic oxo form (chlorpyrifos oxon) (Choi *et al*. 2006; Eaton *et al*. 2008).

1.3. Bioremediation

The development of remediation techniques became a necessity since POPs cannot be efficiently detoxified through natural processes due to their recalcitrance (Sakshi *et al*. 2019). Bioremediation refers to a group of processes that seek the removal or transformation of pollutants present in an environment through the use of biological systems (bacteria, plants, algae, fungi, and enzymes) (Sharma 2021; Vishwakarma *et al*. 2020). The organisms use pollutants as enzyme substrates in their metabolic activity and transform them into less complex metabolites (Babu *et al*. 2019; Vishwakarma *et al*. 2020). Through physical or chemical anthropological processes, the mass extracted from the polluted site can be prepared before treatment to concentrate and homogeneously distribute the pollutants and then placed in an environment with optimal conditions for the biological system applied to transform the pollutants. Those processes include vapor or organic oil/solvent extraction (Figure 1.2), flocculation, adsorption or size-exclusion membranes, and chromatography techniques (Adeola and Forbes 2021; Lombi and Hamon 2005; Mojiri *et al*. 2019).

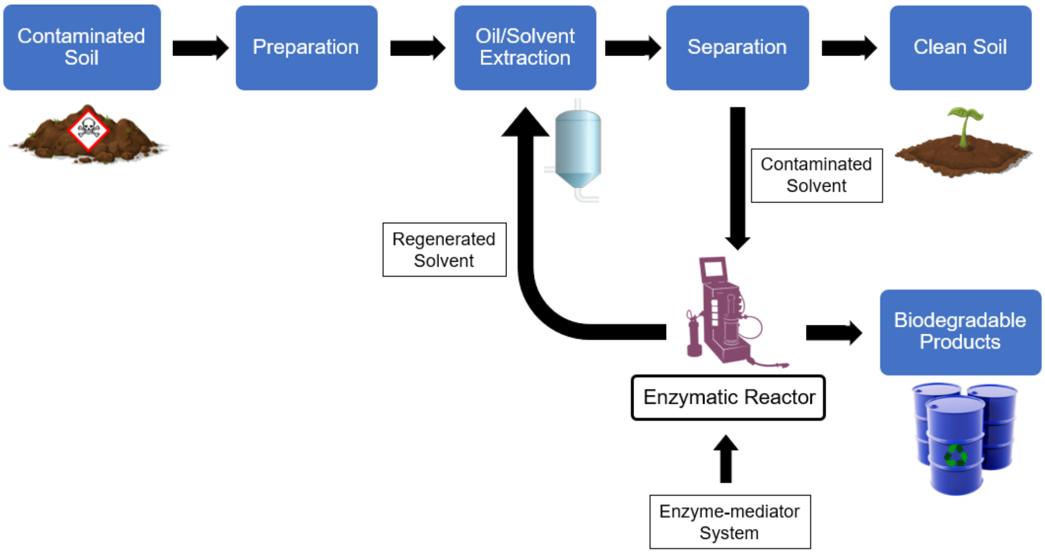

Figure 1.2 – A representative scheme of an enzymatic remediation process. Adapted from (Mousavi *et al*. 2021; Arca-Ramos *et al*. 2015)

Microbial bioremediation is the most common type of bioremediation, using isolated strains individually or in consortia. However, this type of bioremediation can be limited by competition for nutrients within the microbial community, clogging from excessive biomass growth (Bennett 1995; Sakshi *et al*. 2019), or by the unavailability of pollutants to the microorganisms (Lyon and Vogel 2011; Stamatelatou *et al*. 2011). POPs can be found dissolved in a nonaqueous liquid or strongly adsorbed to solid matrixes such as soil components (*e.g*, humic acid) due to their characteristic hydrophobicity, reducing the contact between microorganisms and pollutants (Sharma 2021).

1.4. Enzymes in remediation of organic pollutants

In recent years, enzymatic remediation has been explored as an alternative to treatments with whole microbial cells. Enzymatic remediation uses isolated enzymes to degrade pollutants, focusing on the use of bacterial and fungal enzymes (laccases, peroxidases, oxygenases, etc.) (Karigar and Rao 2011; Sharma *et al*. 2018). This allows the application of only enzymes with pollutant degradation capacities, increasing the efficiency of the process (Rao *et al*. 2010) and reducing the need for nutrients, but it may require supplementation with co-substrates (*e.g*, H_2O_2) or cofactors. Enzymes can be applied in harsher and more extreme conditions (pH, temperature, salinity, pollutant concentration, etc.) in comparison to microorganisms (Kumar and Bharadvaja 2019). However, the application of enzymes in remediation processes can be expensive, due to costs of enzyme production, eventually in purified forms, and immobilization (Babu *et al*. 2019; Kumar and Bharadvaja 2019).

1.4.1. Laccase

Laccase (benzenediol: oxygen oxidoreductase, EC 1.10.3.2) is an extracellular enzyme from the blue-multicopper oxidase family produced by bacteria, fungi, and plants (Baldrian 2006; Arregui *et al*. 2019; Alcalde 2007). It catalyzes a four-electron reduction of molecular oxygen into water coupled to a substrate oxidation reaction in which the substrate acts as a single electron donor (Figure 1.3) (Shraddha *et al*. 2011). Laccase is a versatile enzyme as it can directly oxidize a wide range of substrates (Janusz *et al*. 2020; Bourbonnais and Paice 1990) however, laccase is also capable of catalyzing redox reactions indirectly through a radical-chain mechanism when in the presence of a suitable redox mediator (Alcalde 2007).

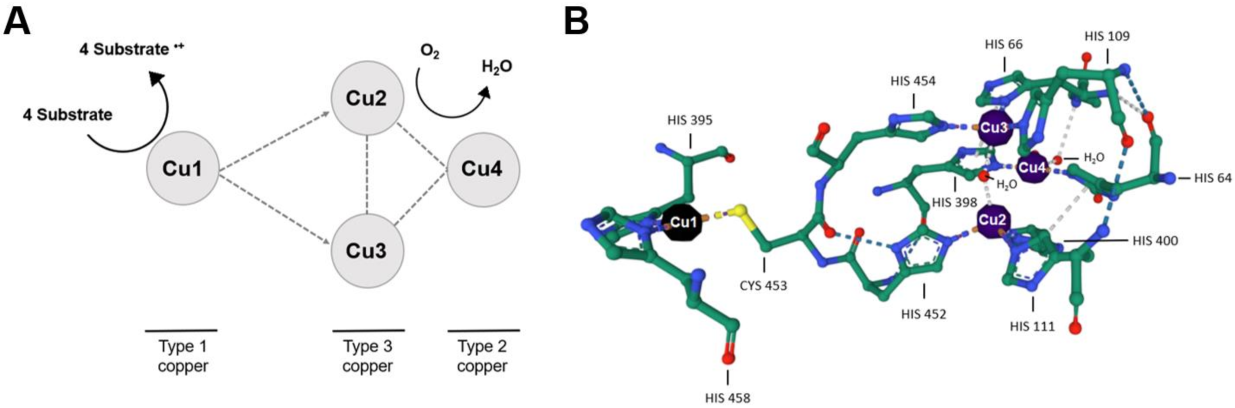

Figure 1.3 – Copper centers in typical fungal laccases and their role in the catalytic process. Type 1 copper captures the electrons from the reducing substrate that are, after, transferred to the trinuclear copper cluster where molecular oxygen is reduced to water. The trinuclear cluster (T2/T3 site) is composed of one binuclear type 3 site and one type 2 site. Laccase PDB entry: 1GYC.

Mediators are low molecular weight compounds able to enhance the rate of enzyme-catalyzed reactions. These compounds act as diffusible electron carriers and shuttle electrons from the electron donors to the electron receptors (Alcalde 2007; Husain and Husain 2007). One of the best described laccase mediators is 2,2′-azino-bis-(3-ethylbenzothiazoline-6-sulphonate) (ABTS), which is also commonly used as a non-phenolic substrate of laccases and peroxidases. ABTS can be semi-oxidized in its cationic radical form ($ABTS^{•+}$) or fully oxidized in its dicationic form ($ABTS^{2+}$) with redox potentials measured as 0.68 and 1.09 V, respectively. In the radical-chain reaction mechanism, in which ABTS mediates laccase oxidoreductase activity (Figure 1.4), ABTS shifts between its reduced form (ABTS) and its oxidized cationic form ($ABTS^{•+}$). Laccase oxidizes ABTS through the four-electron reduction of molecular oxygen into water described previously. Subsequently, the target substrate is oxidized in a non-enzymatic step by $ABTS^{•+}$ via an electron-transfer mechanism. In this step, the oxidizing agent $ABTS^{•+}$ is reduced back to ABTS until it is oxidized again by laccase, restarting the cycle (Christopher *et al*. 2014; Scott *et al*. 1993; Cantarella *et al*. 2003).

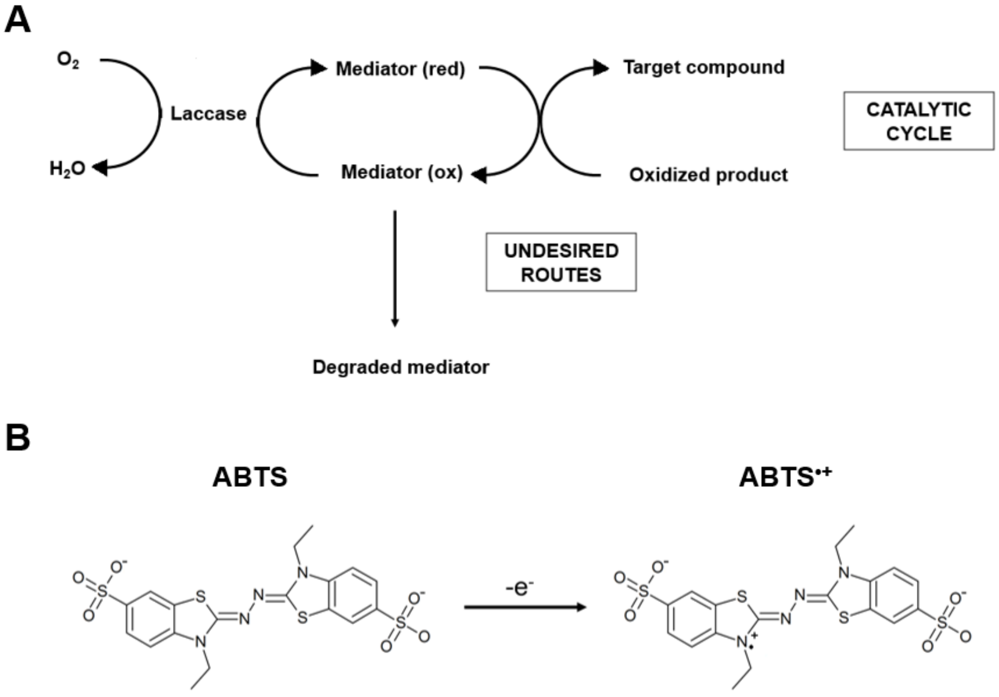

Figure 1.4 – (A) The catalytic cycle of a laccase-mediator system in the oxidation of a non-phenolic substrate and possible undesired side-reactions of the mediator. (B) Oxidation of ABTS to ABTS radical. Retrieved from (D’Acunzo and Galli 2003).

Mediator substances increase the substrate range of an enzyme by bypassing substrate specificity and steric hindrance limitations of the enzyme (Alcalde 2007; Tadesse *et al*. 2008). The most used laccase mediators are ABTS, syringaldehyde, and 1-hydroxybenzotriazole, but many others have been described (Cañas and Camarero 2010; Hilgers *et al*. 2018). The diversity of biocatalytic processes and mechanisms that can be employed with laccase have increased the interest in exploring the use of this enzyme for bioremediation applications (Arregui *et al*. 2019; Gianfreda *et al*. 1999). Fungal laccases have been the center of many degradation studies of organic pollutants (*e.g.,* PAHs, synthetic dyes, PCBs) and of enzymatic activity enhancement studies (*e.g.,* immobilization, use of mediators, protein engineering) (Mikolasch and Schauer 2009; Cañas and Camarero 2010; Guzik *et al*. 2014).

1.4.2. Peroxidases

Peroxidases (EC 1.11.1.7) are a group of oxidoreductase enzymes that catalyze an one-electron oxidation of substrates using H_2O_2. Compounds such as phenols, amines, and dyes are typical substrates known to be oxidized by peroxidases (Morsi *et al*. 2020; Bansal and Kanwar 2013). Peroxidases are produced by a diverse range of sources (bacteria, fungi, animals, and plants), differing in their characteristics depending of the source of but requiring the reduction of H_2O_2 or organic peroxides for their enzymatic activity (Bansal and Kanwar 2013; Patricia Twala *et al*. 2020). Peroxidases play an important role in the defense system of the host. Its antioxidative activity controls the levels of ROS and contributes to the detoxification of toxic substances by oxidizing them through the consumption of H_2O_2 (Vlasova 2018; Khan *et al*. 2014; Brigelius-Flohé and Maiorino 2013).

Heme peroxidases may reach high redox potential due to the stabilization of the higher redox states of iron by the heme group (Ayala 2010; Everse 2004). As a result, the application of hemic peroxidases such as manganese peroxidase (MnP) and horseradish peroxidase (HRP) as biotechnological tools is very interesting (Akbar *et al*. 2018; Azevedo *et al*. 2003).

Horseradish peroxidase and manganese peroxidase

HRP (donor:hydrogen-peroxide oxidoreductase, EC 1.11.1.7) is a monomeric hemic glycoprotein with a molecular weight of 40 kDa. The heme group of HRP possesses a Fe(III) atom pentacoordinated by four tetrapyrrole nitrogens from the heme and a histidine residue from the protein structure (Veitch 2004). This enzyme is often used as a peroxidase model since its catalytical mechanism is the best known and described (Figure 1.5.A). The two-electron H2O2 reduction reaction occurs in the hemic iron, oxidizing the Fe3+ heme group into a Fe4+-porphyrin-radical complex (Compound I). Two molecules of peroxidase substrate are oxidized in sequence by the compound I, which is reduced to Fe^{4+}-porphyrin complex (Compound II) and then reduced to the native ferric state of the enzyme, concluding the catalytical cycle (Veitch 2004; Mousavi *et al*. 2021).

Manganese peroxidase (MnP) (Mn^{2+}: H_2O_2 oxidoreductases, EC 1.11.1.13) is a heme peroxidase with a monochelated manganese atom (Chang *et al*. 2021; Abdel-Hamid *et al*. 2013; Hofrichter 2002). The H_2O_2 reduction reaction and iron-heme complexes formed are similar to those described for HRP. However, in MnP the manganese atom acts as a diffusible charge-transfer mediator between the hemic iron and the substrate, being oxidized by the iron atom and subsequently oxidizing the substrate (Figure 1.5.B) (Mousavi *et al*. 2021; Morsi *et al*. 2020; Hofrichter 2002).

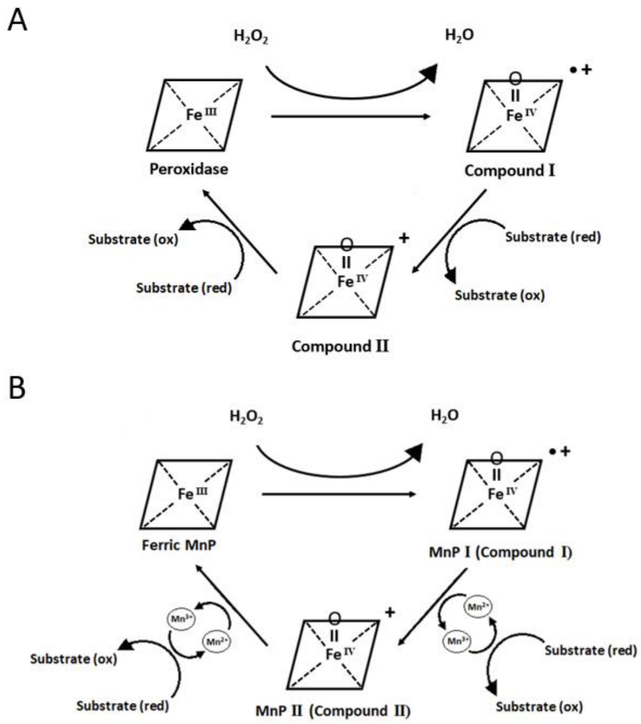
A
H2O2
H2O
Fe III
Peroxidase
O
II
Fe IV
•+
Compound I
Substrate (ox)
Substrate (red)
+
Compound II
Substrate (red)
Substrate (ox)
B
H2O2
H2O
Fe III
Ferric MnP
•+
MnP I (Compound I)
Mn3+
Mn2+
Substrate (ox)
Substrate (red)
+
MnP II (Compound II)
Mn2+
Mn3+
Substrate (red)
Substrate (ox)

Figure 1.5 – Catalytic mechanism of (A) HRP and (B) MnP. Adapted from (Abdel-Hamid *et al*. 2013).

These enzymes have potential for bioremediation applications and have been employed in the treatment of industrial wastewater effluents in the removal of toxic aromatic substances (Chang *et al*. 2021; Na and Lee 2017; Dalal and Gupta 2007) and have been reported to transform more impactful organic pollutants such as PAHs and pesticides (Morsi *et al*. 2020; Abdel-Hamid *et al*. 2013), but with a more limited capacity. Enhancing the efficiency of peroxidases has been sought and enzymatic immobilization is one of the most explored strategies to develop peroxidase-based tools for remediation (Zdarta *et al*. 2021).

Immobilized peroxidases have also been explored to degrade more recalcitrant pollutants. Acevedo *et al.* (2010) evaluated the ability of MnP from *Anthracophyllum discolor* immobilized on nanoclay to degrade PAHs. Immobilized MnP demonstrated higher thermal and pH stability, storage time, and more efficient degradation of degrading anthracene, fluoranthene, phenanthrene, and pyrene

(Acevedo *et al*. 2010). Gholami-Borujeni *et al*. (2011) reported the immobilization of HRP on alginate gel beads and its application on pollutant removal from textile industrial effluents. The results showed that the immobilization of HRP increased the reaction time and the pH and thermal stability of the enzyme. Applications of the encapsulated HRP in 90 min incubations achieved removal efficiencies of 80% and 70% for the textile dyes Acid Orange 7 and Acid Blue 25, respectively (Gholami-Borujeni *et al*. 2011).

Other peroxidases in the transformation of organic pollutants

The enzymes of the cytochrome P450 monooxygenase superfamily are the best known human hemic peroxidases due to their importance in human metabolism (Manikandan and Nagini 2018), making cytochrome P450 the focus of many human toxicology studies while their catalytic versatility raised interest in its exploration for biotechnological purposes (Lamb *et al*. 1998; Gorinova *et al*. 2005). Human hemeproteins pseudo-peroxidases, like hemoglobin and cytochrome *c*, also display peroxidase activity but only after being converted into peroxidases by the influence of external factors (Vlasova 2018; Díaz-Quintana *et al*. 2020).

Hemoglobin is a tetrameric hemoprotein with a molecular weight of 64 kDa well known for its physiological function of oxygen and carbon dioxide transport in the circulatory system (Everse 2004) but hemoglobin also plays antioxidant functions under certain physiological conditions (Coates and Decker 2017). It has been evidenced that hemoglobin exhibits peroxidase-like activity (Reeder 2010) that is triggered under uncontrolled pathological conditions, adopting an antioxidant function through a catalytical cycle similar to the one described for HRP (S. Wang *et al*. 2017). Hemoglobin can oxidize substrates specifically in its hydrophobic pocket and non-specifically through a tyrosyl radical exposed in the surface of the protein (Vlasova 2018; Reeder *et al*. 2008) however, hemoglobin can self-oxidate and aggregate as a result of its peroxidase-like activity and inactivate (Reeder 2010). The best known purpose of hemoglobin peroxidase-like activity is the detoxification of ROS but its toxicological role may not be fully understood yet (Kapralov *et al*. 2009). Recently, Keum *et al.* (2021) evidenced the capacity of hemoglobin to transform BaP in the presence of H_2O_2 through heme-catalyzed reactions (Keum *et al*. 2021). This protein can be easily produced in bulk and was shown to be capable to degrade organic recalcitrant pollutants (Stark *et al*. 2008). Hence, the study of hemoglobin concerning its applicability in bioremediation processes and its toxicological importance in the transformation of organic pollutants is of great interest.

Cytochrome *c* (Cc) is a hemeprotein with a molecular weight of 12 kDa that acts as an electron carrier in the respiratory chain bound in the inner mitochondrial membranes (Wallace and Clark-Lewis 1992). Cc also plays a critical role in apoptosis by being released from the mitochondria to the cytosol and mediating signals of the intrinsic apoptotic pathway (Díaz-Quintana *et al*. 2020). Similar to cytochrome P450, Cc has been reported to be capable of peroxidase activity to detoxify ROS (Min and Jianxing 2007) and to oxidize organic molecules (Radi *et al*. 1991; Maiti *et al*. 2012) but this peroxidase activity is only unlocked or increased after significant structural changes (Diederix *et al*. 2002). The partial unfolding and oxidation of Cc can be induced by the interaction of phospholipidic membranes with the protein. Cardiolipin (CL), a mitochondrion-specific phospholipid, is associated with the gain of peroxidase activity of Cc as it has been reported to complex with Cc, induce structural modifications and trigger a strong peroxidase activity in the presence of H_2O_2 (Barayeu *et al*. 2019; Díaz-Quintana *et al*. 2020). However, the mechanism behind the catalytical activity of Cc is not fully understood and only a few substrates have been reported for this protein. Little is known about the ability of Cc for transforming recalcitrant toxicants. ABTS is among the few organic molecules to have been reported to be oxidized by Cc, therefore, it is possible that the catalytical activity of this pseudo-peroxidase can be mediated by ABTS to transform a wider range of organic compounds, including environmental toxicants.

1.5. Aims of the Thesis

In this work, the transformation of common environmental toxicants catalyzed by oxidoreductase enzymes was investigated in different conditions of toxicological and biotechnological interest. Biotechnological studies were performed for laccase from *Tramates versicolor*, HRP, bovine serum hemoglobin, and horse heart Cc to compare their potential for enzymatic remediation applications. The studies with hemoglobin and Cc were carried also persuing the hypothesis that they play a role in the toxicology of pollutants.

In the studies on the bioremediation perspective, it was decided to test the catalytical capacity of the enzymes and enzyme-like proteins in the transformation of PAHs (mainly, anthracene and BaP), an organophosphate pesticide (chlorpyrifos), and an azo dye (MO). For this, the enzymatic activity of the enzymes was initialy measured using ABTS and the influence of pH was assayed. The degradation of organic pollutants was investigated with the enzymes and enzyme-like proteins with and without ABTS as a mediator. Reactional conditions of degradation studies were optimized using the designed laccase-ABTS systems through MO decolorization and anthracene oxidation assays. The ability of the proteins alone and in systems with ABTS to decolorize MO was assessed through kinetic assays monitored by UV-Vis spectroscopy and the ability to degrade PAHs and chlorpyrifos was assessed through incubation assays analyzed afterward by HPLC.

In addition, the catalytic efficiency in pollutant degradation was investigated in the presence of humic acid (HA) to determine how the enzymatic systems can be influenced by the presence of this soil/water component in bioremediation processes. The influence of HA in enzymatic activity was tested for ABTS oxidation, MO decolorization, and anthracene oxidation. The observed effect of HA motivated the investigation of the possible quenching of radicals by HA.

Regarding the studies of toxicological interest, the capacity to transform the pollutants was studied for hemoglobin and Cc since their role in the metabolism of organic toxicants is still not clear. The cellular environments of hemoglobin and Cc contain lipid membranes that can modulate both the availability of toxicants and the peroxidase-like activity of the hemeproteins. Therefore, the catalytic efficiency of these pseudo-peroxidases in the degradation of organic toxicants was investigated at physiologic pH and in the presence of lipid membranes.

2.
Materials and Methods

2.1. Chemicals, buffers, humic acid, and liposomes

2.1.1. Chemicals

Table 2.1 presents the main and more important reagents used in this work. The proteins are presented in a dedicated section below (Section 2.2).

Table 2.1 – Specifications of the more important reagents used in this work.

Material/Reagent	Supplier	Catalog number	CAS	Additional Information
1,2-Dioleoyl-sn-glycero-3-phosphocholine	Tokyo Chemical Industry	D4250	4235-95-4	Purity >97.0%
1',3'-bis[1,2-dioleoyl-sn-glycero-3-phospho]-glycerol (sodium salt)	Avanti	710335P	115404-77-8	Purity ≥ 99%
2,2'-Azino-bis(3-ethylbenzo-thiazoline-6-sulfonic acid) diammonium salt (ABTS)	Alfa Aesar	J65535	30931-67-0	Purity ≥ 98%
Acetic Acid (CH_3COOH)	Thermo Fisher Scientific	33209	64-19-7	Purity ≥ 99.7%
Acetone (C_3H_6O)	LabChem	6084772	67-64-1	Purity ≥ 99.5%
Acetonitrile (C_2H_3N)	Honeywell	AC03782500	75-05-8	HPLC grade Purity ≥ 99.9%
Anthracene ($C_{14}H_{10}$)	Sigma-Aldrich	A89200	120-12-7	Purity ≥ 97%
Anthraquinone ($C_{14}H_8O_2$)	Acros	104930500	84-65-1	Purity ≥ 98%

Benz[a]anthracene ($C_{18}H_{12}$)	Tokyo Chemical Industry	B0017	56-55-3	HPLC grade Purity ≥ 98%
Benzo[a]Pyrene ($C_{20}H_{12}$)	Sigma-Aldrich	B1760	50-32-8	HPLC grade Purity ≥ 96%
Benzo[b]fluoranthene ($C_{20}H_{12}$)	Tokyo Chemical Industry	B2982	205-99-2	HPLC grade Purity ≥ 98%
Calcium Chloride ($CaCl_2$)	Panreac	1023820500	10035-04-8	Purity ≥ 99%
Chlorpyrifos ($C_9H_{11}Cl_3NO_3PS$)	Sigma-Aldrich	45395	2921-88-2	Analytical standard grade Purity ≥ 98.0%
Copper Chloride (II) ($CuCl_2.2H_2O$)	Acros	206345000	10125-13-0	Purity ≥ 98%
di-Sodium Hydrogen Phosphate (Na_2HPO_4)	Panreac	131679.1211	7558-79-4	Purity ≥ 99%
Diethylenetriaminepentaacetic Acid (DTPA)	Merck	D6518	67-43-6	Purity ≥ 99% (Titration)
Glycerol	Avantor	MFCD00004722	56-81-5	Purity ≥ 99%
Hexane (C_6H_{14})	Thermo Fisher Scientific	H/0355/17	110-54-3	Purity ≥ 99%
Humic Acid, sodium salt	Acros	120861000	68131-04-4	Purity 50-60%
Hydrogen Peroxide (H_2O_2)	Chem-Lab NV	CL00.2308.1000	7722-84-1	30% (w/w)
Iron Chloride (III) ($FeCl_3.6H_2O$)	Panreac	131358.1209	10025-77-1	Purity ≥ 97%
Methanol	Thermo Fisher Scientific	M/4056/17	67-56-1	HPLC grade Purity ≥ 99.9%
Methyl orange ($C_{14}H_{14}N_3NaO_3S$)	Panreac	281432.1209	547-58-0	No information available
Naphthalene ($C_{10}H_8$)	Merck	91-20-3	820846	HPLC grade Purity ≥ 99%
Sodium Dihydrogen Phosphate (NaH_2PO_4)	Scharlau	SO03301000	7558-80-7	Purity ≥ 98%
Sodium Acetate ($C_2H_3NaO_2$)	Merck	1.06268.0250	127-09-3	Purity ≥ 99.7%

2.1.2. Preparation of buffers

Acetate buffer was prepared by mixing acetic acid and sodium acetate aqueous solutions prepared with distilled water at the same concentration intended for the buffer. Buffer pH was adjusted through the addition of volumes of acetic acid or sodium acetate solution until the desired pH is achieved (AAT Bioquest 2021).

Phosphate buffer was prepared by mixing Na_2HPO_4 and NaH_2PO_4 aqueous solutions prepared with distilled water at the same concentration intended for the buffer. Buffer pH was adjusted by the addition of volumes of the reagents until the desired pH is achieved (AAT Bioquest 2020).

2.1.3. Preparation of humic acid solutions

HA solutions were prepared by a method adapted from Zahmatkesh *et al.* (2016) (Zahmatkesh *et al*. 2016). HA powder (4 g) was dissolved in 200 mL of NaOH (100 mM) and stirred at room temperature for 30 minutes. The suspension was centrifuged at 7000 rpm, 4˚ C for 20 minutes. The supernatant was collected, and the pellet formed was discarded. Afterward, 100 mL of phthalate buffer (0.5 M) was added to the collected supernatant, and pH was adjusted to 4.5 using HCl. Posteriorly, the solution was centrifuged again with the same parameters (7000 rpm, 4˚ C, 20 minutes), the supernatant was collected, and the pellet formed was discarded. The HA solutions were filtered (0.2 µm) before experimental use.

In parallel to the preparation of the HA solutions, a blank solution was prepared by following the same method but omitting the addition of the HA powder. This blank solution was used for control assays in the studies of the effects of HA. The concentration of the stock solutions of HA was determined by drying (48 h, 100 °C): 10 mL of the solution and 10 mL of the blank solution, both in triplicate, and subtracting the weight of the dried blank solution to the weight of the dried HA solution. Throughout the work, 3 solutions of HA were prepared with concentrations of 7.33 ± 0.31 g/L.

2.1.4. Preparation of liposomes

Small unilamellar vesicles (SUV) prepared by sonication were used as lipid membranes, as in (Lagoa *et al*. 2017). Chloroform stock solutions of phosphatidylcholine (PC) alone or PC and CL mixture, at a 4:1 molar ratio (PC/CL), were dried and resuspended in 20 mM phosphate buffer (pH 7, supplemented with 100 µM DTPA), to a final lipid concentration of 10 mM. Afterward, SUV were prepared by sonication of 200 µL aliquots of the lipid suspension, in ice, until clarity using a titanium-microtip-equipped Hielscher UP100H sonicator, usually 3-4 pulses of 50 W of 10 s duration each.

2.2. Proteins and their stock solutions

Table 2.2 presents the proteins used in this work.

Table 2.2 – Proteins used in this work and their specifications according to the commercial information.

Protein	Supplier	Catalog number	CAS	Additional Information
Cytochrome *c* (from equine heart)	Sigma-Aldrich	C7752	9007-43-6	Purity ≥ 95%
Cytochrome *c* (from equine heart)	Sigma-Aldrich	C2506	9007-43-6	Purity ≥ 95%
Hemoglobin (from bovine blood)	Sigma-Aldrich	H2625	9008-02-0	From washed, lysed and dialyzed erythrocytes
Laccase (from *Trametes versicolor*)	Sigma-Aldrich	38429	80498-15-3	≥0.5 U/mg solid (using catechol)
Peroxidase (from horseradish)	Sigma-Aldrich	P6782	9003-99-0	950-2000 U/mg solid (using ABTS) ≥250 U/mg solid (using pyrogallol)

2.2.1. Protein stock solutions and determination of concentration

Laccase stock solution was prepared in a final concentration of 10 mg/mL by dissolving laccase (solid) in acetate buffer (100 mM, pH 5.0) containing 20% glycerol. HRP stock solution was prepared by dissolving 5 mg of solid HRP in 5 mL of acetate buffer (100 mM, pH 5.0). Hemoglobin stock solution was prepared in a final concentration of 50 mg/mL by dissolving hemoglobin (solid) in phosphate buffer (100 mM, pH 7.0). Cc stock solution was prepared in a final concentration of 10 mg/mL by dissolving cytochrome *c* (solid) in phosphate buffer (100 mM, pH 7.0). Protein stock solutions were conserved at -65˚ C in the absence of light.

Molar concentrations of the protein solutions were determined through UV–Vis spectroscopy. For laccase and HRP, samples were diluted in acetate buffer (100 mM, pH 5.0) and analyzed using the extinction coefficient $\varepsilon_{611nm} = 7.3\times10^3$ $M^{-1}cm^{-1}$ for laccase and $\varepsilon_{403nm} = 1.02\times10^5$ $M^{-1}cm^{-1}$ for HRP (Chernykh *et al*. 2008; Zatón and Ochoa de Aspuru 1995). For horse heart Cc, samples were prepared in phosphate buffer (100 mM, pH 7.0) and reduced using sodium dithionite. Cc was analyzed using the extinction coefficient $\varepsilon_{550nm} = 27.6$ mM^{-1} cm^{-1} (Errede et al. 1976).

2.3. Stock solutions of PAHs and chlorpyrifos

Anthracene, benzo[a]anthracene, BaP, benzo[b]fluoranthene, and chlorpyrifos stock solutions were prepared by dissolving the dry solid solutes in acetonitrile with moderate stirring at room temperature. Stock solutions of PAHs were prepared in a final concentration of 100 mg/L and chlorpyrifos stock solution was prepared in a final concentration of 10 g/L. Stock solutions were stored at 4 ˚C, in the absence of light, and showed to be stable for at least 3 months.

2.4. Methods of analysis of the target pollutants

MO dye was monitored in the decolorization assays by UV-Vis spectrophotometry using a GENESYS 10 Scanning UV/Visible spectrophotometer (Thermo Scientific). The details are given in the methods relative to enzyme activity and decolorization of MO.

PAHs and chlorpyrifos were analyzed by high-performance liquid chromatography (HPLC) of hexane extracts of the reaction mixtures. The details of extraction and analysis are given in the following sections.

2.4.1. Hexane extraction of target pollutants

The reaction mixtures from the enzymatic degradation assays were mixed with hexane to extract the target pollutants (and reaction products) to the organic solvent, before HPLC analysis.

Extraction assays using hexane were innitialy performed to establish a simple and efficient extraction procedure that achieves precise and accurate results. The assays were performed with 1 mL solutions of PAHs or chorpyrifos in acetate buffer (100 mM, pH 5.0) and evaluated the use of successive extractions and different stirring times. Controls were carried with the target pollutants dissolved in hexane at the concentrations used in degradation studies. Upon phase separation, organic phases were collected and analyzed by HPLC.

After the initial studies of the influence of time and other factors in the extraction efficiency (Section 3.1), an extraction procedure was established for the remaining work: 1 mL of reactional sample was extracted with the addition of 500 µL of hexane in two successions with 30 seconds of vigorous stirring (protected from light). The organic phases were collected after each stirring step and aggregated for analysis.

2.4.2. UV-Vis spectra of PAHs and chlorpyrifos

To study the UV-Vis spectra of the target pollutants in acetonitrile, two sets of sample solutions of each organic pollutant were prepared in a final concentration of 1 mg/L. One set was prepared by diluting volumes of stock solution with acetonitrile and another set of sample solutions using water as a dilution media. The UV-Vis absorption spectra of these solutions were measured at room temperature on a Varian Cary 50 UV-Vis spectrophotometer (Agilent). The spectra of anthracene, at a concentration of 1 mg/L, were also collected in mixtures of acetonitrile and water at different ratios. Absorption maxima were recorded with an accuracy of 1 nm in the 200-800 nm wavelength interval using a 1 cm standard quartz cell. The absorption baselines were established with the corresponding dilution media of the sample solutions: acetonitrile, or distilled water, or mixtures acetonitrile:water at the same ratio as the sample solutions.

2.4.3. High-Performance Liquid Chromatography

HPLC using an Agilent 1100 system with a C18 column was used to analyze PAHs, chlorpyrifos, and corresponding reaction products. HPLC methods using methanol were routinely used on the pre-run and post-run to clean the HPLC column and flow was gradually increased and decreased on the pre-run and post-run respectively to avoid damaging the HPLC column.

The hexane extracts of the reactional mixtures were analyzed by reverse-phase HPLC with a mobile phase of acetonitrile (85%) and water (15%), flux 1 mL/min. Anthracene and reaction products were measured through UV detection at 251 nm. BaP and reaction products were measured through UV detection at 266 nm. The mixtures of different PAHs and reaction products were analyzed through UV detection at 266 nm. Chlorpyrifos was measured through UV detection at 225 nm.

2.5. Studies of enzyme activity using ABTS as substrate

2.5.1. Determination of enzymatic activity

The enzymatic activity of the proteins used in this work was determined through a method based on the oxidation of the nonphenolic dye ABTS catalyzed by laccase to $ABTS^{\bullet+}$. This cation is a blue-green chromophore whose formation can be correlated to enzyme activity and can be followed spectrophotometrically at 420 nm, the wavelength correspondent to the maximum molar extinction coefficients of $ABTS^{\bullet+}$ (ε_{420}, 3.6×10^4 $M^{-1}\cdot cm^{-1}$).

The activity of the proteins was assayed with 1 µg/mL of laccase, 1×10^{-3} µg/mL of HRP, 10 µg/mL of hemoglobin and 100 µg/mL of Cc, in reactional mixtures of 1 mL using 0.5 mM of ABTS in acetate buffer (100 mM, pH 5.0).

Assays of peroxidase-type proteins were carried with 100 µM of H_2O_2 and the buffer solution contained 0.1 mM of DTPA. The H_2O_2 working solutions were prepared by dilution in distilled water of the commercial 30% (w/w) solution. The actual concentration of H_2O_2 in the daily working solutions was measured considering the 240 nm extinction coefficient 39.4 M^{-1} cm^{-1}. The influence of DTPA on the peroxidase activity of the hemeproteins in study was checked and the effect of concentrations of DTPA up to 2 mM was determined by comparing the ABTS oxidation rates in the presence and in the absence of DTPA.

$ABTS^{\bullet+}$ formation was monitored at 420 nm in a spectrophotometer at 25° C. Some assays were equally carried at 436 nm, 600 nm, and 734 nm, wavelengths at which the ABTS radical also absorbs. Blank assays were also carried without the addition of the protein. One unit of enzymatic activity was defined as the amount of enzyme that oxidized 1 µmol of ABTS substrate per min.

2.5.2. Effect of humic acid on enzyme-catalyzed ABTS oxidation

Stock solutions of HA were prepared as described in the above Section 2.1.3. The effect of HA in laccase-catalyzed ABTS oxidation was studied with 1 µg/mL of laccase, using 50 µM of ABTS, by adding small volumes of HA to the reactional mixtures to reach final concentrations between 0.5 mg/L and 100 mg/L in acetate buffer (100 mM, pH 5.0). Control assays were carried in parallel using the same volumes of blank solution instead of HA solution. The effect of HA in laccase activity was calculated through the comparison of ABTS oxidation rates between assays in the absence and in the presence of HA and normalized by subtracting the effect of the blank solution in the ABTS oxidation rate of laccase.

Studies with peroxidase-type proteins were carried for the same concentrations of enzymes and H_2O_2 used in the studies of ABTS oxidation (Section 2.5.1) and the effect of HA was assayed by adding a small volume of HA in a final concentration of 50 mg/L to the reactional mixture. The effect of HA in ABTS oxidation by HRP and Cc was calculated through the comparison of ABTS oxidation rates between assays in the absence and in the presence of HA. ABTS oxidation was monitored at 420 nm as described previously (Section 2.5.1).

2.5.3. Effect of pH and liposomes on enzyme-catalyzed ABTS oxidation

The effect of pH on the ABTS oxidizing activity of laccase, HRP, and Cc was studied using the same ABTS oxidation method previously described (Section 2.5.1). Reactional mixtures at different pHs were achieved by using acetate buffers (100 mM) with pH 5.0, 5.5 or 6.0, or phosphate buffers (100 mM) with pH 7.0 or 8.0. ABTS oxidation assays were carried using 1 µg/mL (3.8×10^{-4} µM) of laccase, 100 µg/mL (8 µM) of Cc with 100 µM H_2O_2 and 1×10^{-3} µg/mL (1.7×10^{-5} µM) of HRP with 100 µM H_2O_2.

The effect of lipid membranes on the ABTS oxidizing activity of Cc and hemoglobin was studied adapting the ABTS oxidation method, in phosphate buffer at pH 7.0. Cc (12.5 µg/mL) and hemoglobin (10 µg/mL) were incubated with the lipid SUVs in the spectrophotometer cuvette, for 5 minutes, before addition of 100 µM of ABTS and 100 µM of H_2O_2. In these assays, ABTS oxidation was followed at 734 nm to avoid eventual interferences caused by absorbance changes of the Soret band due to changes in the heme group during reaction.

2.6. Decolorization of methyl orange

2.6.1. Decolorization of methyl orange by laccase

The effect of ABTS as a redox mediator was investigated through methyl orange decolorization assays using 100 µg/mL of laccase and increasing amounts of ABTS ranging between 0.5 and 10 µM to degrade 10 mg/L of MO in acetate buffer (100 mM, pH 5.0) at 25 ̊C. Absorbance changes were observed spectrophotometrically at 477 nm. Control assays were carried without the enzyme to test the eventual non-enzymatic degradation of the dye in the absence and in the presence of ABTS. The influence of the presence of ABTS in MO degradation was calculated through a comparison of absorbance decrease rates before and after the addition of different ABTS concentrations to the reactional mixtures.

2.6.2. Decolorization of methyl orange by peroxidase-type proteins

MO decolorization catalyzed by HRP, hemoglobin, and Cc was assayed with 0.2 µg/mL (3.4×10^{-3} µM) of HRP, 10 µg/mL of hemoglobin, and 100 µg/mL (8 µM) of Cc in acetate buffer (100 mM, pH 5.0 containing 0.1 mM DTPA) at 20˚ C. Reaction was triggered by the addition of 100 µM H_2O_2 and followed at 477 nm. The effect of ABTS in MO decolorization catalyzed by peroxidase activity was tested by the addition of 5 µM and 10 µM of ABTS to the reactional mixtures. Controls without protein were carried out in parallel with the same reactional conditions described but without the addition of ABTS. The effect of ABTS in MO decolorization catalyzed by peroxidase-type proteins was measured as described in laccase studies (Section 2.6.1).

MO decolorization at pH 7.0 was assayed in the same conditions, except that the assays were performed in phosphate buffer (100 mM, pH 7.0 containing 0.1 mM DTPA) and without the addition of ABTS. Reaction was triggered by the addition of 100 µM H_2O_2 and followed at 477 nm.

For MO decolorization activity of Cc and hemoglobin in the presence of lipid membranes, the proteins were incubated in the same conditions described previously for ABTS oxidation assays (Section 2.5.1) before addition of 10 mg/mL of MO and 100 µM of H_2O_2. Control assays were carried in the same conditions but without the presence of SUVs. MO decolorization was followed at 477 nm and the induction of Cc- and hemoglobin-catalyzed MO decolorization by SUVs was calculated through the comparison of absorbance decrease rates of Cc and hemoglobin assays incubated with SUVs and the respective control assays.

2.6.3. Influence of metal ions on methyl orange decolorization by laccase-ABTS system

For the studies with metal ions (Fe^{3+}, Cu^{2+} and Ca^{2+}), stock solutions were prepared in acetate buffer (100 mM, pH 5.0) and added in small volumes to the assays to reach final concentrations between 1 µM and 1 mM. The MO decolorization assays were carried as described above using 100 µg/mL of laccase and 5 µM of ABTS. To calculate the effect of the metal ions on the activity of laccase-ABTS in MO decolorization the decolorization rates in the presence of the metal ions were compared with the degradation rates in the absence of the metal ions, which were taken as 100%.

2.6.4. Effect of humic acid on enzyme-catalyzed methyl orange decolorization

The effect of HA in laccase-, HRP- and Cc-catalyzed MO decolorization was studied through the same general methods described previously (Section 2.5.1 and 2.5.2). Assays were carried for laccase 300 µg/mL, HRP 0.2 µg/mL and Cc 100 µg/mL.

In laccase assays, HA was added in volumes corresponding to final concentrations of HA ranging between 1 mg/L and 100 mg/L to reactional mixtures. Separate laccase assays were additionally carried with a higher amount of HA in the reaction media (200 mg/mL). Assays of HRP and Cc were carried with 100 µM of H_2O_2 and 50 mg/L of HA were added to the reactional mixtures. The effect of HA in laccase-, HRP- and Cc-catalyzed MO decolorization was calculated through the comparison of absorbance decrease rates before and after the addition of HA to the reactional mixture.

The effect of HA in MO decolorization by ABTS mediated laccase activity was also assayed following a procedure similar to the one described for the study of the influence of metal ions (Section 2.6.3). MO decolorization assays were performed for 100 µg/mL of laccase in the presence of different ABTS concentrations (5 µM and 50 µM). Control assays were performed using the blank solution instead of HA. The effect of HA was measured as described for the previous MO decolorization assays and normalized as described for the ABTS studies (Section 2.5.2).

2.7. Degradation of PAHs and chlorpyrifos

2.7.1. Enzyme-catalyzed degradation of PAHs and chlorpyrifos

The oxidative ability of enzymes and enzyme-like proteins was studied against anthracene, BaP, BbF, chlorpyrifos, and, also, facing a mixture of PAHs composed by 20 mg/L of BbF, 5 mg/L of BaP, 5 mg/L of BaA, and 0.5 mg/L of naphthalene. The degradation of anthracene, BaP, and chlorpyrifos catalyzed by laccase, HRP and Cc was investigated through incubation assays performed in 5 mL reaction tubes using initial concentrations of 1 mg/L of anthracene, 1 mg/L of BaP, and 25 mg/L chlorpyrifos. Incubation assays were performed with laccase (100 µg/mL), or HRP (0.2 µg/mL) or Cc (100 µg/mL) with 100 µM H_2O_2. The oxidative capacity in the transformation of the mixture of PAHs was studied only with Cc at pH 5 and pH 7.

The effect of ABTS in laccase-catalyzed degradation of anthracene (1 mg/L) was assayed with 100 µg/mL of laccase incubated with different concentrations of ABTS ranging from 0.5 µM to 50 µM.

The ability of ABTS to mediate PAHs and chlorpyrifos enzymatic degradation was also investigated for laccase and HRP through the same method. Incubation assays were performed using the same reactional conditions but in the presence of 50 µM of ABTS.

The influence of the presence of CL-containing SUVs in the ability of Cc to transform BbF (1 mg/L) was investigated using 12.5 µg/mL of Cc with 100 µM of H_2O_2 in phosphate buffer (20 mM, pH 7.0). Incubation assays were performed using the same reactional conditions in the presence and in the absence of 200 µM of PC/CL SUVs.

Control assays of anthracene, BaP, and chlorpyrifos were carried out for each set of incubations with the respective target pollutant incubated in acetate buffer (100 mM, pH 5.0), target pollutant in the presence of 50 µM of ABTS and target pollutant in the presence of 50 µM of ABTS, and 100 µM H_2O_2. Control assays of BbF were carried with BbF incubated in the presence of 100 µM H_2O_2 in phosphate buffer (20 mM, pH 7.0). Control assays of the mixture of PAHs were carried with the mixture of the PAHs incubated in the presence of 100 µM H_2O_2 in acetate buffer (100 mM, pH 5.0) or phosphate buffer (100 mM, pH 7.0) for assays performed at pH 5.0 and pH 7.0, respectively.

Incubation tubes were tightly sealed and incubated in the absence of light, at 20ºC, for 24 hours. Afterward, target pollutants and reaction products were extracted with hexane and analyzed by HPLC as described above in Sections 2.4.1 and 2.4.3. Percentages of remaining target pollutants were calculated through comparison with the results of the controls consisting in the target pollutant in acetate buffer (100 mM, pH 5.0), which was taken as 100% of initial target pollutant concentration (0% degradation).

2.7.2. Effect of humic acid on anthracene degradation by laccase-ABTS system

The influence of HA in anthracene oxidation was assayed with the same method used for the anthracene degradation studies described above (Section 2.7.1). Experiments were conducted for 100 µg/mL of laccase in the absence of ABTS and in the presence of 50 µM of ABTS and adding volumes of HA to the reactional mixture in final concentrations ranging between 0 mg/L and 500 mg/L. Control assays consisted in anthracene in acetate buffer (100 mM, pH 5.0) and anthracene in the presence of 500 mg/L of HA, both without laccase. A set of control incubation assays was also carried in parallel to the HA assays described but using equivalent volumes of blank solution instead of HA.

Afterward, anthracene and degradation products were extracted with hexane and analyzed by the HPLC method described previously. Percentages of remaining anthracene were calculated as described above (Section 2.7.1) and normalized by subtracting the effect observed in the set of incubation with the blank solution.

2.7.3. Anthraquinone degradation by laccase-ABTS system

Anthraquinone degradation by laccase-ABTS systems was studied following the same method as for anthracene. Anthraquinone initial concentration was 1 mg/L and ABTS was used at 50 µM. Anthraquinone incubation in acetate buffer (100 mM, pH 5.0) without laccase was used as a control for this study.

Afterward, anthraquinone and reaction products were extracted and analyzed by HPLC as described previously. Percentages of anthraquinone degradation were determined through the same method as described previously (Section 2.7.1).

2.8. Quenching of radicals by humic acid

The ability of HA to scavenge the ABTS and MO products generated by laccase was investigated by two methods: (1) interrupting laccase catalysis with azide and (2) using chemically produced ABTS radical.

The first method was based on the laccase ABTS oxidation and MO decolorization assays carried in the same conditions as described previously (Section 2.5.2 and 2.6.4). When the absorbance of $ABTS^{\bullet+}$ at 420 nm reached approximately 0.5 or, in the case of MO decolorization, the absorbance at 477 nm decreased to approximately 0.1, sodium azide was added to the cuvette to a final concentration of 0.1 mM for the $ABTS^{\bullet+}$ assay and 0.2 mM for the MO assay, enough to block the enzymatic activity (Nagai *et al*. 2002). Then, HA was added at different concentrations and the changes in the absorbance of the reaction media were followed.

For the assays based on the second method, an ABTS radical solution was previously produced by oxidation with persulfate. The radical was pre-formed by mixing 10 mL of ABTS 7 mM with 10 mL potassium persulfate 4.9 mM and leaving the mixture in the dark at room temperature for 12–16 h, as indicated in Re. *et al.* (Re *et al*. 1999). In this proportion, persulfate is limiting and ABTS is not completely oxidized. For the HA assays, an aliquot of pre-formed $ABTS^{\bullet+}$ (14 µM) was diluted in the acetate buffer (100 mM, pH 5) and a small volume of HA was added. Absorbance changes were followed at 420 nm after HA addition.

3.
Results and Discussion

3.1. Environmental toxicants in this work and their analysis

The present work investigated the ability of different enzymes and enzyme-like proteins to transform organic pollutants, namely, PAHs, an azo dye, and an organophosphate pesticide. Most of the work was developed with anthracene, used as a model for PAHs in water and soil pollution (Sakshi *et al*. 2019; Tobiszewski and Namieśnik 2012). Chlorpyrifos was the model organophosphate pesticide studied in the work (Dar *et al*. 2019; John and Shaike 2015). The degradation of the PAHs and the organophosphate pesticide was studied by incubation assays of the compounds with the enzymes and enzyme-like proteins, followed by extraction with hexane and chromatographic analysis of the extracts. The degradation potential of the proteins was also investigated with MO dye, which offered the additional advantage of using a more convenient test assay (UV-Vis kinetic assay) than the degradation assay of PAHs, circumventing some of the difficulties of the analysis of PAHs, such as organic solvent extraction, and allowed real-time monitorization of the enzymatic reactions. The UV-Vis absorption spectra of MO and the selection of the wavelength for its monitorization are presented in Section 3.3. Being based on a more convenient test assay, the enzymatic studies with MO were useful to unravel some catalytic abilities of each protein and optimize reaction conditions before the degradation assays with anthracene and chlorpyrifos.

3.1.1. Basic physico-chemical properties

Table 3.1 presents physico-chemical properties of the studied PAHs and chlorpyrifos. Details on the reagents and stock solutions of these compounds employed throughout the work can be found in Sections 2.1 and 2.3. From the data gathered in Table 3.1, it can be confirmed that most of the PAHs are characterized by a low logP and low water solubility, and that naphthalene and anthracene are the most volatile. These properties and other molecular features promote the precipitation or aggregation of the compounds in aqueous media and hinder their monitoring in the typical (aqueous) enzymatic reaction/assay conditions. Hence, before the enzymatic studies, the behavior of the PAHs and chlorpyrifos in solution was inspected by UV-Vis spectroscopy and the methods for their analysis were established.

Table 3.1 – Chemical structures and physico-chemical properties of the polycyclic aromatic hydrocarbons and the organophosphate pesticide chlorpyrifos used in this work.

Substance and Molecular structure	Molecular Weight (g/mol)	Log P (Octanol:Water) (a)	Solubility (water, mg/L) (b)	Polar Surface Area ($\mathrm{Å}^2$) (c)	Melting Point (°C) (d)	Molar Extinction Coefficient ($M^{-1}\ cm^{-1}$) (e)	Equilibrium Vapor Pressure (mmHg) (f)
Naphthalene 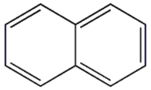	128.17	3.30	66 31	0	80.2	$\varepsilon_{275nm} = 5700$ (acetonitrile)	0.08
Anthracene 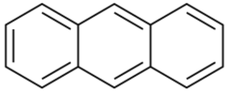	178.23	4.45	65×10^{-3} 15×10^{-3}	0	215-218	$\varepsilon_{252nm} = 155000$ (acetonitrile) $\varepsilon_{323nm} = 2430$ (acetonitrile) $\varepsilon_{341nm} = 4670$ (acetonitrile) $\varepsilon_{356nm} = 9700$ (cyclohexane) $\varepsilon_{357nm} = 6400$ (acetonitrile) $\varepsilon_{357nm} = 6860$ (acetonitrile) $\varepsilon_{376nm} = 6290$ (acetonitrile)	6.5×10^{-6}

Benz[a]anthracene 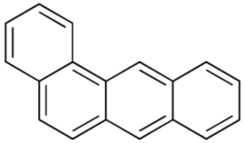	228.3	5.33 5.76	9.4×10^{-3}	0	155-157	$\varepsilon_{286nm} = 83300$ (acetonitrile)	2.1×10^{-7}
Benzo[b]fluoranthene 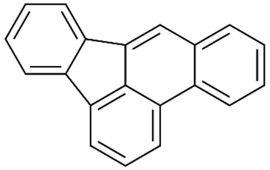	252.3	6.04	1.5×10^{-3} 1.2×10^{-3}	0	168	$\varepsilon_{300nm} = 37100$ (acetonitrile)	5.0×10^{-7}
Benzo[a]pyrene 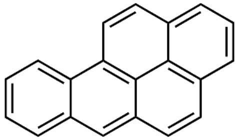	252.3	6.36 6.13	3.8×10^{-3} 2.3×10^{-3}	0	179	$\varepsilon_{364nm} = 24069$ (ethanol) $\varepsilon_{384nm} = 29040$ (ethanol) $\varepsilon_{295nm} = 53500$ (acetonitrile)	5.49×10^{-9}
Chlorpyrifos 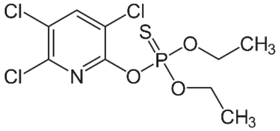	350.6	4.96	1.12	72.7	42	UV maxima at 208, 230, and 290 nm	2.02×10^{-5}

[a] Values for partition coefficient from (Hansch *et al*. 1995; NCBI 2020a; IARC 2005; Stamatelatou *et al*. 2011; de Maagd *et al*. 1998; Bowman and Sans 1983)

[b] Values for solubility in water were collected from (NCBI 2020a; Stamatelatou *et al*. 2011; Speigth 2011; May *et al*. 1978; Mallick 2019; Yap *et al*. 2012; Samuel *et al*. 2010)

[c] Values for polar surface area in water were collected from (NCBI 2020a; 2020b; 2020c; 2020d; 2020e; 2020f)

[d] Values for melting point in water were collected from (IARC 2005; Stamatelatou *et al*. 2011; Speigth 2011; Collin *et al*. 2003; R. Lide 2016)

[e] Values for molar extinction coefficient were collected from (NCBI 2020a; Thomas and Brogat 2017; Castegnaro *et al*. 1983; Lauer 2010)

[f] Values for vapor pressure were collected from (NCBI 2020a; 2020b; 2020c; 2020d; 2020e; 2020f; IARC 2005; Fowler *et al*. 1968)

3.1.2. UV-Vis absorption spectra of the PAHs and chlorpyrifos

Solvents influence the physical-chemical properties of the solutes, therefore, the UV-Vis spectra of some of the pollutant compounds were analyzed in different solvents. The solute-solvent interactions may affect properties of the solute molecules such as geometry, electronic structure, polarity and consequently affect their stability and solubility. Solvent interactions may also change the spectral properties of the solute and consequently cause bathochromic shifts and alter the absorption intensity and shape of the absorption bands of the spectra (Sancho *et al*. 2011; Zheng *et al*. 2018; Gündüz 2013). This is particularly important for PAHs and chlorpyrifos having a low solubility in water and a high logP (Table 3.1).

For this work, it was essential to control the preservation and structure integrity of the organic pollutant solutions during storage, extraction, experimental use, and analysis without changes potentially caused by factors such as the solvent, temperature, or light. Stock solutions degradation must be avoided to guarantee the integrity of the solutions and, consequently, to guarantee the reliability of the results obtained. During the transformation studies, the organic pollutant substances will be present in different media (aqueous/organic) which may interfere with the analytical methods used in this work. Therefore, studying the effect of solvents in the chemical structure of organic pollutants is important to select the appropriate solvent to prepare the pollutant solutions and to determine its influence on the detection techniques for each substance.

UV-Vis spectroscopy was used to investigate the influence of different solvents on the pollutant molecules in the study since PAHs and chlorpyrifos typically absorb radiation in the UV range due to the aromatic ring systems on their structure (Dong *et al*. 2002). Furthermore, UV-Vis spectroscopy is used as a detection method for the transformation studies in the present work. Hence, studying the influence of solvents on the spectra of the pollutant substances provides information about how the analytical methods can be affected by different solvents and help to design appropriate experimental methods.

The absorption spectra of PAHs and chlorpyrifos in acetonitrile and aqueous solutions were recorded and compared (Figure 3.1 to 3.5). The aqueous solutions contained a small amount of acetonitrile (1% v/v) from the compound stock solution.

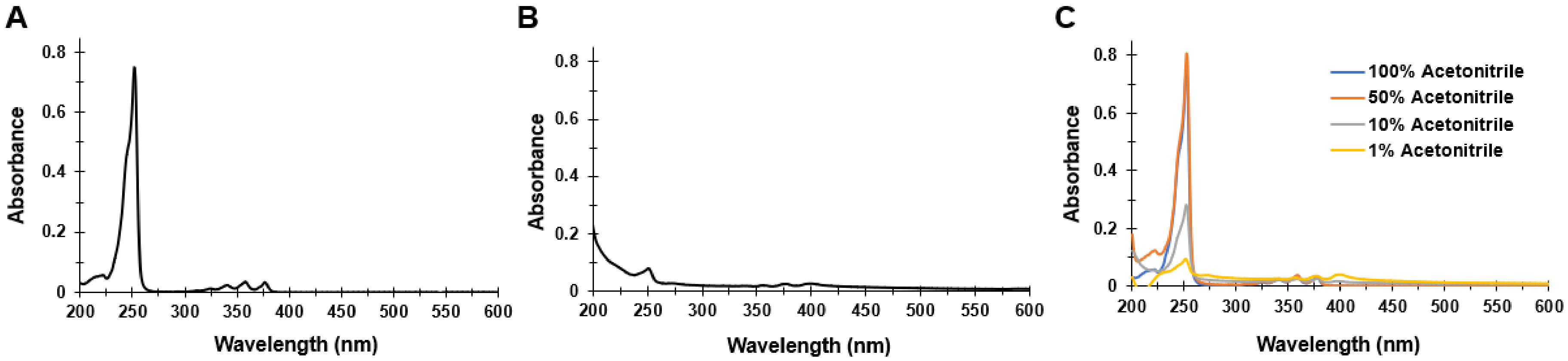

Figure 3.1 – UV-Vis spectra of anthracene (1 mg/L) in (A) acetonitrile; (B) water with 1% (v/v) acetonitrile; and (C) mixtures of acetonitrile:water (% v/v is indicated).

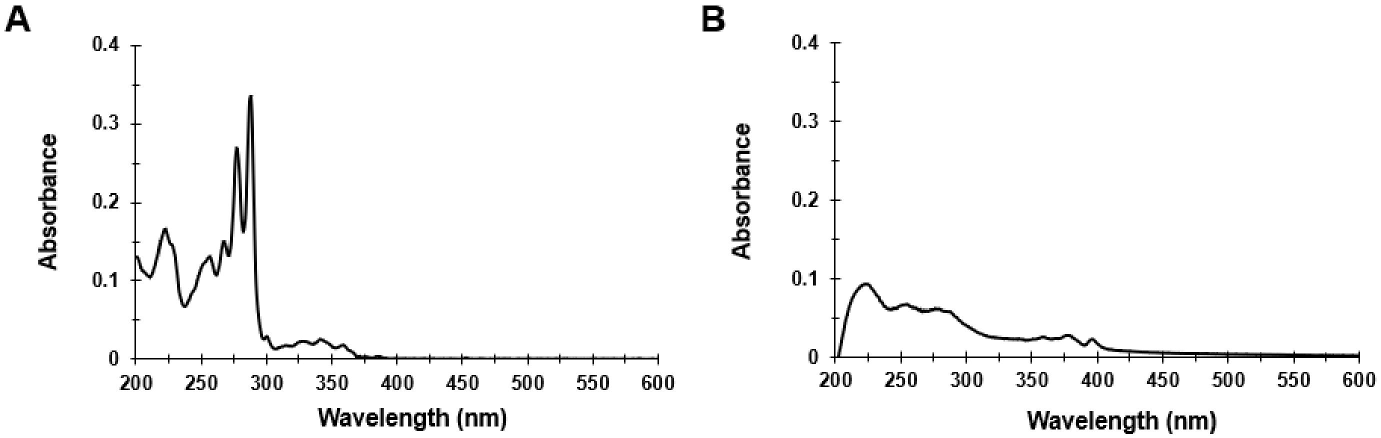

Figure 3.2 – UV-Vis spectra of benz[a]anthracene (1 mg/L) in (A) acetonitrile; (B) water with 1% (v/v) acetonitrile.

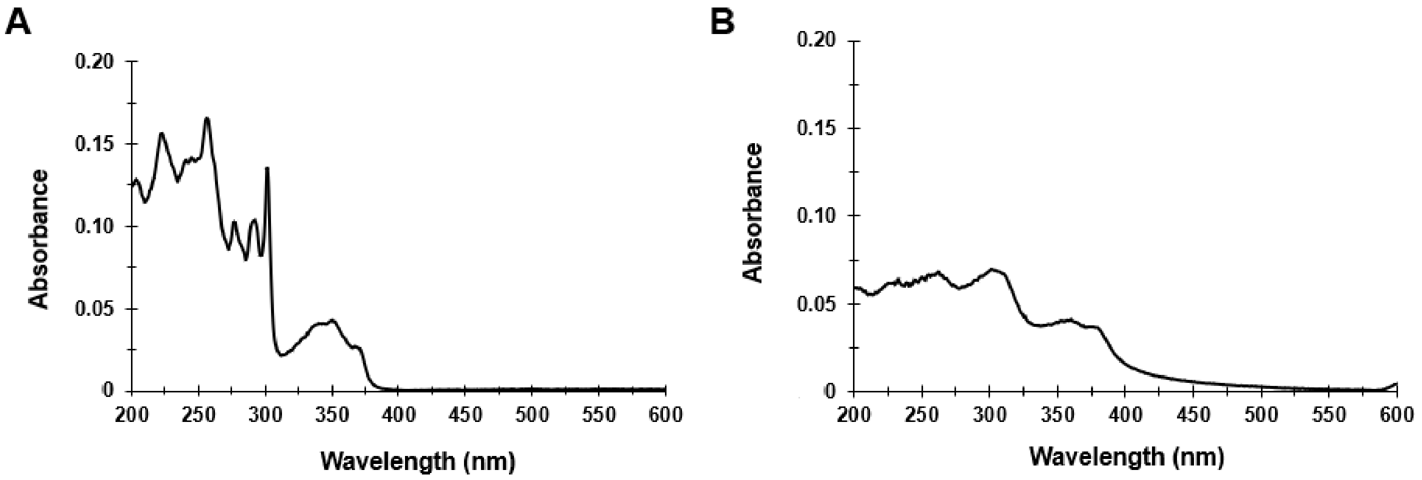

Figure 3.3 – UV-Vis spectra of benzo[b]fluoranthene (1 mg/L) in (A) acetonitrile; (B) water with 1% (v/v) acetonitrile.

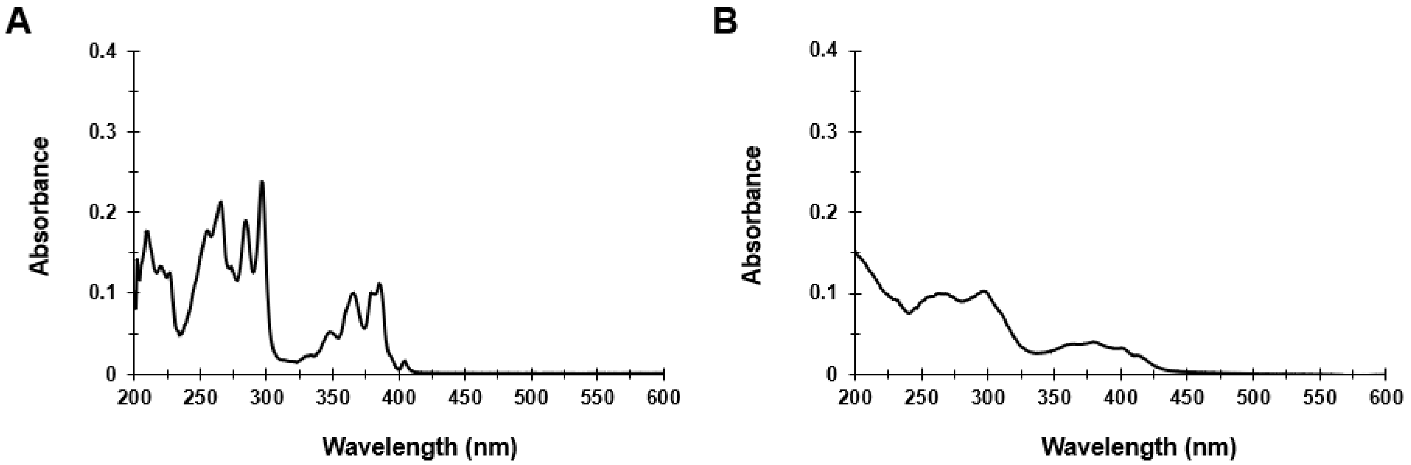

Figure 3.4 – UV-Vis spectra of benzo[a]pyrene (1 mg/L) in (A) acetonitrile; (B) water with 1% (v/v) acetonitrile.

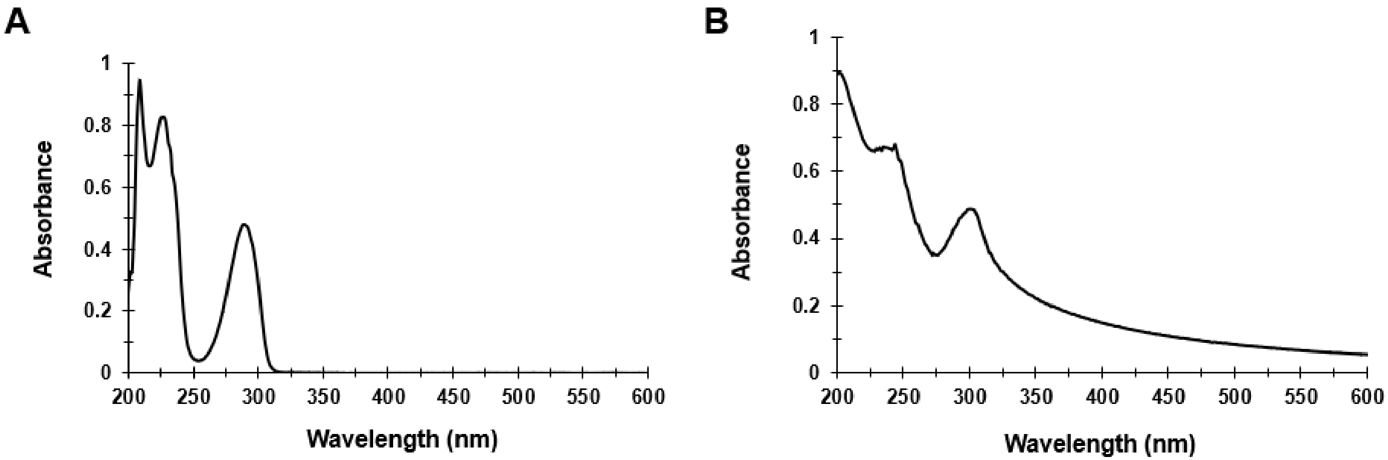

Figure 3.5 – UV-Vis spectra of chlorpyrifos (25 mg/L) in (A) acetonitrile; (B) water with 1%(v/v) acetonitrile.

All 4 PAHs exhibited absorption bands in the 200-450 nm region. The absorption spectrum produced by a 1 mg/L (5.6 µM) anthracene solution in acetonitrile (Figure 3.1.A) exhibits one intense band on the 225-275 nm region and 4 weaker bands on the 300-400 nm region. The spectrum of 1 mg/L (4.4 µM) BaA in acetonitrile (Figure 3.2.A) presents 2 intense absorption bands in the 250-300 nm region and weaker absorption bands in the 300- 370 nm region. The spectrum of 1 mg/L (4.0 µM) BbF in acetonitrile (Figure 3.3.A) presents 5 intense absorption bands on the 200-315 nm region and a weaker absorption band in the 315-380 nm region. The spectrum of 1 mg/L (4.0 µM) BaP in acetonitrile (Figure 3.4.A) presents 3 intense absorption bands on the 250-300 nm region and weaker absorption bands in the 325- 410 nm region. The spectrum of 25 mg/L (7.1 µM) chlorpyrifos in acetonitrile (Figure 3.5.A) presents 2 intense absorption bands on the 200-250 nm region and weaker absorption bands in the 250- 325 nm region. In aqueous solutions (Figure 3.1.B, 3.2.B, 3.3.B, 3.4.B, and 3.5B), the intensity of the absorption bands of all pollutant compounds decreased considerably. The shape of the absorption bands was also changed from separate bands with well-defined peaks to a merge of shoulder-like bands. On this basis, the direct UV monitoring of the PAHs in aqueous media degradation assays does not seem a reliable method, although it would be very practical to follow the enzymatic reactions with these compounds.

The results show that the PAHs in acetonitrile produce absorption spectra with well-defined absorption bands. In water, the spectra obtained show lower absorption intensities, and the shape of the bands is deformed (Thomas and Brogat 2017; Lopes *et al*. 2005; PatenaudeE *et al*. 1962). This effect was greater on the less water-soluble PAHs, such as BbF (Table 3.1 and Figure 3.3). The spectrum of chlorpyrifos showed the least deformation in the shape of the absorption bands and, despite observing an intensity decrease in water, it still presented strong absorbance intensities (Figure 3.5). All concentrations of pollutant compounds used surpassed the water solubility of each substance (Table 3.1) which causes them to aggregate to form more stable conformations (Ma *et al*. 2016; Rapacioli *et al*. 2005; Zheng *et al*. 2018). The chlorpyrifos and the anthracene spectra were the least affected because they have higher water solubility and, therefore, water solutions have more dissolved free molecules of these solutes in comparison to BbF or BaP, which have lower water solubility. Nevertheless, it was evident that increasing proportions of water in acetonitrile mixture solution of anthracene causes a gradual decrease in UV-Vis absorption (Figure 3.1.C).

The spectra of anthracene, BaA, BbF, BaP, and chlorpyrifos in acetonitrile present λmax of absorbance bands at 251 nm, 288 nm, 301 nm, 296 nm, and 209 nm respectively (Figure 3.1.A, 3.2.A, 3.3.A, 3.4.A, 3.5.A), which are in accordance with the reported λmax (Table 3.1). The information obtained on UV absorption maxima of the target pollutants was useful to design the HPLC methods employed in the following degradation studies.

3.1.3. Analytical methods

As indicated previously, MO transformation in the enzymatic assays was followed directly by UV-Vis spectroscopy, making use of a distinct absorption band of the dye. Details on the methods of MO decolorization assays are described in Section 2.6 and discussed in Section 3.3.

Concerning PAHs and chlorpyrifos, these toxicants were analyzed by HPLC, as described in detail in Section 2.7 and resumed in Table 3.2.

Table 3.2 – HPLC parameters used for pollutant analysis. For all the analyses, a C18 column was used in an Agilent 1100 system.

Pollutant	**Mobile phase**	**Flux (mL min^{-1})**	**Wavelength (nm)**
Anthracene and Anthraquinone	Water:acetonitrile 3:17	1.0	251
Benzo[a]pyrene and mixture of PAHs	Water:acetonitrile 3:17	1.0	266
Benzo[b]fluoranthene	Water:acetonitrile 3:17	1.0	256
Chlorpyrifos	Water:acetonitrile 3:17	1.0	225

In order to analyze the pollutant degradation in the enzymatic assays, it was necessary to extract the remaining pollutant and the formed reaction products from the aqueous incubation media to an organic solvent. Hexane was used as extraction solvent and 4 different protocols were initially tested to develop an optimal procedure (protocols A-D in Table 3.3).

Table 3.3 – Optimization of anthracene extraction with hexane. The recovery of 0.3 mg/L anthracene from 1 mL aqueous solutions (100 mM acetate buffer pH 5) achieved with each extraction protocol is presented as Mean ± SE.

Protocol	Number of extraction steps	Stirring time of each step (s)	Hexane volume added in each step (µL)	Anthracene recovery (%)
A	1	600	1000	93.6 ± 1.5
B	2	15	500	93.1 ± 9.8
C	2	30	500	100.7 ± 5.3
D	2	60	500	98.2 ± 4.3

Based on the optimization results, an extraction procedure was established for the following degradation studies: 1 mL of incubation media was extracted with the addition of 500 µL of hexane in two successions with 30 seconds of vigorous stirring (protected from light). The organic phase was collected after each stirring step. This protocol allows a high recovery of anthracene (C in Table 3.3), and it is low time-consuming. The efficiency of this extraction protocol (2 times 30 s) was also assessed with anthraquinone, BaP, and chlorpyrifos at different concentrations and, in some cases, also in the presence of HA (Table 3.4).

The results showed that the extraction procedure afforded a high recovery of the PAHs and chlorpyrifos (approximately 100%) in the different cases, except for anthracene solutions in the presence of a high concentration of HA. The effect of HA in enzymatic degradation of anthracene will be presented in Sections 3.5 and 3.6, and the present data indicates that high concentrations of HA in the media can reduce the recovery of anthracene, but not of anthraquinone (Table 3.4).

Table 3.4 – Efficiency of extraction of target pollutants with the hexane extraction protocol. The recovery of anthracene, anthraquinone, benzo[a]pyrene, and chlorpyrifos from aqueous solutions (acetate buffer 100 mM, pH 5) is presented as Mean ± SE. Recovery of anthracene and anthraquinone was also measured in the presence of humic acid.

Pollutant	Pollutant concentration (mg/L)	Humic acid (mg/L)	Recovery (%)
Anthracene	0.3	0	103.4 ± 6.1
	1	0	96.0 ± 0.4
		250	86.4 ± 7.7
Anthraquinone	0.3	0	98.8 ± 9.4
	1	0	101.5 ± 1.5
		250	109.8 ± 4.9
Benzo[a]pyrene	1	0	103.0 ± 5.2
Chlorpyrifos	0.1	0	99.8 ± 3.1
	0.3		99.5 ± 0.2
	1		111.8 ± 6.0
	25		102.5 ± 4.9

3.2. Activity of laccase and peroxidase-type proteins using ABTS as substrate

As presented in the Introduction, enzymatic remediation technologies applied to organic pollutants are being developed employing mostly oxidoreductase enzymes such as laccase, HRP, and MnP. Since laccase-mediator systems can be very potent in the degradation of PAHs, with the advantage of using molecular O_2 as oxidant, enzymatic studies were initiated with a common laccase and a standard substrate and mediator (ABTS), before investigating less conventional peroxidase-type enzymes.

3.2.1. Activity of laccase using ABTS as substrate

The activity of laccase from *Trametes versicolor* was determined by the ABTS oxidation method described by Attala *et al.* (Atalla *et al*. 2013). This assay is based on the oxidation of ABTS to its more stable state of cation radical ($ABTS^{\bullet+}$). This cation is a blue-green chromophore whose formation can be correlated to enzyme activity and its formation can be easily followed spectrophotometrically.

Figure 3.6 illustrates the spectral changes of laccase-catalyzed oxidation of ABTS to $ABTS^{\bullet+}$ in pH 5.0 acetate buffer. The spectra show absorption bands with maximums at approximately 420, 653, and 735 nm which falls in accordance with previous studies (Potthast *et al*. 2001). It is to be noted that, despite the large alteration in the spectrum of ABTS with oxidation, minor changes were observed in the range 470-490 nm that became useful for the studies with MO in following sections.

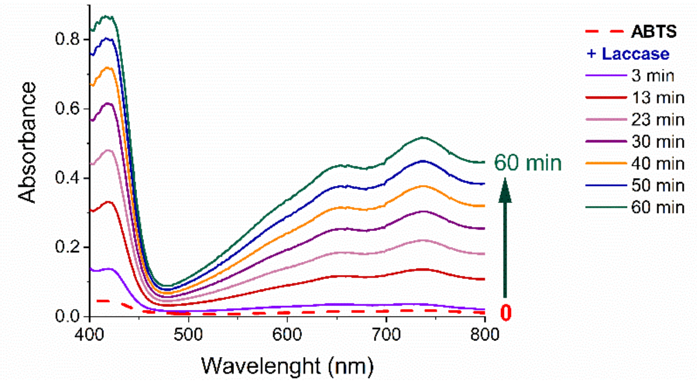

Figure 3.6 – Changes in the UV-Vis spectra of 0.5 mM ABTS during the oxidation catalyzed by laccase (1 µg/mL) in 100 mM acetate buffer pH 5.0, at 25 ºC.

Table 3.5 – Molar extinction coefficients of $ABTS^{\bullet+}$ radical at pH 5.0.

Wavelength (nm)	ε (M^{-1} cm^{-1})	Reference
420	36000	(Shin and Lee 2000)
436	29300	(Kohler *et al*. 2018)
734	12867	(Riedl and Hagerman 2001)

ABTS oxidation is commonly monitored at 420, 436, or 734 nm (Shin and Lee 2000; Kohler *et al*. 2018; Riedl and Hagerman 2001). On this basis, kinetic assays were carried to investigate further the oxidation of ABTS by laccase and determine the specific activity of the enzyme used in the work. For this set of assays, reactional mixtures were prepared with 0.5 mM of ABTS and a suitable amount of laccase in acetate buffer pH 5.0. ABTS oxidation was monitored spectrophotometrically at different wavelengths, and the possible enzyme-independent oxidation was evaluated in blank assays (Figure 3.7). The rate of ABTS oxidation was calculated by determining absorbance increase rates.

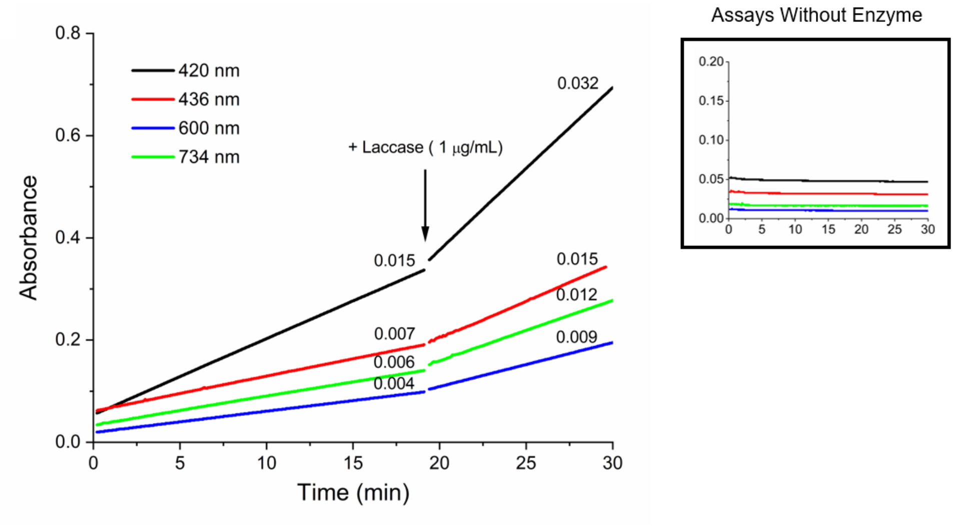

Figure 3.7 – Enzymatic activity of laccase (0.5 μg/mL and 1 μg/mL) with 0.5 mM ABTS measured in 100 mM acetate buffer pH 5.0 and 25 ºC. The oxidation of ABTS was followed at 420 nm, 436 nm, 600 nm, and 734 nm. The observed ΔAbs/Δt (min^{-1}) are indicated for each wavelength after the addition of laccase, first to a final concentration of 0.5 μg/mL and then 1.0 μg/mL to check the response of the assay. Experimental traces from blank assays (ABTS without addition of enzyme) are shown in the lateral graphic.

The results obtained from these assays showed an increase in absorbance at the respective wavelengths indicating the formation of $ABTS^{\bullet+}$. The slopes of the absorbance increase with the different concentrations of laccase have a ratio of approximately 2, at all the wavelengths tested, which is in agreement with the laccase concentration ratio. Furthermore, it indicates that the assays were performed in substrate saturated conditions since the absorbance increase maintained linearity. The absorbance slopes also follow in accordance with the $ABTS^{\bullet+}$ molar extinction coefficients as the biggest slopes correspond to wavelengths with higher molar extinction coefficients of $ABTS^{\bullet+}$ (Figure 3.7 and Table 3.5).

Laccase specific activity was calculated in units per mg of protein by using the data obtained at 420 nm since this wavelength corresponds to the maximum molar extinction coefficient of $ABTS^{\bullet+}$ (Table 3.5) and, therefore, it is more sensitive to ABTS concentration variations. One unit of laccase is defined as the amount of laccase required to oxidize 1 μmol of ABTS substrate per min. The assays at 420 nm, like the one in Figure 3.7, indicated that the laccase used had a specific activity of 0.85 ± 0.04 U/mg (freshly prepared solution), which is similar to the 0.5 U/mg value indicated by the commercial supplier (Table 2.2).

ABTS oxidation by laccase was also followed at 436 nm and 734 nm, as these wavelengths correspond to other absorption bands of $ABTS^{\bullet+}$ (Figure 3.7). Additionally, ABTS oxidation was investigated at 600 nm, having in mind that peroxidase activities have been reported in antioxidant activity studies using this method (Rubio *et al*. 2016; Lagoa *et al*. 2017; Cano *et al*. 2002). This wavelength is used to monitor ABTS oxidation as an alternative to 420 nm and 436 nm since antioxidant heme proteins exhibit a Soret Peak and strongly absorb at these wavelengths. Nevertheless, the present results (Figure 3.6 and 3.7) indicate that 734 nm is a more suitable wavelength to follow ABTS oxidation avoiding the absorption band of the proteins, and this method was used in some assays shown in following sections.

3.2.2. Oxidation of ABTS catalyzed by horseradish peroxidase

HRP is well known to oxidize ABTS in the presence of H_2O_2 and its peroxidase activity was determined using an adapted version of the ABTS oxidation method followed with laccase. Details on the method of ABTS oxidation are described in Section 2.5.1 and information about the peroxidase-type proteins and solutions used can be found in Section 2.2.

The assays of peroxidase activity were carried in acetate buffer containing 0.1 mM of DTPA to avoid ABTS oxidation via Fenton reaction (Buettner 2008). The introduction of H_2O_2 in the reactional media can originate a Fenton or a Fenton-like system with the transition metals dissolved in the water used to prepare buffers (M. Wang *et al*. 2019; Cai *et al*. 2018). Transition metals can activate H_2O_2 and generate hydroxyl radicals which oxidize ABTS and, indeed, in some initial assays it was observed ABTS oxidation in reaction buffer in the absence of enzyme. DTPA is a chelating agent able to bind strongly to di- and trivalent metal cations, forming stable water-soluble metal complexes (Hart 2011; Swati and Hait 2017), reducing the reactivity of the dissolved metal ions present in the water. Therefore, DTPA was routinely included in the reaction buffers used to assay peroxidase activities with ABTS and, in these conditions, no significant enzyme-independent oxidation of the probe was observed. DTPA control assays showed that the presence of DTPA up to 2 mM did not interfere with the peroxidase activity of HRP, hemoglobin, and Cc.

Figure 3.8 shows experimental traces of HRP assays. These were carried with HRP at the concentration of 1×10^{-3} μg/mL, which corresponds to 1.7×10^{-5} μM. The initial concentration of ABTS was 500 μM, identical to the laccase assays, and H_2O_2 was at 100 μM.

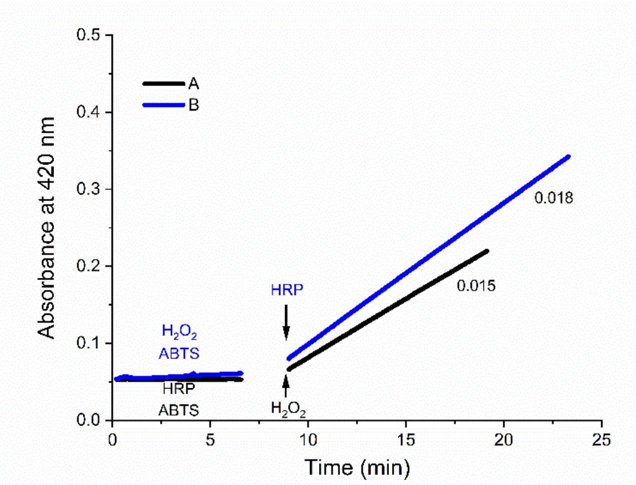

Figure 3.8 – Enzymatic activity of HRP (1×10^{-3} µg/mL) with 100 µM of H_2O_2 and 0.5 mM ABTS measured in 100 mM acetate buffer pH 5.0, at 25 ºC. In the assay A, ABTS was incubated with the enzyme before addition of H_2O_2. In the assay B, ABTS was incubated with H_2O_2 before addition of HRP. The ΔAbs/Δt (min^{-1}) observed in each assay are indicated.

Blank assays performed in buffer containing DTPA, ABTS, and H_2O_2, but in the absence of HRP, showed no changes in absorbance indicating that the uncatalyzed H_2O_2 oxidation of ABTS is negligible in the time period of the assays (results not shown). ABTS oxidation assays with HRP confirmed that the enzyme was unable to oxidize ABTS when in the absence of H_2O_2 as no absorbance increase was detected, indicating that $ABTS^{\bullet+}$ was not being formed (Figure 3.8). When in the presence of H_2O_2, reactional mixtures containing HRP showed an absorbance increase at 420 nm, indicating ABTS oxidation (Figure 3.8). In the presence of 100 µM of H_2O_2, the HRP used showed a specific activity of 465 ± 43 U/mg.

3.2.3. Peroxidase activity of hemoglobin using ABTS as substrate

The peroxidase activity of bovine hemoglobin was also studied using the ABTS oxidation method as for HRP. Figure 3.9 shows experimental traces of the assays carried with 10 µg/mL of hemoglobin.

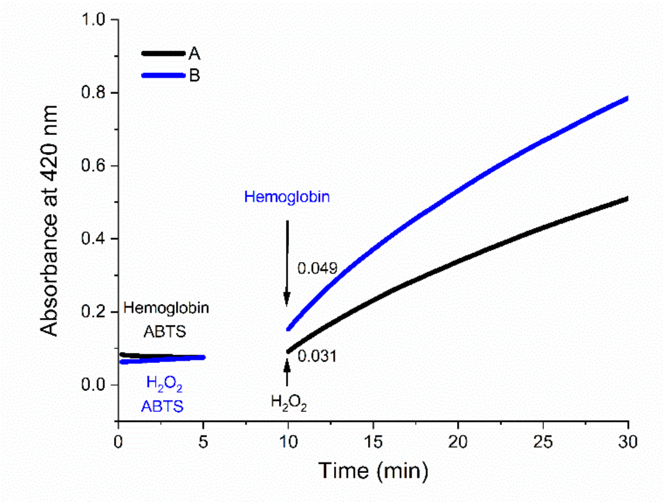

Figure 3.9 – Enzymatic activity of hemoglobin (10 µg/mL) with 100 µM of H_2O_2 and 0.5 mM ABTS measured in 100 mM acetate buffer pH 5.0 and 25 ºC. In the assay A, ABTS was incubated with the protein before addition of H_2O_2. In the assay B, ABTS was incubated with H_2O_2 before addition of hemoglobin. The initial ΔAbs/Δt (min^{-1}) observed in each assay are indicated.

Hemoglobin was unable to oxidize ABTS in the absence of H_2O_2 as it can be seen in Figure 3.9, however, when H_2O_2 was added to the reactional mixtures, an increase of absorbance at 420 nm was observed, indicating ABTS oxidation. However, the rate of ABTS oxidation decreased over time, probably due to inactivation of the protein by H_2O_2. The initial rates of absorbance change, while the absorbance increase was still linear, were used to calculate the specific activity of hemoglobin. In the presence of 100 µM of H_2O_2, the hemoglobin used showed a specific activity of 0.178 ± 0.002 U/mg.

3.2.4. Peroxidase activity of cytochrome c using ABTS as substrate

Cc was previously reported to oxidize ABTS in the presence of H_2O_2 and/or of certain cardiolipin liposomes (Barayeu *et al*. 2019; Radi *et al*. 1991; Lagoa *et al*. 2017). Oxidation of other organic compounds was also reported (Radi *et al*. 1991), as well as of peroxidase activity in immobilized forms of Cc (Deere *et al*. 2003). However, the toxicological implications and biotechnological value of the peroxidase function of Cc are still poorly investigated. The peroxidative activity of horse heart Cc was studied using the ABTS oxidation method in the same conditions as above for HRP and hemoglobin. These assays were carried with Cc at the concentration of 100 µg/mL, which corresponds to 8 µM

(Figure 3.10). In long kinetic assays, such as curve B in Figure 3.10, it was possible to follow increases in absorbance at 420 nm superior to 0.3, which correspond to accumulation of ABTS radical in concentrations above 8 µM, the same Cc concentration in the reaction media. These results indicate that Cc is not participating in the ABTS oxidation reaction as a reagent, but as a catalyst.

Horse heart Cc is a common commercial form of Cc and two preparations were used in this work: Sigma C7752 and C2506. According to the commercial information (Sigma-Aldrich n.d.), C7752 is purified with acetic acid, may have higher contamination by superoxide dismutase and lower proportion of dimeric Cc, whereas C2506 is prepared by harsher trichloroacetic acid treatment that tends to cause dimerization or acid-modified structures of the protein.

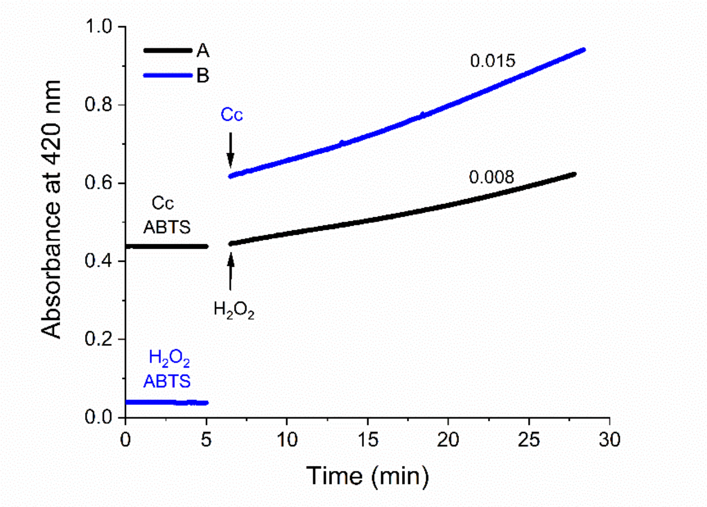

Figure 3.10 – Enzymatic activity of Cc (100 µg/mL) with 100 µM of H_2O_2 and 0.5 mM ABTS measured in 100 mM acetate buffer pH 5.0 and 25 ºC. This assay was carried with Sigma C7752 product of Cc. In the assay A, ABTS was incubated with the protein before addition of H_2O_2. In the assay B, ABTS was incubated with H_2O_2 before addition of Cc. The ΔAbs/Δt (min^{-1}) observed in each assay are indicated.

The Cc assays in the absence of H_2O_2 did not register absorbance increase, indicating that Cc was unable to oxidize ABTS however, absorbance increases were registered after the addition of H_2O_2 to the reactional mixture (Figure 3.10). Like in HRP and hemoglobin assays, it was verified that the observed ABTS oxidation was due to enzymatic activity and not direct ABTS oxidation by H_2O_2 since no absorbance increase was observed in the absence of Cc (Figure 3.10).

These studies with Sigma C7752 indicated that, in the presence of 100 µM of H_2O_2, this Cc has a specific activity of 8 ± 1 mU/mg. However, the ABTS oxidation rate of Cc is dependent on H_2O_2 concentration on the medium, as it can be seen in the results displayed in Figure 3.11. These results indicate that higher peroxidase activities can be reached by using higher concentrations of H_2O_2, which can be interesting for biotechnological applications, but a 100 µM concentration was maintained in the continuing work with peroxidases for its toxicological relevance and to avoid protein inactivation as observed with hemoglobin. ABTS oxidation assays were also carried with the other form of Cc, Sigma C2506, and similar results were observed (assays not shown). Although this form of Cc might have more dimeric and unfolded proteins, the peroxidase-like activity (9 ± 1 mU/mg) was not significantly different from the Sigma C7752.

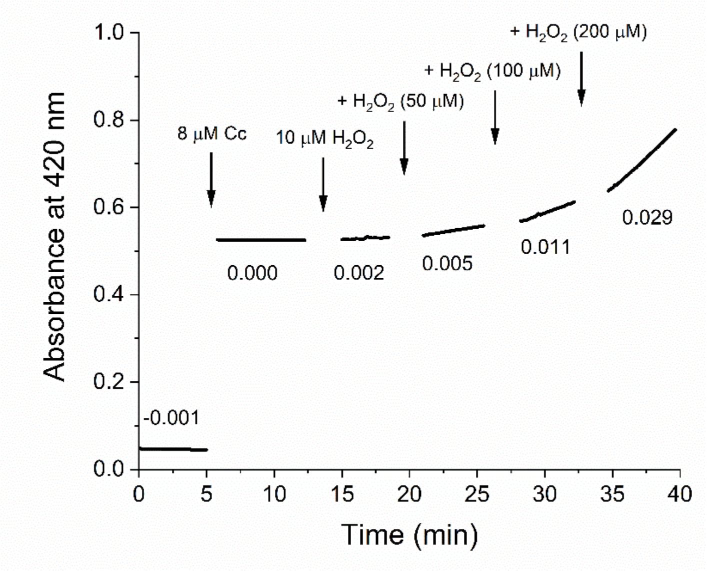

Figure 3.11 – Effect of H_2O_2 concentration on the enzymatic activity of Cc measured in 100 mM acetate buffer pH 5.0 and 25 ºC. Enzymatic reaction was initiated with the addition of 100 µM of H_2O_2. Reactional mixture contained Cc (100 µg/mL), 0.5 mM ABTS and H_2O_2 concentrations ranging between 10 µM and 200 µM. The assay was carried with Sigma C7752 product of Cc. The ΔAbs/Δt (min^{-1}) observed after each addition of H_2O_2 are indicated.

3.2.5. Comparison of ABTS oxidation efficiencies of the enzymes and enzyme-like proteins at different pH

Table 3.6 summarizes the ABTS oxidation rates catalyzed by the enzymes and enzyme-like proteins studied in this work, all at pH 5 and other comparable conditions. At pH 5.0, HRP showed a much higher specific activity and Cc seems a less efficient catalyst, both on a molar and mass basis. Although the results in the previous section indicate that by increasing the concentration of H_2O_2 it is still possible to augment the catalytic capacity of Cc, it is unlikely to reach the efficiency of HRP or laccase (at pH 5). Laccase presented an intermediate activity in catalyzing ABTS oxidation, with the advantage of reducing atmospheric oxygen and not requiring H_2O_2 as oxidizing agent.

Table 3.6 – Comparison of the specific ABTS oxidizing activity of laccase, HRP, hemoglobin, and Cc measured in 100 mM acetate buffer pH 5.0 at 25 ºC. Two commercial forms of Cc were studied.

Protein	Laccase	Horseradish Peroxidase	Hemoglobin	Cytochrome *c* (C7752)	Cytochrome *c* (C2506)
Assay conditions	500 µM ABTS 3.8×10^{-4} µM Laccase (1 µg/mL)	500 µM ABTS 100 µM H_2O_2 1.7×10^{-5} µM HRP (1×10^{-3} µg/mL)	500 µM ABTS 100 µM H_2O_2 Hemoglobin 10 µg/mL	500 µM ABTS 100 µM H_2O_2 8 µM Cc (100 µg/mL)	500 µM ABTS 100 µM H_2O_2 8 µM Cc (100 µg/mL)
Specific Activity (U/mg of solid)	0.85 ± 0.04	465 ± 43	0.178 ± 0.002	0.008 ± 0.001	0.009 ± 0.001

To determine the effect of pH on the enzymatic activity of the proteins under study, ABTS oxidation assays were performed at pHs ranging between 5.0 and 8.0. Assays were carried in the same way for laccase and for HRP and Cc in the presence of H_2O_2, following the ABTS oxidation methods described in Section 2.5.3. Hemoglobin was not included in this set of assays because the gradual inactivation observed previously (Figure 3.9) would limit the analysis of the effect of pH.

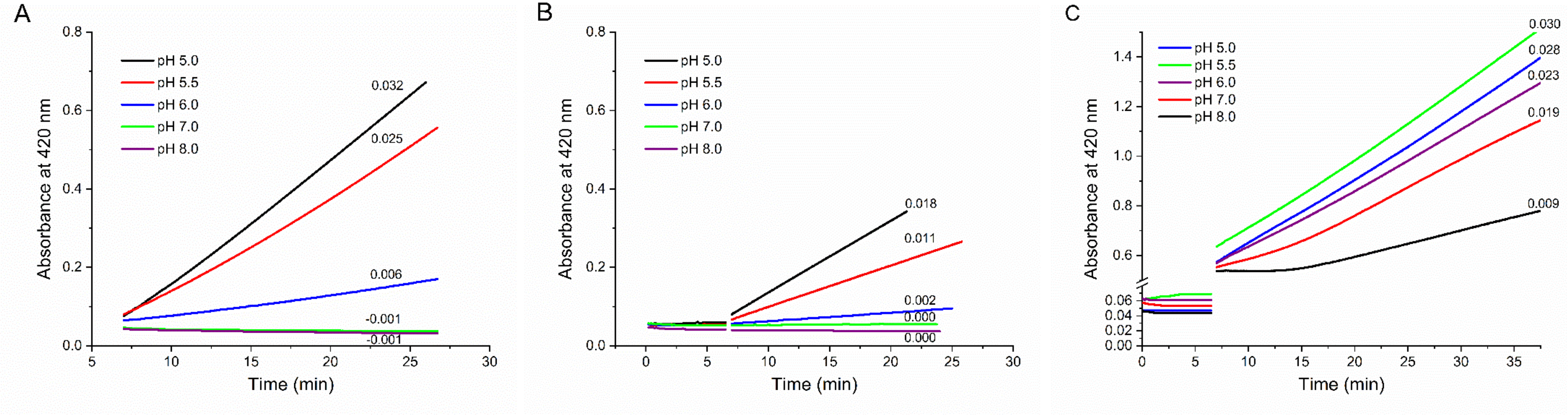

Figure 3.12 – Effect of pH in enzymatic activity of (A) laccase (1 µg/mL), (B) HRP (1 × 10^{-3} µg/mL) with 100 µM of H_2O_2 and (C) Cc (100 µg/mL) with 100 µM of H_2O_2, using 0.5 mM ABTS as substrate. Reactional mixtures were prepared in 100 mM acetate buffer pH 5.0 or 5.5, or 100 mM phosphate buffer pH 6.0, 7.0 or 8.0. In all the assays, the reaction was triggered by addition of the protein, and the ABTS oxidation was monitored at 420 nm. Sigma C7752 Cc was used in these assays.

The results in Figure 3.12 show that laccase, in the pH range studied, exhibits higher activity at the more acid conditions. At pH 7.0 and 8.0 no ABTS oxidation was detected, indicating that laccase loses enzymatic activity at these pH values (Figure 3.12.A), in good agreement with the reported in the bibliography (Yaropolov *et al*. 1994; More *et al*. 2011). The results with HRP (Figure 3.12.B) are similar to the ones obtained with laccase. Higher absorbance increase rates were observed at lower pH values and no absorbance increase was detected at pH 7.0 and 8.0. For these latter pHs, a phosphate buffer was used instead of the acetate buffer used for pH 5.0 and 5.5, but a phosphate buffer was also used for pH 6.0 and enzymatic activity was detected in this condition, in good accordance with a gradual activity decrease from acid to neutral conditions irrespective of the different buffers used (Figure 3.13).

In the kinetic assays of Cc, it was observed ABTS oxidation at all the pHs studied (Figure 3.12.C). Higher ABTS oxidation rates were registered at the slight acid conditions (pH 5.0 to 6.0) followed by pH 7.0 and pH 8.0 (Figures 3.12.C and 3.13). The lowest activity of Cc was detected at pH 8.0, which not only exhibited a slower ABTS oxidation rate but also was unable to oxidize ABTS immediately (Figure 3.12.C). Indeed, the activation of the peroxidase-like activity of Cc (in the presence of H_2O_2) is also apparent in the experimental traces in Figure 3.10 and was registered previously in other conditions (Lagoa *et al*. 2017; Radi *et al*. 1991; Barayeu *et al*. 2019). Therefore, the assays at different pH in Figure 3.12.C were extended for a longer time, confirming the occurrence of an activation phase taking some minutes and more obvious at pH 7.0 and 8.0.

Since the ABTS oxidizing activity of Cc is less characterized in the bibliography, in comparison to HRP or hemoglobin, the assays at different pH were performed in triplicate for a more complete study and confirmation of the Cc activity at pH 7-8. The pH dependences of the proteins under study summarized in Figure 3.13 evidence the advantage of Cc at neutral pHs.

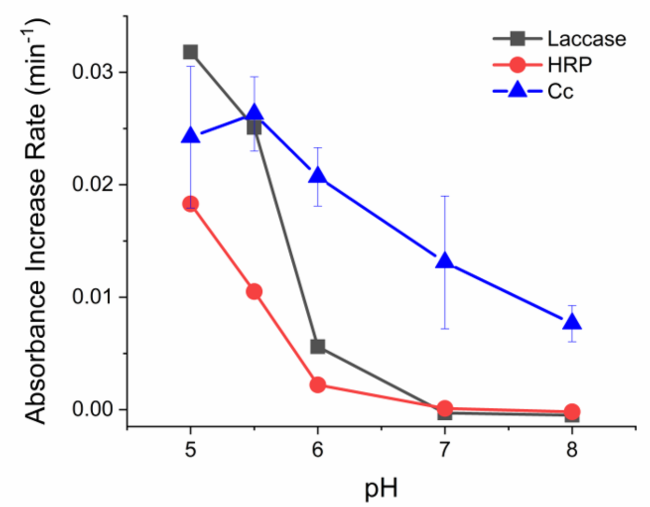

Figure 3.13 – Comparison of the ABTS oxidation rate catalyzed by laccase, HRP, and Cc at different pH. Assays were carried with ABTS initial concentration 0.5mM, at 25 ºC. Acetate buffer (100 mM) was used for pH 5.0 and 5.5, while phosphate buffer (100 mM) was used for pH 6.0, 7.0, and 8.0. Enzymatic assays were performed using a final concentration of 1 µg/mL of laccase, 1 × 10^{-3} µg/mL of HRP, or 100 µg/mL of Cc in the presence of 100 µM of H_2O_2. The measurements with Cc (Sigma C7752) were triplicated and the mean ± SE is represented.

3.3. Studies of methyl orange decolorization by laccase

In order to increase laccase activity and pollutant degradation potential, this work investigated the effect of a mediator in laccase catalytic systems. For this study, the azo dye MO was used as a representative organic test pollutant to evaluate the effect of different reactional conditions (Ambatkar and Mukundan 2015). The ability of ABTS to behave as a laccase mediator has been studied and reported in other studies, thus being selected for this work (Alcalde 2007; Morozova *et al*. 2007). It should be noted that the addition of such synthetic mediators to the remediation processes raises toxicity concerns and increases the cost (Cañas and Camarero 2010), so it is important to be optimized.

MO transformation was monitored spectrophotometrically at 477 nm, which corresponds to a wavelength that MO strongly absorbs (Figure 3.14) due to a band caused by the n–π* transition of its azo bond (Hou *et al*. 2007; Fan *et al*. 2009). Furthermore, laccase, acetate buffer, copper, and ABTS do not absorb significantly at this wavelength, including the ABTS radical (Figure 3.6), thus not interfering with the analytical method for MO. Since the oxidation mechanism of MO by laccase occurs at the diazo bond level, the decrease of absorption at 477 nm is correlated with the degradation of MO and consequently, with the laccase activity as well (Hou *et al*. 2007; Fan *et al*. 2009).

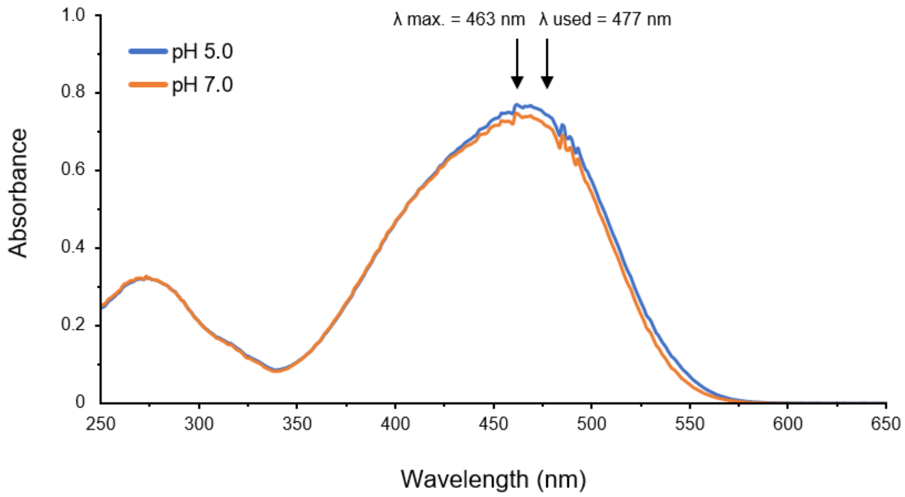

Figure 3.14 – UV-Vis spectrum of 10 mg/L (30.6 µM) of methyl orange at pH 5.0 in acetate buffer (100 mM) and at pH 7.0 in phosphate buffer (100 mM) at 25 ºC. At the wavelength used to monitor the decolorization in this work (477 nm), methyl orange shows an absorbance close to that at the maximum (463 nm).

3.3.1. Methyl orange decolorization by laccase alone and with ABTS mediation

The laccase-catalyzed MO decolorization was assayed in the absence and in the presence of ABTS to determine the capacity of laccase alone to degrade MO and if the presence of ABTS affects the decolorization rate. These assays were carried with a concentration of laccase of 100 µg/mL, which corresponds to 85 mU/mL based on the ABTS oxidizing activity calculated in the previous section.

Incubation of MO with laccase in the absence of mediators demonstrated a decrease of the dye characteristic absorbance, indicating the transformation of the dye catalyzed by the enzyme. However, the rate of transformation was very slow (Figure 3.15). In the presence of ABTS, it was observed that the decolorization rate greatly increased, responding to micromolar ABTS concentrations (Figure 3.15). Blank assays in identical conditions, but without laccase, confirmed that MO, even in the presence of a high concentration of ABTS (50 µM), is stable for time periods longer than the enzymatic decolorization assays and no significant enzyme-independent reaction was observed (results not shown).

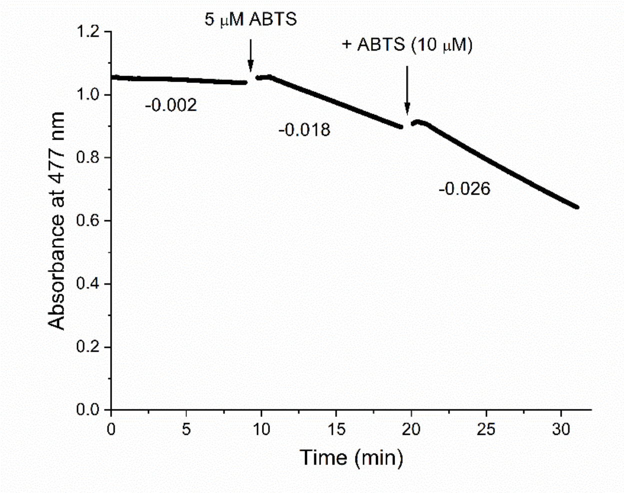

Figure 3.15 – Representative assay of methyl orange decolorization by laccase and the effect of ABTS. The absorbance of methyl orange, initial concentration 10 mg/L (30.6 µM), in 100 mM acetate buffer pH 5.0, was followed at 477 nm, at 25 ºC. The concentration of the enzyme was 100 µg/mL. The decolorization rates in ΔAbs/Δt (min^{-1}) are indicated for each reactional condition, in the absence and after additions of ABTS to reach a final concentration of 5 and 10 µM.

The influence of ABTS concentration on the laccase-catalyzed transformation of MO was studied in more detail, varying the ABTS concentration between 0 µM and 10 µM. The results plotted in Figure 3.16 demonstrate an increase in MO decolorization at all ABTS concentrations studied, more evidently at the higher concentrations of ABTS. These observations are in agreement with previous studies that investigated the ability of ABTS to enhance laccase activity in dyes decolorization

(Kagalkar *et al*. 2015; Almansa *et al*. 2004). It was observed an increase in MO decolorization of approximately 1100% with 10 µM of ABTS when compared to the decolorization rate in the absence of ABTS. These results confirmed that ABTS acts as a laccase mediator, greatly increasing the capacity of the enzyme to degrade organic pollutants, and pointed us the use of low micromolar concentrations is enough for significant effects.

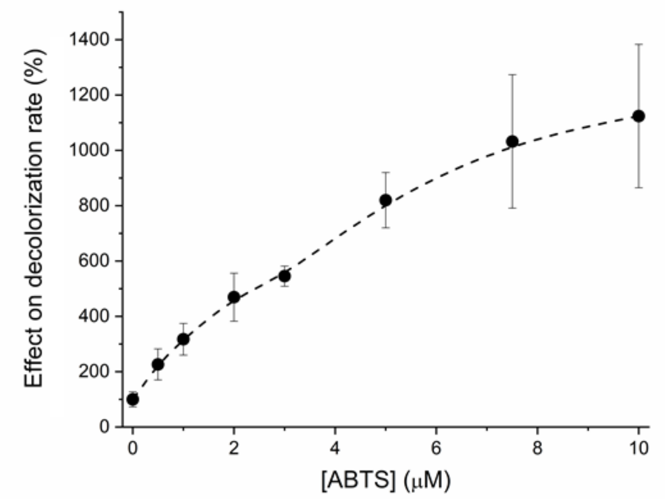

Figure 3.16 – Effect of ABTS on laccase-catalyzed decolorization of methyl orange. Assay conditions indicated in Figure 3.15 caption. The decolorization rates in the presence of ABTS were normalized to the rate observed in the corresponding control in the absence of ABTS, which was taken as 100%. The control decolorization rates in $\Delta Abs/\Delta t$ (min^{-1}) in absence of ABTS were -0.002 ± 0.001 min^{-1}.

3.3.2. Influence of metal ions in laccase-ABTS system

Metal cations such as Fe^{3+}, Cu^{2+}, and Ca^{2+} are present in media relevant for laccase applications, like industrial wastewaters (Varma and Misra 2018; Agrawal *et al*. 2009). Transition metal ions such as copper and iron are redox active and can behave as electron carriers as they can donate and accept electrons, mediating electron transfer processes. This ability allows these ions to participate in oxidation-reduction reactions which can be observed in a wide variety of fundamental biologic reactions (Vuorilehto 2008; Zhu *et al*. 2016; Xu *et al*. 2013; Yashnik *et al*. 2005; Dev and Babitt 2017). In addition, it should be remembered that copper is essential at the catalytic center of laccases (Janusz *et al*. 2020; Alcalde 2007; Morozova *et al*. 2007) (Figure 1.3). Therefore, these metal cations may produce some effect on the catalytic efficiency of the laccase-ABTS system.

It was investigated how the laccase-catalyzed MO decolorization mediated by ABTS was influenced by the presence of Fe^{3+}, Cu^{2+}, and Ca^{2+}. Enzymatic MO decolorization assays were performed with MO (10 mg/L), laccase (85 mU/mL), and 5 µM of ABTS in different reactional conditions varying metallic cation concentrations between 1 µM and 1 mM. Iron absorbs radiation at the wavelength used (477 nm), but the absorbance of the metal ions at the low concentrations that were studied did not interfere substantially with MO absorbance (Figure 3.17.A). The effect of each metal concentration was determined by comparing the dye absorbance decrease rates before and after the addition of the metal ions (Figure 3.17). The ABTS concentration was chosen to be 5 µM because it is enough to observe a substantial transformation rate, while simultaneously not excessively enhancing MO decolorization by laccase that could deplete the available MO in a short time of the assay.

The assays showed that Fe^{3+} and Cu^{2+} caused a decrease in the rate of MO decolorization by the laccase-ABTS system, more evident at the higher concentrations (Figure 3.17). The pH of the reactional mixtures was checked and no significant changes were observed, indicating that the effects of the metal ions in laccase-ABTS system activity were not due to pH changes. In the case of iron, as represented in Figure 3.18, some effect on the reaction rates was noticed also with low micromolar concentrations (experimental traces not shown). However, none of these metal cations seem strong antagonists of the laccase-ABTS system, because even the higher concentrations (1 mM) did not cause decreases of the reaction rates greater than 50% (Figure 3.18). Previous studies on the effect of iron and copper in laccase activity have reported similar observations. Murugesan *et al.* (2009) have demonstrated that the presence of heavy metal ions, including Fe^{3+} and Cu^{2+}, inhibit the decolorization of Remazol dyes by laccase (Murugesan *et al*. 2009). No significant effect was observed in the MO decolorization rate after Ca^{2+} addition (Figure 3.17.C and 3.18), suggesting that Ca^{2+} does not influence laccase activity at the concentrations studied. These results are similar to those reported by Zhou *et al*. (2017) about laccase catalyzed dye decolorization not being significantly affected by Ca^{2+} up to 10 mM (Zhou *et al*. 2017). In the study by Murugesan *et al.* (2009), calcium was also one of the metal ions showing less effect on the laccase system (Murugesan *et al*. 2009).

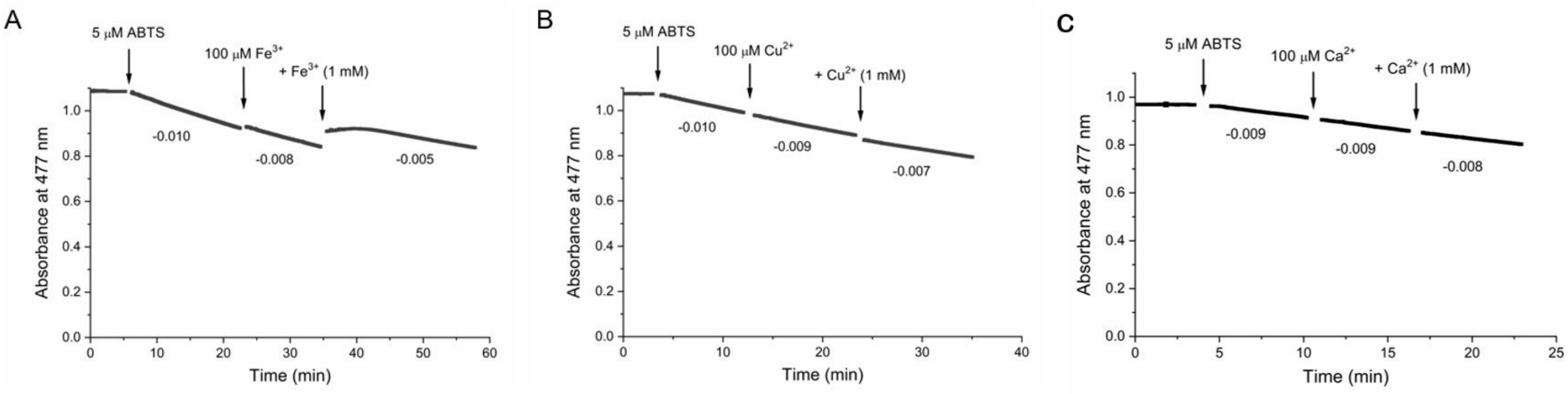

Figure 3.17 – Assays of methyl orange decolorization by laccase and 5 µM ABTS in the presence of 0.1- and 1-mM concentrations of (A) Fe^{3+}, (B) $Cu^{2+}$and (C) Ca^{2+} ions. Methyl orange decolorization in 100 mM acetate buffer pH 5.0 was monitored at 477 nm, at 25 ºC. The dye initial concentration was 10 mg/L (30.6 µM) and the enzyme concentration was 100 µg/mL. The decolorization rates in ΔAbs/Δt (min^{-1}) are indicated for each reactional condition.

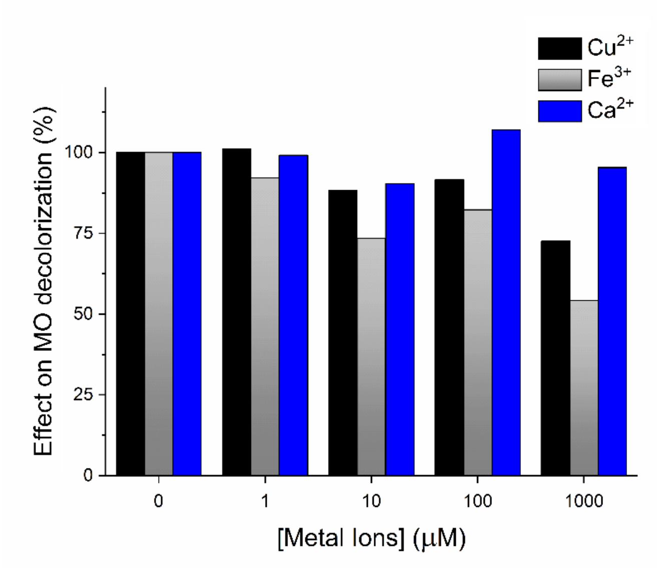

Figure 3.18 – Effect of Fe^{3+}, Cu^{2+}, and Ca^{2+} ions on methyl orange decolorization rate by laccase-ABTS system. Assay conditions indicated in Figure 3.17 caption. The decolorization rates in the presence of the metal cations were normalized to the rate observed in the corresponding control in the absence of the metal, which was taken as 100%. The control decolorization rates in $\Delta Abs/\Delta t$ (min^{-1}) in absence of added metal cations were -0.010 ± 0.003 min^{-1}.

3.4. Studies of anthracene degradation by laccase

The ability of laccase to degrade more recalcitrant POPs was investigated using anthracene as a model compound of PAHs. Previous studies have pointed that laccase alone can oxidize anthracene, converting it mostly into 9,10-anthraquinone and anthrone (Ike *et al*. 2019), but the rate of this catalyzed reaction is not satisfactory enough for applications in remediation processes.

However, combining laccase with redox mediators can enhance laccase activity by overcoming potential limitations described previously in the Introduction. It was clear from the MO degradation studies (Section 3.3) that ABTS acts as a mediator and greatly enhances the laccase-catalyzed transformation of MO. In addition, ABTS has already been reported to considerably enhance anthracene transformation by laccase (Alcalde *et al*. 2002; Johannes *et al*. 1996; Cañas *et al*. 2007) indicating that it can be used to form enzymatic degradation systems. However, the influence of low mediator concentrations has not been described and, as indicated before, optimization of conditions is important for safe and cost-effective processes. Following the studies with MO, different concentrations of ABTS were investigated to understand the effect in anthracene degradation and to determine a suitable concentration that can provide a system with a satisfying efficiency (Figure 3.19).

Anthracene transformation by laccase activity was studied through incubation assays with laccase in the presence of different concentrations of ABTS. As in the MO degradation studies, laccase was used at a concentration of 100 μg/mL (85 mU/mL ABTS oxidizing activity), but the interval of ABTS concentrations tested was widened up to 50 µM. Laccase incubation assays were performed, extracted, and analyzed as described in Section 2.7.1.

The assays without ABTS (Figure 3.19 and 3.20) indicated that laccase alone was unable to transform anthracene significantly, as in these assays it was not observed the formation of degradation products and there was no significant anthracene signal decrease. The results obtained in the assays containing the redox mediator ABTS showed that anthracene degradation increases with the presence of higher ABTS concentration studied, confirming that ABTS acts as a redox mediator in laccase activity in anthracene degradation. The incubation assays with 50 µM of ABTS yielded an anthracene conversion greater than 60% (Figure 3.19). Control assays with anthracene in the presence of ABTS, but without laccase, did not show anthracene degradation, discarding the hypothesis of direct reaction between ABTS and anthracene. It is possible that higher anthracene degradation percentages can be achieved by using ABTS concentrations superior to 50 µM, however, the reactional condition containing this concentration already offers anthracene degradation percentages satisfactory enough for further studies of the laccase-ABTS system.

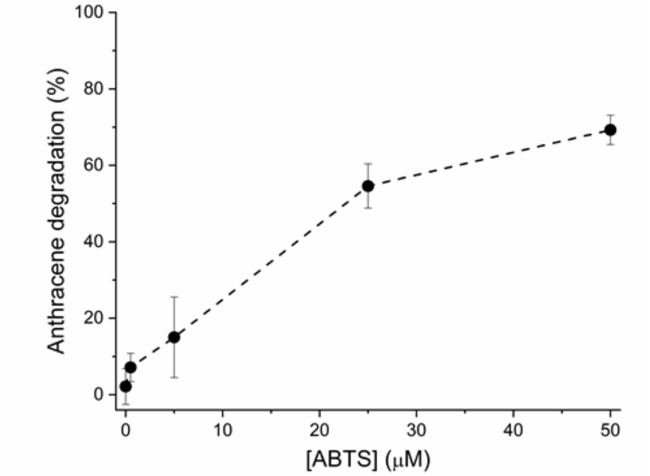

Figure 3.19 – Effect of ABTS on laccase-catalyzed degradation of anthracene. Assays were carried with an anthracene initial concentration of 1 mg/L (5.6 µM) and laccase 100 µg/mL. Incubation assays were carried in 100 mM acetate buffer pH 5.0, in the absence of light, at 20 ºC. After 24 h incubation, the remaining anthracene concentration in the presence of ABTS was compared to the control without enzyme, which was taken as 0% degradation. Results from duplicate assays are shown as Mean ± SE.

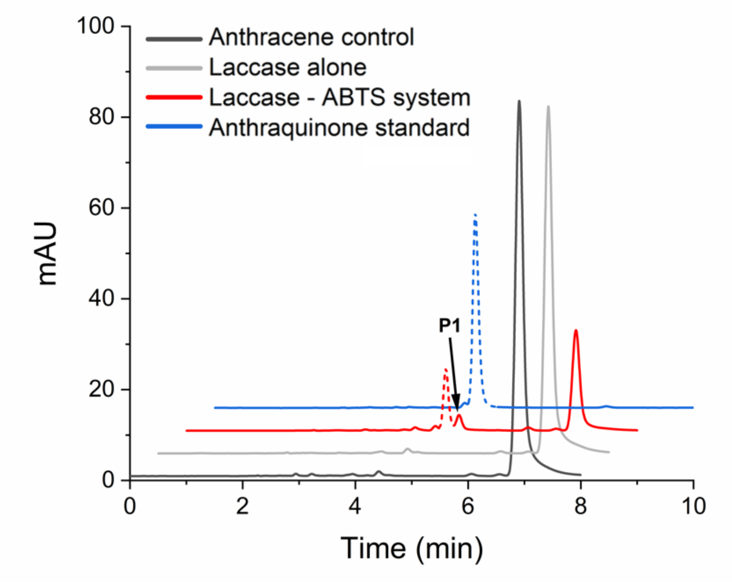

Figure 3.20 – HPLC chromatograms of anthracene and degradation products generated by the laccase-ABTS system. Chromatograms are shown for an anthracene (1 mg/L) control incubation in the absence of enzyme, and anthracene after 24 h incubation with laccase (100 µg/mL) without and with ABTS 50 µM. A chromatogram of an anthraquinone (1 mg/L) standard is also shown, and anthraquinone peaks (t_R=4.5min) are highlighted by dashed lines. The unidentified oxidation product P1 (t_R=4.8min) is indicated in the red chromatogram. Incubation assays were carried in 100 mM acetate buffer pH 5.0, in the absence of light, at 20 ºC. The chromatograms are displaced in the vertical and horizontal axis for better observation. The chromatograms shown are representative results of at least triplicate assays for each reaction condition.

HPLC chromatograms of the incubation assays showed the presence of a very small peak at 4.3 minutes (Figure 3.20) however, this peak was also observed in chromatograms of control assays and blank chromatograms with hexane without anthracene (not shown). This peak did not interfere significantly in the analysis of the reaction products of anthracene incubation assays.

The peak at 4.5 minutes present in the HPLC chromatograms of the incubation assays evidenced the presence of another chemical substance which was identified as 9,10-anthraquinone since its peak presented the same t_R (retention time) of a standard anthraquinone sample (Figure 3.20). The amount of anthraquinone produced by the laccase-ABTS system was quantified (Figure 3.21) and, as expected, it increased with higher ABTS concentrations and anthracene degradation.

It should be noted that an additional degradation product was observed at the end of every incubation assay of anthracene with laccase and ABTS (Figure 3.20 and 3.21). This reaction product appeared at the chromatograms approximately 15 s after the anthraquinone peak and it was not identified (P1). The anthracene degradation pathway is not yet fully established, however, previous studies have pointed out the formation of intermediates for the anthraquinone formation (Gemma Eibes et al. 2006; Ahmed et al. 2012). In anthracene degradation studies conducted by Ye *et al.* (2011), in addition to 9, 10-anthraquinone, it was detected the simultaneous formation of other metabolites such as anthrone (Ye *et al*. 2011). Other studies have suggested that anthrone is an intermediate on the anthracene degradation pathway to form anthraquinone (Wu *et al*. 2010; Ike *et al*. 2019). However, other anthracene degradation pathways have been proposed suggesting that anthracene is first oxidized in 9, 10-anthracenediol that, posteriorly, is oxidized to anthraquinone (Swaathy *et al*. 2014; Moody *et al*. 2001). Studies of anthracene degradation by bacteria have observed the presence of 9, 10-anthracenediol and anthraquinone which might indicate that 9, 10-anthracenediol is an intermediate of the formation of anthraquinone or produced by further enzymes (Bibi *et al*. 2018; Swaathy *et al*. 2014). Additionally, biodegradation studies of anthracene conducted by Ahmed *et al.* (2012), have detected the presence of both anthrone and 9, 10-anthracenediol simultaneously in the extract of biodegradation products (Ahmed *et al*. 2012). Anthrone and 9, 10-anthracenediol have logP (octanol/water partition coefficient) equal to 3.7 both, and molecular weights 194.23 g/mol and 210.23 g/mol, respectively. Therefore, it is possible that both anthrone and 9, 10-anthracenediol are being formed simultaneously and the HPLC peaks of each substance possess very similar t_Rs and overlap each other, appearing as only one peak in the chromatograms obtained. In reverse-phase HPLC, peaks with higher t_R correspond to lower polarity substances. The logP of anthrone and 9, 10-anthracenediol is slightly higher than the logP of anthraquinone (3.4), hence they are slightly less polar. Since P1 has a slightly higher t_R than the peak corresponding to anthraquinone (Figure 3.20), it is possible that P1 corresponds to anthrone or 9, 10-anthracenediol.

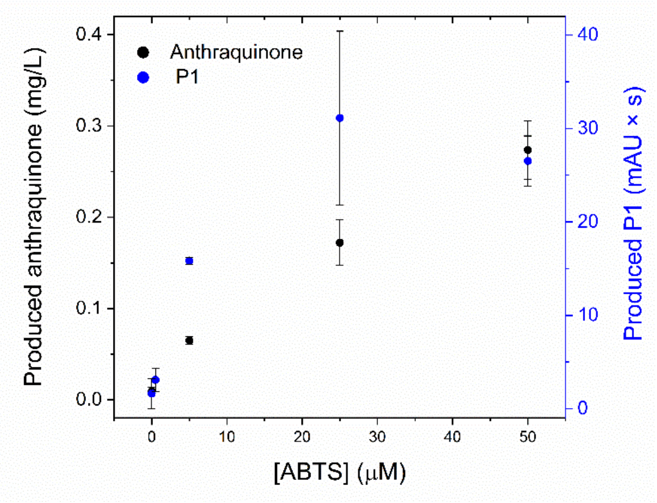

Figure 3.21 – Effect of ABTS on anthraquinone and P1 formation during laccase-catalyzed degradation of anthracene. Assay conditions indicated in Figure 3.19 caption. Results from triplicate assays are shown as Mean ± SE.

It is interesting to note that the anthraquinone measured at the end of the degradation assays does not completely match with the amount of anthracene degraded. As studied in Section 3.1, the hexane extraction method applied at the end of the incubations achieved recoveries of anthracene and anthraquinone from the assay media close to 100%. However, the extracts of the incubation assays with 50 µM of ABTS had an anthraquinone concentration of 1.31 µM (Figure 3.21), which corresponds to approximately 23% of initial anthracene, and approximately 56% of the total degraded anthracene registered. Studies conducted by Eibes *et al.* (2005), observed a 1:2 ratio of degraded anthracene and formed anthraquinone, similarly to the results obtained in the present work, and pointed out the formation of intermediates to account for the remaining degraded anthracene (G. Eibes et al. 2005). Part of the remaining 44% of the degraded anthracene registered on these assays might be attributed to the formation of P1, the potential intermediate of the formation of anthraquinone from anthracene however, it is unlikely that the registered P1 alone corresponds to all the unaccounted degraded anthracene. Anthracene can also be transformed into alcohol derivatives such as anthracenols and anthracenediols (Moody *et al*. 2001; Ahmed *et al*. 2012; Van Herwijnen *et al*. 2003). Anthraquinone has a lower logP than anthracenols (4.2) and similar values to the ones of anthracenediols (3.7), therefore, both substances should also be able to be extracted and identified by HPLC however, no new peaks that may correspond to these substances appear in the chromatograms obtained from assays of ABTS-mediated laccase degradation of anthracene. As a result, the unaccounted degraded anthracene does not correspond to the formation of anthracenols or anthracenediols. Degradation studies of anthracene have identified many other smaller mass metabolites such as phthalic acid and catechol (Ahmed *et al*. 2012; Van Herwijnen *et al*. 2003; Zeinali *et al*. 2008). These degradation products are hydrophilic, meaning that the hexane extraction may be less efficient for them. Therefore, the remaining percentage of degraded anthracene may correspond to other non-detected, low molecular weight and hydrophilic products that were not extracted and remained in the aqueous reactional media.

An additional hypothesis for the unaccounted degraded anthracene is that smaller mass metabolites, such as phthalic anhydride or phthalic acid, are formed from anthraquinone or P1 degradation occurring simultaneously to anthracene oxidation. This hypothesis was investigated through incubation of anthraquinone with the laccase-ABTS system. Assays were performed with 1 mg/L of anthraquinone (4.8 µM) using 0.1 mg/L of laccase and 50 µM of ABTS.

As illustrated in Figure 3.22, no decrease of the anthraquinone peak nor formation of new peaks was observed in the HPLC chromatograms obtained from anthraquinone assays. This indicates that anthraquinone is not degraded by ABTS-mediated laccase activity, confirming anthraquinone as a dead-end product of anthracene as suggested by other studies (Zeinali et al. 2008; G. Eibes et al. 2005; Field et al. 1992). The present results demonstrate that, in the anthracene degradation assays, the anthraquinone formed is not further degraded to form smaller mass metabolites proposed. This discards the hypothesis that the unaccounted degraded anthracene observed in anthracene degradation assays was composed by hydrophilic reactional products formed by anthraquinone degradation. However, it is still possible that the proposed reactional products are formed from P1 degradation. This would mean that P1 might be an intermediate for the formation of more than one anthracene metabolite (Figure 3.23).

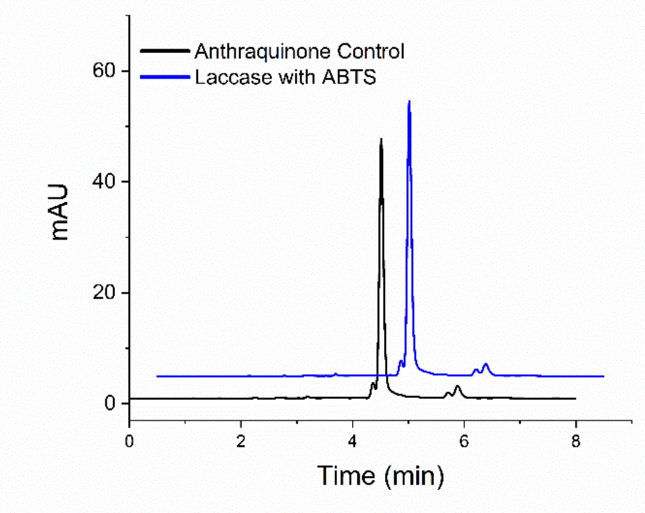

Figure 3.22 – HPLC chromatograms of anthraquinone after incubation with the laccase-ABTS system. Chromatograms are shown for a 24h incubation of anthraquinone (1 mg/L) with ABTS but without the enzyme (Control) and with the laccase-ABTS system. A 100 µg/mL concentration of laccase and 50 µM ABTS was used. Incubation assays were carried in acetate buffer (100 mM, pH 5.0), in the absence of light, at 20 ºC. The chromatograms are displaced in the vertical and horizontal axis for better observation. The chromatograms shown are representative results of triplicate assays for each reaction condition.

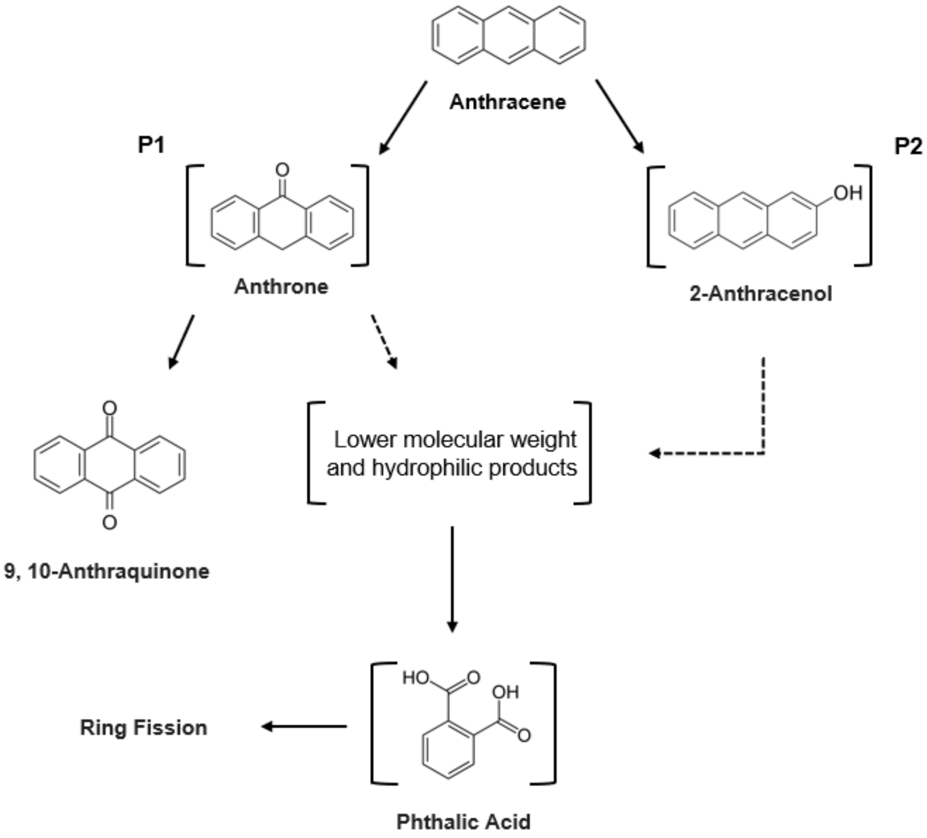
Anthracene
P1
P2
O
Anthrone
OH
2-Anthracenol
O
O
9, 10-Anthraquinone
Lower molecular weight
and hydrophilic products
HO
O
OH
O
Ring Fission
Phthalic Acid

Figure 3.23 – Hypothetical pathway of anthracene oxidation. Compounds between brackets were not identified in the present work.

3.5. Influence of humic acid in laccase catalytic systems

The interaction between environmental factors, enzymatic systems, and pollutants is currently a major challenge in bioremediation. It is of great importance to investigate the synergistic and antagonistic effects caused by soil and aquatic substances to understand how detoxification processes and the performance of biological systems can be affected (Vishwakarma *et al*. 2020).

HA is the fraction of organic matter from soil, sediment, or peat that coagulates under acidic conditions while the other fraction, the fulvic acids, remains soluble after acidification (Bleam 2017). HAs are a complex heterogeneous mixture of polydisperse polyelectrolyte-like molecules with a molecular weight around 5 to 100 kDalton and mainly contain three types of functional groups: carboxylic acids, phenolic alcohols, and methoxy carbonyls (Islam *et al*. 2005).

HA can interact with pollutants and affect their environmental fate, as mentioned in the Introduction, but can also interfere with pollutant removal processes (Zouboulis *et al*. 2004). HA has been reported to interact with enzymes (Allison 2006; Cozzolino and Piccolo 2002) and act as an inhibitor of oxidoreductase enzymes such as laccase, catalase, and lignin peroxidase (Pukalchik *et al*. 2019; Criquet *et al*. 2000; Serban and Nissenbaum 1986).

The potential influence of HA on the laccase-based systems for MO and anthracene transformation was investigated.

3.5.1. Humic acid solutions and spectra

The HA solutions used in this study were prepared as described in Section 2.1.3. The solutions obtained contained 7.33 ± 0.31 g/L of HA. It should be remembered that, in parallel to the preparation of the HA solutions, blank solutions were obtained following the same preparation procedure, except that no HA was added in the initial mixtures (Section 2.1.3). These blank solutions were used as controls in all the studies with HA to assess any eventual confounding effect of buffer constituents.

Figure 3.24 presents the UV-Vis spectra of the HA solutions prepared and used for the HA studies.

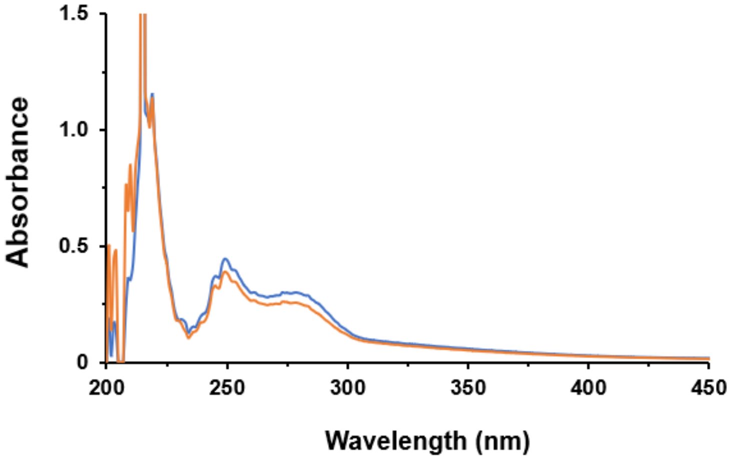

Figure 3.24 – UV-Vis spectra of representative humic acid solutions prepared in the work. The stock solutions were diluted in water to a final concentration of humic acid of 10 mg/L.

3.5.2. Influence of humic acid in laccase activity with ABTS as substrate

A set of assays was carried to determine and characterize the effect of HA on the ABTS oxidizing activity of laccase, performed as described in (Section 2.5.2). These assays were carried with ABTS at an initial concentration of 50 µM and laccase 1 µg/mL, which corresponds to 0.85 mU/mL based on the ABTS oxidizing activity calculated previously. In assays with 50 mg/L of HA, pH values of 4.94 ± 0.01 were verified at the end of the assays, indicating that no significant pH changes occurred in the presence of the highest concentration of HA tested. ABTS oxidation rates were calculated, and the inhibition produced by the presence of the different HA concentrations was determined as described in Section 2.5.2.

The results from this set of assays confirmed that the presence of HA produces an inhibitory effect on laccase activity (Figure 3.25). Control assays carried with the blank solutions (buffer without HA) showed no significant effect on laccase activity. Increasing HA concentration causes a higher inhibitory effect in laccase, reaching up to 60% inhibition of ABTS oxidation with 100 mg/L of HA (Figure 3.26). HA concentrations smaller than 5 mg/L did not affect laccase activity significantly. Experimental traces illustrating HA inhibition of the ABTS oxidizing activity of laccase, using a high and a low HA concentrations, are shown in Figure 3.25. The sudden absorbance increase on addition of HA (at high concentration) to the reaction media is justified by the absorbance of HA at the wavelengths used in the method as can be observed in the HA spectra in Figure 3.24. After the addition of HA, absorbance increase due to ABTS radical formation is not observed and a small absorbance decrease can be observed for some minutes (HA 50 mg/L in Figure 3.25), possibly indicating the reduction of the ABTS radical previously produced by laccase. After this initial effect, the absorbance increase is gradually re-observed, but not reaching the rate measured before addition of HA.

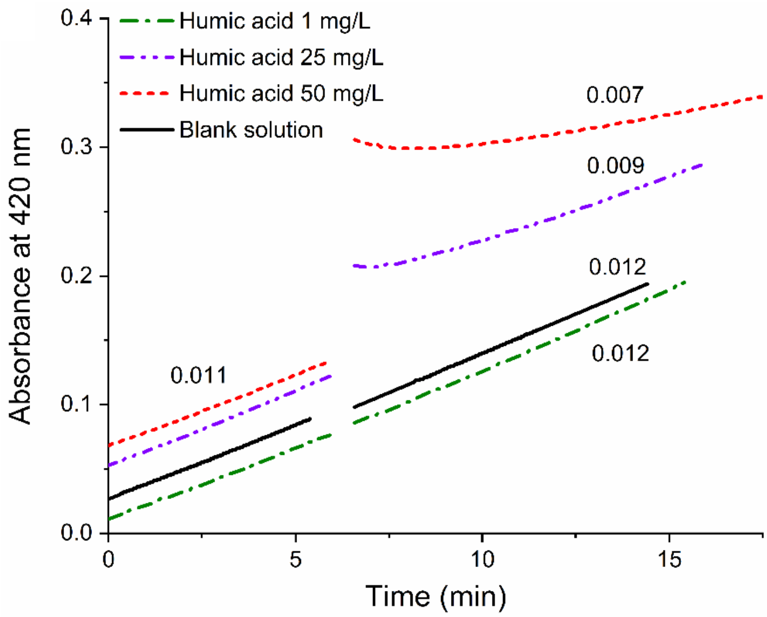

Figure 3.25 – Representative assays of the effect of humic acid on ABTS oxidation by laccase. The ABTS initial concentrations was 50 µM and laccase 1 µg/mL, in 100 mM acetate buffer pH 5.0 at 25 ºC. Small volumes of humic acid stock solution were added to the spectrophotometer cuvette to reach the final concentrations indicated. In the assay with the Blank solution (buffer without humic acid), a volume equivalent to the 50 mg/L humic acid was added to the cuvette. The oxidation rates in ΔAbs/Δt (min^{-1}) are indicated for each reactional condition. The experimental traces shown are representative of at least triplicate assays.

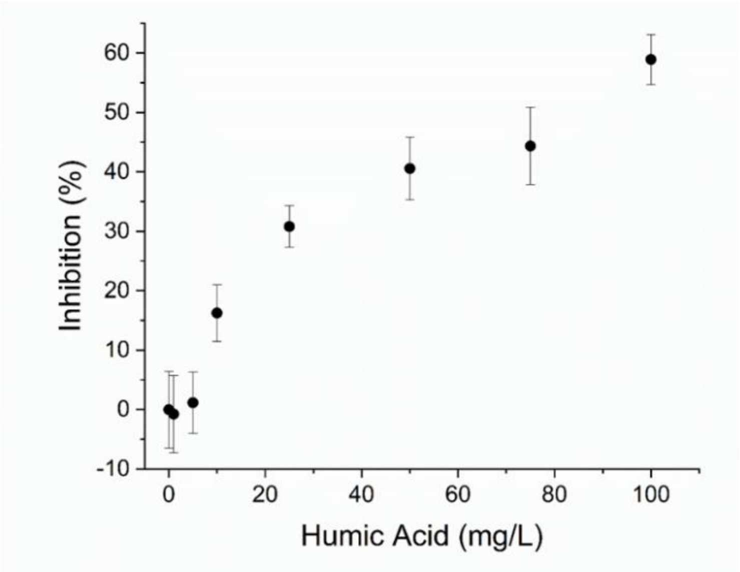

Figure 3.26 – Effect of humic acid on laccase oxidation of ABTS. Assay conditions indicated in Figure 3.25 caption. The control oxidation rates in ΔAbs/Δt (min^{-1}) in absence of humic acid were 0.012 ± 0.003 min^{-1}. The data plotted is the Mean ± SE from three independent experiments.

3.5.3. Influence of humic acid in laccase decolorization of methyl orange

3.5.3.1. Laccase alone

The study of the influence of HA in laccase activity was followed using MO as a different substrate. Even in the absence of mediators, laccase can oxidize MO but at a slow rate as it was seen in previous experiments (Section 3.3). Laccase-catalyzed MO decolorization was assayed in the presence of HA to determine how it is affected by the presence of HA. These assays were carried with greater concentrations of laccase (300 µg/mL) to achieve substantial decolorization rates and to reduce experimental errors. MO decolorization assays by laccase were performed using the method described in Section 2.6.4. In the assays containing the highest HA concentrations (100 mg/L), it was registered pH values of 4.95 ± 0.02, indicating that no significant pH changes occurred during the assays.

Similar to what was observed with ABTS, the presence of HA shows an inhibitory effect on MO decolorization by laccase (Figure 3.27). Experimental results indicate that the presence of concentrations of HA as small as 5 mg/L are sufficient to reduce the rate of MO decolorization significantly (11%). It was also possible to observe that, in the presence of 20 mg/L of HA there is an inhibition of MO decolorization of 30% and plateaus for higher concentrations of HA. The apparent saturation behavior of the inhibition caused by HA observed for ABTS oxidation and MO decolorization assays suggests that the inhibition mechanism of HA might not be dependent on interactions between HA and the substrate. Instead, since a plateauing of the inhibition on laccase activity is observed with both substrates (ABTS and MO), it is possible that the inhibitory effect caused by HA could be due to a direct interaction with laccase.

The inhibition of MO decolorization by high concentrations of HA was further investigated in additional assays as shown in Figure 3.28. These assays confirmed that the laccase catalyzed reaction can be further inhibited, but not even 200 mg/L of HA was able to completely inhibit the enzymatic activity.

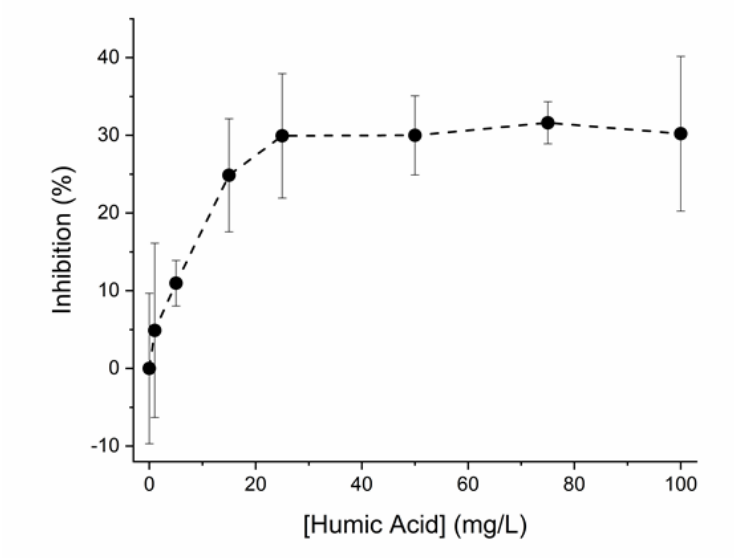

Figure 3.27 – Effect of humic acid on methyl orange decolorization by laccase. Decolorization assays were carried with 300 µg/mL laccase and an initial dye concentration of 10 mg/L (30.6 µM), in 100 mM acetate buffer pH 5.0. Dye decolorization was followed at 477 nm at 25 ºC in the absence and in the presence of different humic acid concentrations from 0.5 to 100 mg/L. The decolorization rates in the presence of humic acid were normalized to the rate observed in the corresponding controls carried using equivalent volumes of Blank solution (buffer without humic acid), which were taken as 0% inhibition. The control decolorization rates in ΔAbs/Δt (min^{-1}) in absence of humic acid were -0.003 ± 0.001 min^{-1}. The data plotted is the Mean ± SE from three independent experiments.

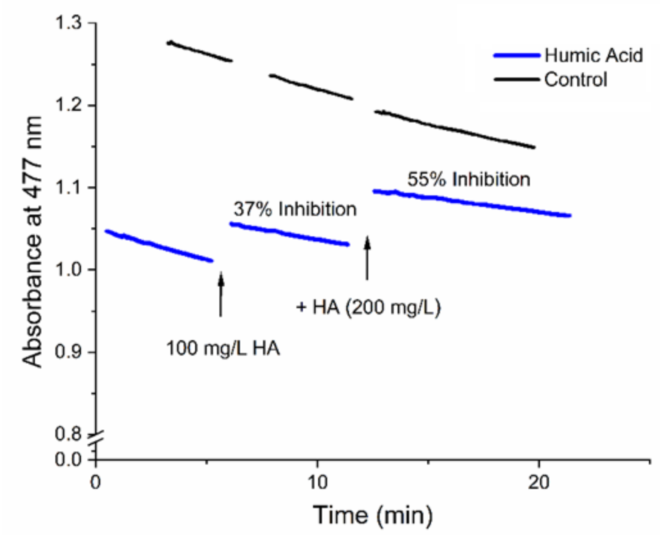

Figure 3.28 – Representative assays of the effect of humic acid on methyl orange decolorization by laccase. The absorbance of methyl orange, initial concentration 10 mg/L (30.6 µM), in 100 mM acetate buffer pH 5.0, was followed at 477 nm, at 25 ºC. The concentration of the enzyme was 900 µg/mL. In the humic acid assay shown, volumes of humic acid stock solution were added to reach the final concentrations indicated, whereas in the Control assay equivalent volumes of blank solution (buffer without humic acid) were added to the spectrophotometer cuvette. The Control assay trace is displaced vertically and horizontally for better visualization.

3.5.3.2. Laccase-ABTS system

It became clear from the experiments performed that HA inhibited laccase activity in both ABTS oxidation and MO decolorization, however, it is still important to investigate how HA affects the activity of the laccase-ABTS mediator system that is being studied in the present work. The inhibitory effect of HA in laccase activity mediated by ABTS was studied using two different concentrations of ABTS (5 and 50 µM).

The results from these assays show that the activity of the laccase-ABTS system is inhibited by the presence of HA. At the resemblance of the results obtained using ABTS as substrate (Section 3.5.2.1), HA concentrations smaller than 5 mg/L did not have a significant effect on the activity of the laccase-ABTS system. HA above 25 mg/L produced a significant inhibitory effect on the activity of laccase-ABTS systems, which is stronger at higher concentrations of HA, reaching around 27% inhibition on the presence of 100 mg/L. However, the inhibitory effect of HA is not directly proportional to the concentration of HA, as inhibition percentages seem to reach a maximum of inhibition at the highest concentrations studied. In these assays, it is verified that the percentages of laccase-ABTS system inhibition are very similar for systems with 5 µM and 50 µM ABTS, suggesting that the inhibitory effect that HA generates on laccase-ABTS systems is independent of the ABTS concentration.

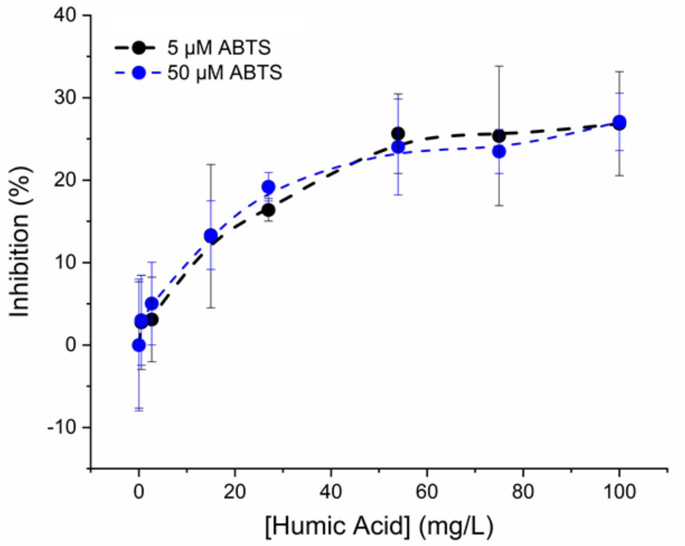

Figure 3.29 – Effect of humic acid on methyl orange decolorization by laccase-ABTS system in the presence of ABTS. Decolorization assays were carried with 100 µg/mL laccase, an initial dye concentration of 10 mg/L (30.6 µM) and ABTS 5 µM or 50 µM, in 100 mM acetate buffer pH 5.0. Dye decolorization was followed at 477 nm, at 25 ºC, in the absence and in the presence of different humic acid concentrations from 0.5 to 100 mg/L. The decolorization rates in the presence of humic acid were normalized to the rate observed in the corresponding controls carried using equivalent volumes of Blank solution (buffer without humic acid), which was taken as 0% inhibition. The control decolorization rates in ΔAbs/Δt (min^{-1}) in absence of humic acid were -0.009 ± 0.002 min^{-1} for assays with 5 µM ABTS and -0.029 ± 0.005 min^{-1} for assays with 50 µM ABTS. The data plotted is the Mean ± SE are representative of at least triplicate assays.

3.5.4. Influence of humic acid in laccase-catalyzed degradation of anthracene

Anthracene might be adsorbed by HA due to its hydrophobicity and that may lead to additional inhibitory mechanisms of the activity of laccase mediated by ABTS. Due to the interest in studying the influence of common organic components present in the environment in the degradation of environmentally relevant pollutants by enzymatic systems, the present work studied the influence of HA in the activity of a laccase-ABTS system on the degradation of anthracene. The influence of HA was investigated through 24 hours incubation assays with HA concentrations up to 500 mg/L using a laccase-ABTS system with 50 µM of ABTS and laccase (100 µg/mL) as in the assays in Section 3.4.

A sample of HA at a high concentration (500 mg/L) was also extracted with hexane and analyzed as a control (Figure 3.32). The chromatogram obtained shows two small peaks around t_R=2.8 min and t_R=3.1 min, but these peaks do not interfere with the analysis of anthracene and the reaction products, observed in the previous section (Section 3.4), since they have very different t_Rs.

It was verified an inhibitory effect in anthracene degradation at all HA concentrations tested, including HA concentrations as low as 5 mg/L (Figure 3.30). Higher concentrations of HA yielded a considerably bigger inhibition of anthracene degradation however, it is noticeable that concentrations above 50 mg/L of HA do not significantly further inhibit anthracene degradation by the laccase-ABTS system in study. These results suggest that, when it comes to anthracene degradation, the presence of 50 mg/L of HA is apparently enough to obtain maximum HA inhibition of the laccase-ABTS system, which corresponds to approximately 65% of inhibition.

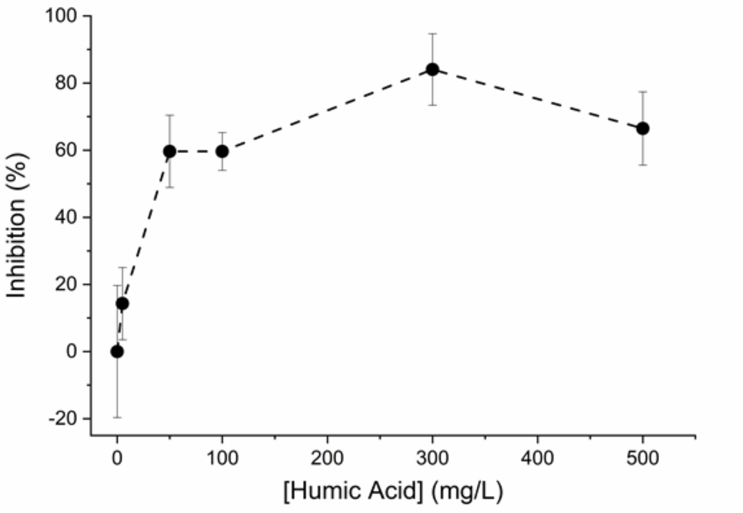

Figure 3.30 – Effect of humic acid on anthracene degradation by laccase-ABTS system. Degradation assays were carried with 100 µg/mL laccase, an initial anthracene concentration of 1 mg/L (5.6 µM), and 50 µM ABTS, in 100 mM acetate buffer pH 5.0. After 24 h incubation, the remaining anthracene concentration was compared to the control without enzyme, which was taken as 0% degradation. Results from at least triplicate assays are shown as Mean ± SE.

The production of anthraquinone and other reaction products of anthracene was also analyzed from the chromatograms of the reaction mixtures after incubation in the absence and presence of HA (Figure 3.32). As expected, lower amounts of anthraquinone were measured when higher concentrations of HA were present in the media (Figure 3.31). The decrease in produced anthraquinone and in anthracene degradation remained proportional with the presence of the different HA concentrations. Approximately 45% of the degraded anthracene was transformed in anthraquinone in the absence of HA and in the presence of the different HA concentrations tested, similar to the observed previously in the studies presented in Section 3.4.

The presence of increasing amounts of HA in the media also caused a decrease of the area of P1 in the chromatograms obtained (Results not shown). In accordance with the results of anthracene degradation and anthraquinone formation, the presence of HA concentrations up to 5 mg/L did not affect the formation of P1 but in the presence of HA concentrations of 500 mg/L P1 was very low. As illustrated in Figure 3.32, no novel reaction products or major interfering components were evident in the enzymatic assay mixtures containing HA.

Considering the relevance of the present results on HA inhibition of laccase-catalyzed transformation of MO and anthracene, the possible underlying mechanisms were investigated further and the results are presented in following sections.

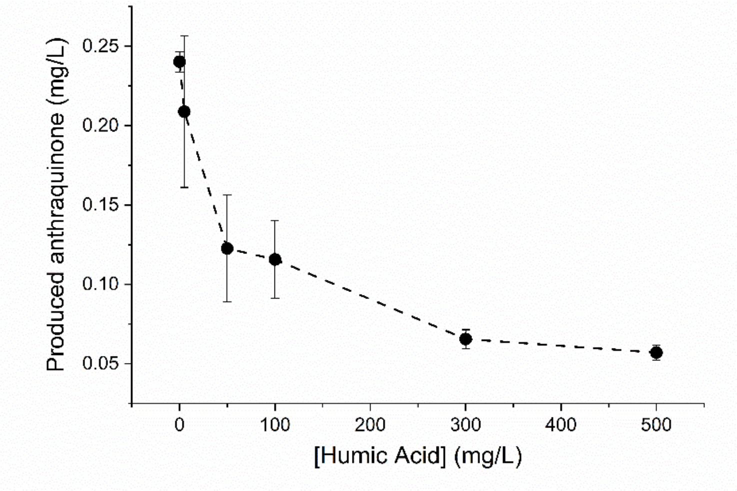

Figure 3.31 – Effect of humic acid on anthraquinone formation by laccase-catalyzed degradation of anthracene. Assay conditions indicated in Figure 3.30 caption. Results from triplicate assays are shown as Mean ± SE.

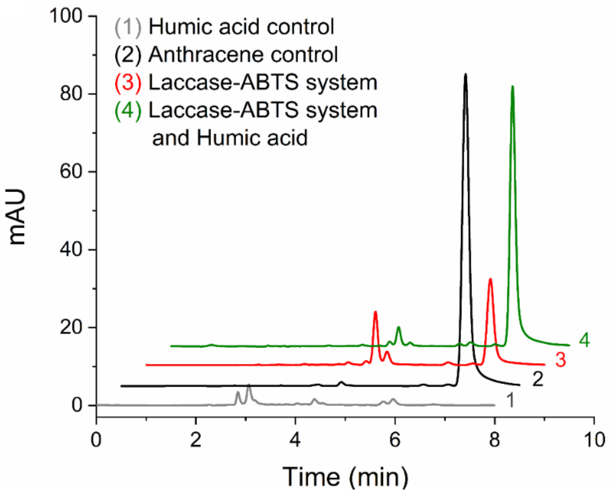

Figure 3.32 – HPLC chromatograms of anthracene degradation by the laccase-ABTS system. Chromatograms are shown for standard humic acid (500 mg/L), an anthracene (1 mg/L) control incubation in the absence of enzyme, and anthracene after 24 h incubation with the laccase-ABTS system without humic acid and with humic acid (500 mg/L). Incubation assays were carried in acetate buffer (100 mM, pH 5.0), in the absence of light, at 20 ºC. The chromatograms are displaced in the vertical and horizontal axis for better observation. The chromatograms shown are representative results of at least triplicate assays for each reaction condition.

3.6. Methyl orange and anthracene degradation studies with peroxidase-type proteins

The studies in Section 3.2 showed the ability of the heme proteins HRP, hemoglobin, and Cc to oxidize ABTS, a good mediator for enzymatic degradation of pollutants. It also revealed the potential advantage of Cc for operation at neutral pH, compared to laccase. Moreover, from the perspective of human toxicology, it is important to characterize the ability of hemoglobin and Cc to catalyze the transformation of environmental toxicants.

3.6.1. Methyl orange decolorization

3.6.1.1. Peroxidase and peroxidase-like proteins alone and with ABTS in methyl orange decolorization

The decolorization of MO by HRP, hemoglobin, and Cc was assayed similarly to the laccase studies. Absorbance decrease rates were measured for each peroxidase and peroxidase-like protein, with 100 µM H_2O_2, in the absence and in the presence of ABTS. Assays were conducted using 0.2 µg/mL of HRP (93 mU ABTS oxidizing activity/mL; 3.4 × 10^{-3} µM), 10 µg/mL of hemoglobin (1.8 mU ABTS oxidizing activity/mL) and 100 µg/mL of Cc (0.8 mU ABTS oxidizing activity/mL; 8 µM). The Sigma C7752 product of Cc was used in these studies.

The results shown in Figure 3.33 demonstrated that HRP, hemoglobin, and Cc were able to decolorize MO when H_2O_2 was present in the reactional media as evidenced by the absorbance decrease registered. In more prolonged assays (Figure 3.33.A, B and C), it was evident that hemoglobin- and Cc-catalyzed MO decolorization rate progressively decreased over time, whereas a more constant rate was maintained by HRP for the duration of these assays (10-15 min). As shown in Figures 3.33.A, 3.35, and 3.36, HRP was able to catalyze the decolorization of MO until low absorbance values, suggesting that the dye is degraded extensively, or at least transformed into products with a lower molar extinction coefficient at the wavelength used. In the case of Cc, it was observed a small initial increase in MO decolorization rate followed by a decrease, possibly due to enzymatic inactivation (Figure 3.33.C, 3.35 and 3.36), as noticed also with hemoglobin (Figure 3.33.B). Inactivation of hemoglobin was already observed in the studies of ABTS oxidizing activity, presented in Section 3.2, and it also seems to affect the MO decolorization by hemoglobin and Cc.

The influence of ABTS in MO decolorization by HRP, hemoglobin, and Cc was studied (Figure 3.33.A, B, and C) and it was observed that ABTS did not accelerate MO decolorization unlike the results with laccase (Section 3.3). On the contrary, the addition of ABTS to the peroxidase and peroxidase-like proteins slowed the decrease in absorbance at 477 nm, suggesting that ABTS may act as an inhibitor of MO decolorization by the peroxidase-type proteins. In the case of HRP (Figure 3.33.A), the effect of ABTS on MO decolorization shown seems less significant, but it should be remembered that the simultaneous oxidation of ABTS might cause an increase in the absorbance at 477 nm that interferes with the method used to monitor MO.

The hypothesis that ABTS oxidation and concomitant increase in absorbance at 477 nm interferes with the MO decolorization rate monitored at this wavelength was further explored with Cc (Figure 3.33.D). The kinetic curve in Figure 3.33.C shows that ABTS 5 µM caused only a small decrease in the absorbance variation rate, but 10 µM caused an almost 50% deceleration, that could be only partially justified by the enzymatic inactivation observable in the more prolonged assay in the absence of ABTS (Figure 3.33.C). Figure 3.33.D shows ABTS oxidation by Cc in the same conditions of the assays in Figure 3.33.C but in the absence of MO. ABTS oxidation was detectable as small increases in the absorbance at 477 nm that can cause only a minor interference on MO monitoring. These results suggest that, at least with 10 µM concentration, ABTS competes with MO for Cc-catalyzed oxidation. In accordance, it is interesting to observe in the curves from hemoglobin and Cc assays (Figure 3.33.B and C) that, in the first minutes after addition to the reaction media, ABTS almost cancels the 477 nm absorbance decrease that afterward is gradually recovered.

Mechanistically, it is possible that ABTS reduces the oxidized iron species at the heme of hemoglobin and Cc that are essential for their peroxidase activity. ABTS oxidation may be competing with MO decolorization by these hemeproteins since both reactions occur through the same catalytic mechanism which could explain the deceleration of MO decolorization rate observed after ABTS addition (Figure 3.33.A, B and C).

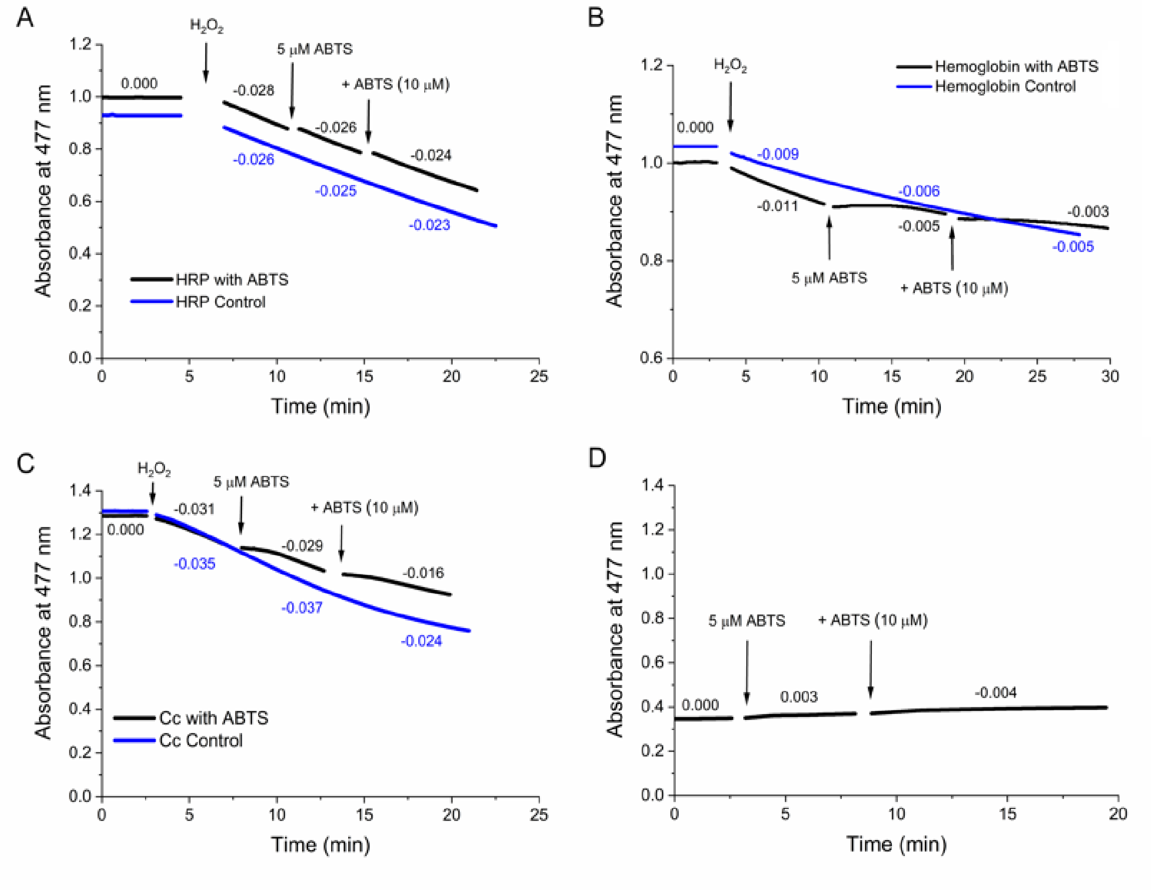

Figure 3.33 – Representative assays of methyl orange decolorization by (A) HRP, (B) hemoglobin, and (C) Cc and the effect of ABTS. The concentration of the proteins used was 0.2 µg/mL of HRP, 10 µg/mL of hemoglobin and 100 µg/mL of Cc, and the concentration of H_2O_2 was 100 µM. The absorbance of methyl orange, initial concentration 10 mg/L (30.6 µM), in 100 mM acetate buffer pH 5.0, was followed at 477 nm at 25 ºC. Panel (D) shows the oxidation of ABTS by Cc in the same conditions as panel (C), but in the absence of methyl orange. The decolorization rates in ΔAbs/Δt (min^{-1}) are indicated for each reactional condition in the absence and after the additions of ABTS to reach a final concentration of 5 and 10 µM.

A peroxidase-ABTS system was further investigated with HRP through MO decolorization assays with 50 µM of ABTS monitored at 477 nm, but also at 734 nm, a wavelength that allows measuring ABTS oxidation without the interference of MO. Figure 3.34 shows that HRP quickly oxidized all the ABTS in the media and ABTS$^{•+}$ concentrations remained constant for long periods (absorbance 0.61 at 734 nm corresponds to 47.4 µM ABTS radical). These results show that the absorbance decrease by MO decolorization at 477 nm is minimized due to the absorbance increase by ABTS oxidation registered in the first moments after ABTS addition in MO assays and because HRP oxidizes ABTS before MO. The detection of ABTS oxidation simultaneous to MO decolorization supports the hypothesis that ABTS and MO compete for the peroxidase and peroxidase-like proteins studied. The deceleration of MO decolorization rate could be explained by this competition if the rate of the ABTS-mediated decolorization of MO reaction is slower than direct decolorization of MO by the peroxidase and peroxidase-like proteins.

Although the details on the effect of ABTS on the catalysis by these proteins requires more studies, the present results indicate that ABTS offers no great advantage for bioremediation processes based on peroxidase and peroxidase-like proteins, at least for decolorization of pollutants like MO that are directly transformed by the proteins.

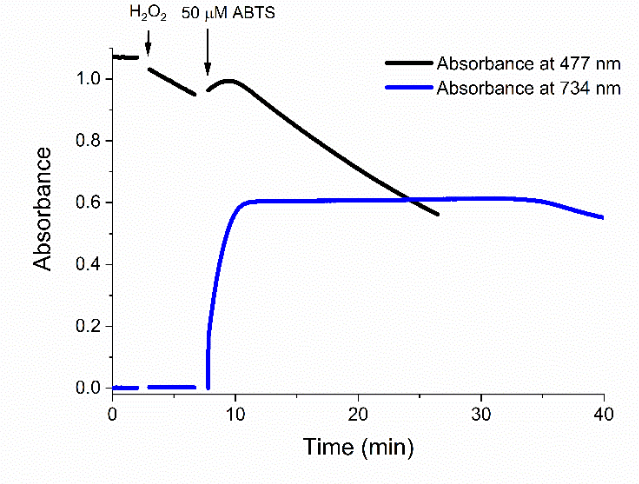

Figure 3.34 – Monitoring of HRP-ABTS system in decolorization of methyl orange. The assay was carried in the same conditions as in Figure 3.33.A, except that with 50 µM of ABTS. The course of the reactions (methyl orange decolorization and ABTS oxidation) were followed at 477 and 734 nm.

Additional assays were performed to better understand MO decolorization catalyzed by HRP and Cc. MO decolorization assays with peroxidase and peroxidase-like proteins and H_2O_2 were monitored for large periods of time, until apparent termination of the enzymatic reaction (>30 min), followed by the addition of more MO and H_2O_2 to determine if the variation of MO and H_2O_2 throughout the assay may influence the results observed (Figure 3.35 and 3.36).

In the HRP assay shown in Figure 3.35, after the deceleration of MO decolorization rate, a new addition of MO to the reactional mixture caused an increase in the decolorization rate, however, it did not increase to the decolorization rate verified at the start of the assay. Later on, MO decolorization halted while there was still a high concentration of MO available on the medium. This suggests that the decrease of MO availability in the reactional medium slows the decolorization rate of MO, but it is not the only factor causing this effect. It is possible that the deceleration of MO decolorization rate can also be caused by other factors such as H_2O_2 depletion. In Cc assays shown in Figure 3.35, a new addition of MO to the medium did not cause a significant effect in the MO decolorization rate, reinforcing that the peroxidase-like protein becomes inactivated.

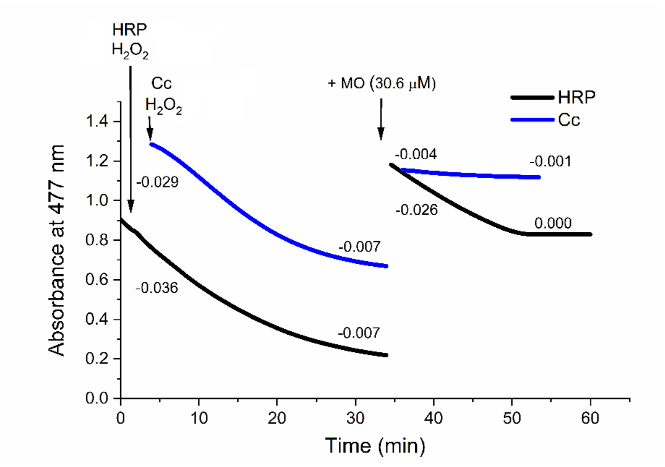

Figure 3.35 – Influence of the methyl orange availability in the medium on the kinetics of decolorization by HRP and by Cc. Assay conditions indicated in Figure 3.33 caption. The kinetics of decolorization can be compared before and after the replenishment of methyl orange in the reactional mixture.

The activity of both HRP and Cc is dependent on H_2O_2, and it was observed previously that H_2O_2 concentration influenced peroxidase and peroxidase-like proteins activity (Figure 3.11). In the assays of peroxidase-catalyzed MO decolorization, H_2O_2 is consumed and its exhaustion can limit the reaction rate. Therefore, the decrease in decolorization rate observed even when reactional medium contains high MO concentrations may be due to the decrease in H_2O_2 concentration throughout the assay. This possibility was tested by new addition of H_2O_2 to the spectrophotometer cuvette during the decolorization assays (Figure 3.36). MO decolorization rates greatly increased shortly after H_2O_2 addition for Cc, despite the low MO concentrations available in the medium, but no effect was observed in HRP assays.

These results show that the exhaustion of the H_2O_2 available in the reactional media limits Cc-catalyzed MO decolorization, but little effect is observed in prolonged HRP assays. Nevertheless, in the conditions of the shorter assays in Figure 3.33, these possible limitations of substrate availability are not critical, because the rate of enzymatic reaction is maintained high throughout the measurement times.

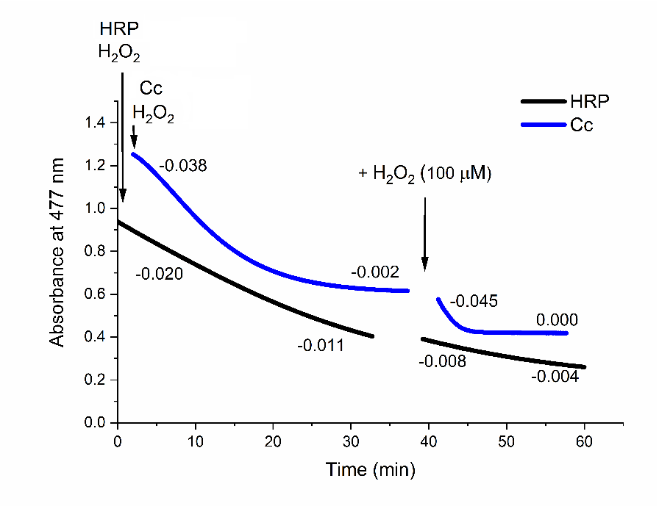

Figure 3.36 – Influence of H_2O_2 exhaustion in the medium on the kinetics of decolorization by HRP and by Cc. Assay conditions indicated in Figure 3.33 caption. The kinetics of decolorization can be compared before and after the replenishment of H_2O_2 in the reactional mixture.

3.6.1.2. Peroxidase-catalyzed methyl orange decolorization at neutral pH

The ability of hemoglobin and Cc to metabolize MO can have important implications for the toxicology of azo dyes and other toxicants, especially if it is observed at neutral pH similar to the physiological pH in the cell compartments containing these proteins. Hence, it was decided to study the transformation of MO by HRP, hemoglobin, and Cc in the same assay conditions as above, but at pH 7.0 by using phosphate buffer. In control assays, MO was incubated in phosphate buffer (100 mM, pH 7.0 containing 0.1 mM DTPA) in the presence of 100 µM of H_2O_2 for the duration of the decolorization assays and no significant spectral changes were registered. The pH of the reactional mixtures was checked at the end of the decolorization assays and no significant pH changes were observed.

The results from the decolorization assays (Figure 3.37) show that, in the presence of 100 µM of H_2O_2, Cc and hemoglobin decolorize MO at pH 7.0 but at a slower rate than what was observed at pH 5.0. HRP assays showed no significant decolorization of MO at pH 7.0. These results fall in accordance with the results obtained in Section 3.2 regarding to ABTS oxidation at different pHs (Figure 3.12). Like the results obtained in MO decolorization assays, HRP did not yield a significant ABTS oxidation rate at pH 7.0, and Cc showed to be capable to oxidize ABTS at pH 7.0, although at a slower rate than at pH 5.0. The MO decolorization rates afforded by the peroxidase-type proteins are presented in Table 3.7.

Considering the low MO decolorization rates and the inactivation of hemoglobin observed in assays both with ABTS and MO substrates, it was decided not to continue the studies with this heme-protein.

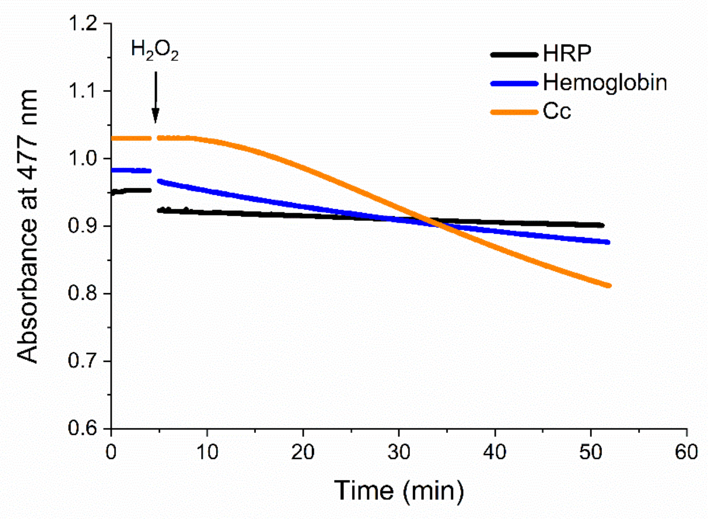

Figure 3.37 – Representative assays of methyl orange decolorization by HRP, by hemoglobin, and by Cc. The concentration of the proteins used was 0.2 µg/mL of HRP, 10 µg/mL of hemoglobin and 100 µg/mL of Cc, and the concentration of H_2O_2 was 100 µM. The absorbance of methyl orange, initial concentration 10 mg/L (30.6 µM), in 100 mM phosphate buffer pH 7.0, was followed at 477 nm at 25 ºC. The decolorization rates in ΔAbs/Δt (min^{-1}) are indicated in Table 3.7 for each peroxidase and peroxidase-like proteins.

Table 3.7 – Comparison of MO decolorization rates of peroxidase-type proteins measured in 100 mM acetate buffer pH 5.0 and in 100 mM phosphate buffer pH 7.0, at 25 ºC.

Protein	Horseradish Peroxidase	Hemoglobin	Cytochrome *c* (C7752)
Assay conditions	30.6 µM MO 3.4×10^{-3} µM HRP (0.2 µg/mL) 100 µM H_2O_2	30.6 µM MO Hemoglobin (10 µg/mL) 100 µM H_2O_2	30.6 µM MO 8 µM Cc (100 µg/mL) 100 µM H_2O_2
Decolorization Rate pH 5.0 ΔAbs/Δt (min^{-1})	0.027 ± 0.001	0.011 ± 0.002	0.030 ± 0.001
Decolorization Rate pH 7.0 ΔAbs/Δt (min^{-1})	Very low (not quantified)	0.0026 ± 0.0001	0.0061 ± 0.0001

3.6.1.3. Inhibition of peroxidase-type proteins by humic acid

For bioremediation applications, it is important to clarify if HRP and Cc are sensitive to HA inhibition as it was observed with laccase (Section 3.5).

The influence of HA in HRP and Cc activity was studied using ABTS and MO as substrates to investigate if the peroxidase activity of HRP and Cc was affected by HA. These studies were carried at pH 5.0, and the pH of the reactional mixtures was checked at the end of the assays and no significant pH changes were observed (5.00 ± 0.01).

Control assays were performed for HRP and Cc assays by addition of a blank solution instead of HA solution and no significant effect was observed in the ABTS oxidation rate nor in MO degradation rate. However, when HA was added to the reactional mixtures, it was observed a 30% decrease in the rate of ABTS oxidation by HRP but, in Cc assays, it was observed an increase of ABTS oxidation rate (Figure 3.38). The results obtained in Cc assays were the opposite of the effect that was observed for the other enzymes studied in this work.

The heme group of Cc and HA absorb at the wavelength used to follow ABTS oxidation of the assays from which these results were obtained. It is possible that interactions between HA and Cc may be occurring that cause conformational changes in Cc at the level of the heme and cause the apparent increase in ABTS oxidation rate. Therefore, further Cc assays were carried following the ABTS oxidation at 734 nm to avoid possible interferences in the absorbance of the reaction mixture due to changes in the heme optical properties. The assays monitored at 734 nm show similar results to the results obtained in assays monitored at 420 nm (Figure 3.38), confirming that HA enhances ABTS oxidation by Cc since the acceleration in the absorbance increase observed in Cc assays in the presence of HA is not caused by the optical properties of the heme of Cc nor of HA.

In MO decolorization assays, the presence of HA caused an inhibitory effect for both HRP and Cc (Figure 3.39). The presence of HA inhibited the Cc-catalyzed MO decolorization more strongly than the HRP-catalyzed reaction.

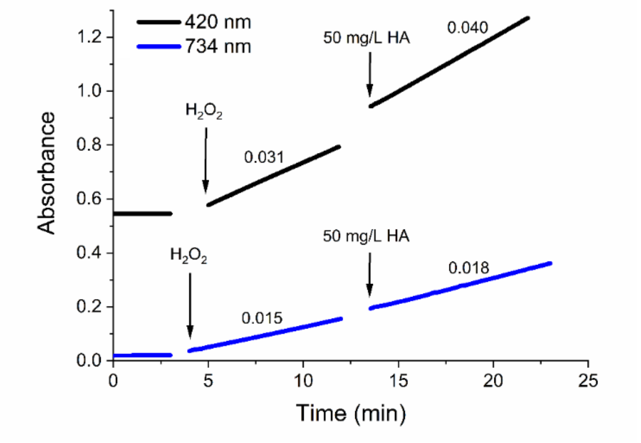

Figure 3.38 – Effect of humic acid in Cc-catalyzed ABTS oxidation. Assays were performed using 100 µg/mL of Cc, 100 µM H_2O_2, 500 µM ABTS and 50 mg/L of humic acid in 0.1 M acetate buffer (0.1 M pH 5.0 containing 0.1 mM DTPA) and 25 ºC. ABTS oxidation was monitored at 420 nm and at 734 nm.

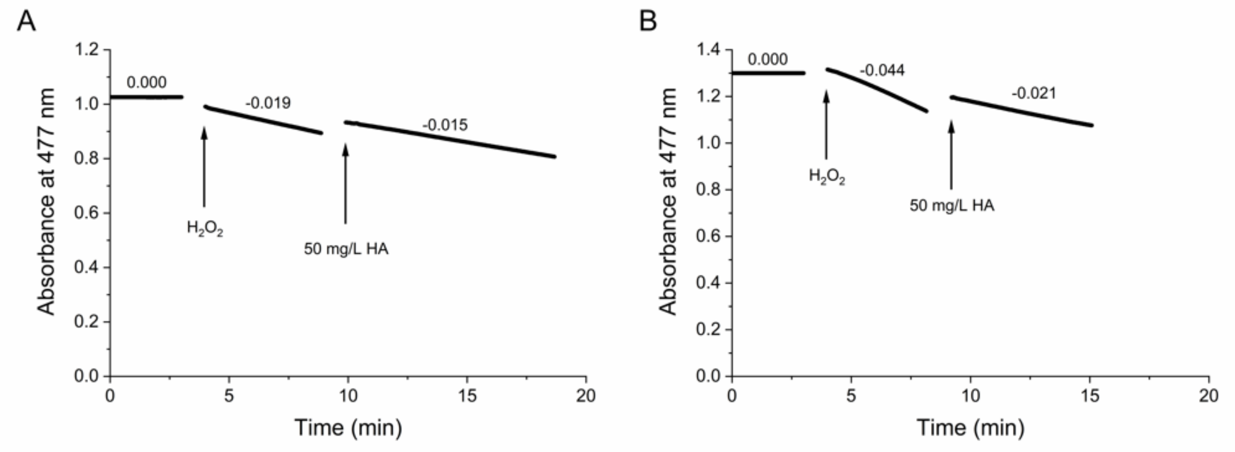

Figure 3.39 – Effect of humic acid on methyl orange decolorization by (A) HRP and (B) Cc. The concentration of the proteins used was 0.2 µg/mL of HRP and 100 µg/mL of Cc, and the concentration of H_2O_2 was 100 µM. The absorbance of methyl orange, initial concentration 10 mg/L (30.6 µM), in 100 mM acetate buffer pH 5.0, was followed at 477 nm at 25 ºC. The decolorization rates in $\Delta Abs/\Delta t$ (min^{-1}) are indicated for each reactional condition in the absence and after addition of humic acid in a final concentration of 50 mg/L.

The histogram in Figure 3.40 resumes the effect of the presence of HA in HRP- and Cc-catalyzed reactions with ABTS and MO. These findings converge with the results from laccase assays on the impact of HA on the ability of oxidoreductases to catalyze the transformation of pollutants. Similar to the inhibition of laccase, HA caused a 30% inhibition of HRP-catalyzed ABTS and MO transformation and even higher inhibition of Cc-catalyzed decolorization of MO. Based on these data, it is plausible that a common mechanism of action underlines HA inhibition of the 3 proteins, a topic to be investigated further in the following section.

The HA-induced increase in the ABTS-oxidizing activity of Cc seems to disagree with the general panorama of the present work. It should be remembered that Cc presents positive patches at the surface known to interact with anionic molecules that activate its peroxidase activity (Díaz-Quintana *et al*. 2020). As mentioned in Section 3.5, HA molecules contain carboxylic acids which are partially ionized at pH 5.0 (Zavarzina *et al*. 2004). These anionic groups might interact with Cc and trigger the peroxidase activity of the protein, similarly to the interaction and structural changes caused by CL previously mentioned in the Introduction.

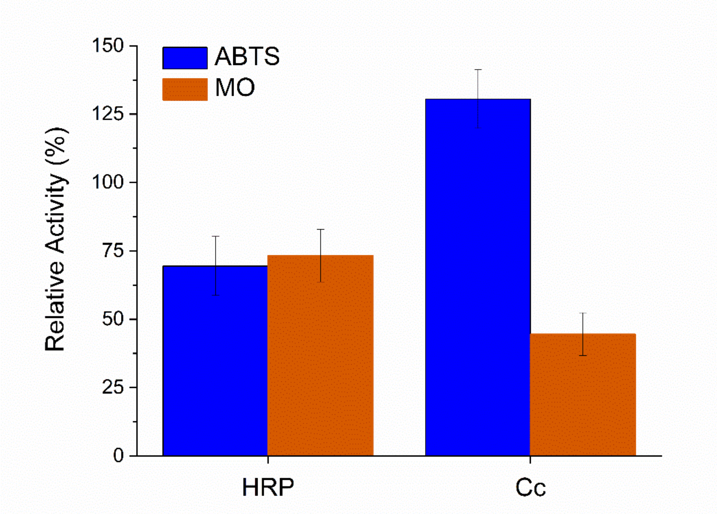

Figure 3.40 – Effect of humic acid (50 mg/L) in HRP- and Cc-catalyzed oxidation of ABTS and MO. Assays were performed in acetate buffer (100 mM pH 5.0 containing 0.1 mM DTPA), at 25 ºC. The inhibitory effect in ABTS oxidation was assayed for HRP (1×10^{-3} µg/mL) and Cc (100 µg/mL for ABTS) with 100 µM of H_2O_2 and 500 µM of ABTS. Conditions of MO assay indicated in Figure 3.39 caption. Relative rates were calculated through the comparison of the ABTS oxidation and MO decolorization rates after the addition of humic acid with the rates obtained in the absence of humic acid, which were taken as 100%.

3.6.2. Peroxidase-catalyzed anthracene degradation

The results of ABTS oxidation and MO decolorization by HRP and Cc encouraged the investigation of the ability of these peroxidase and peroxidase-like proteins to degrade anthracene.

Studies of anthracene degradation through peroxidase activity by HRP and Cc were performed through incubation assays as described in Section 3.6.1. The Sigma C2506 product of Cc was used in these studies. After 24h, reactional media was extracted with hexane and the remaining anthracene and generated products were analyzed. Assays were carried without and with the addition of ABTS to the reactional media.

Figure 3.42 shows the chromatograms of the hexane extracts of anthracene incubated with HRP and Cc with and without ABTS. No anthracene degradation was observed in HRP incubations without

ABTS. In HRP assays with ABTS (50 µM), it was observed a degradation of 17.1 ± 7.0% of initial anthracene and the detected reaction products were anthraquinone and P1 (Figure 3.42.A and 3.43, and Table 3.8). Different from what was observed for laccase and HRP assays, incubation assays with Cc showed evident degradation of anthracene without the presence of ABTS on the media, while in the presence of ABTS registered a very low or depreciable transformation of anthracene (Figure 3.42.B). It was observed a degradation of initial anthracene greater than 75% in Cc assays without ABTS (Figure 3.43). However, in Cc incubation assays with ABTS (50 µM) it was observed a very small anthracene degradation (5%), only confirmed as significant because the formation of anthraquinone and P1 was detected (Table 3.8). In all Cc assays it was detected the formation of anthraquinone as the major reaction product, and P1 was detected in small amounts. Another unidentified reaction product (P2) was detected in Cc assays without ABTS, which was not detected in assays with Cc in the presence of ABTS, nor with laccase or HRP (t_R =5.6 min, in Figure 3.42.B). As mentioned previously (Section 3.4), anthracene can be transformed into alcohol derivatives such as anthracenols and anthracenediols. It is possible that P2 corresponds to anthracenols (Figure 3.23) or 1-methoxy-2-hydroxyanthracene. This novel peak detected possesses a t_R in-between the one of anthracene and the one of anthraquinone and the Kow of both reactional products proposed is also in-between the one of anthracene and the one of anthraquinone.

It is interesting to notice again that, in HRP with ABTS and Cc without ABTS assays, where higher anthracene degradation percentages were observed, the anthraquinone formed corresponded to approximately 50% of the degraded anthracene, like the results obtained with the laccase-ABTS system (Section 3.4).

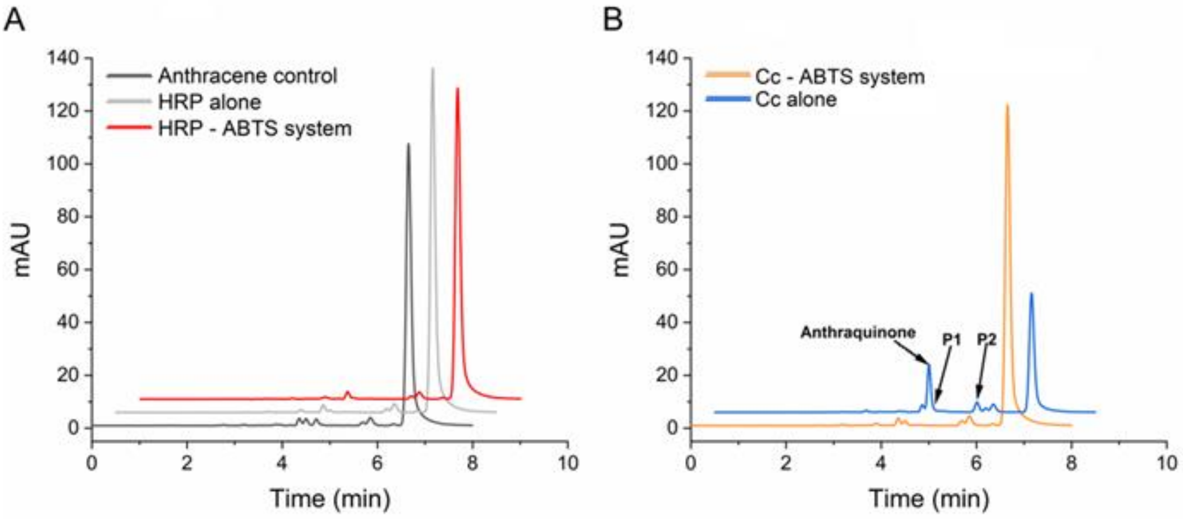

Figure 3.41 – HPLC chromatograms of anthracene and degradation products generated by HRP (A) and Cc (B) systems. Chromatograms are shown for (A) an anthracene (1 mg/L) without protein nor ABTS, anthracene with HRP 0.2 µg/mL in the presence of H_2O_2 100 µM without ABTS and with ABTS 50 µM, and (B) with Cc 100 µg/mL with H_2O_2 100 µM without ABTS and with ABTS 50 µM after 24 h incubation. The unidentified oxidation product P2 (t_R=5.6min) is indicated in the blue chromatogram, in addition to anthraquinone and P1. Incubation assays were carried in 100 mM acetate buffer pH 5.0, in the absence of light, at 20 ºC. Some chromatograms are displaced in the vertical and horizontal axis for better observation. The chromatograms shown are representative results of at least triplicate assays for each reaction condition.

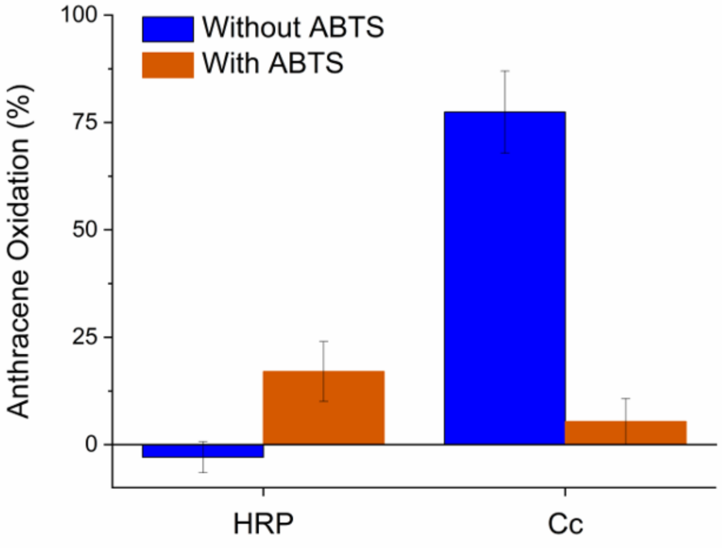

Figure 3.42 – Effect of ABTS in HRP- and Cc-catalyzed degradation of anthracene. Assay conditions indicated in Figure 3.41 caption. Results from triplicate assays are shown as Mean ± SE.

Overall, the anthracene degradation studies with the hemeproteins indicated that HRP behaves like laccase, showing the HRP-ABTS system some potential for bioremediation processes, and pointed a significant ability of Cc (alone) to transform anthracene. This ability of Cc prompted further studies with other PAHs, presented in a following section.

Table 3.8 – Anthracene reaction products generated by HRP- and Cc-catalyzed degradation, alone and in the presence of ABTS. Assay conditions indicated in Figure 3.41 caption. Results from triplicate assays are shown as Mean ± SE.

Reaction Products	HRP		Cc	
	Without ABTS	With ABTS	Without ABTS	With ABTS
Anthraquinone (mg/L)	0.019 ± 0.011	0.087 ± 0.033	0.401 ± 0.042	0.033 ± 0.001
P1 (mAU × s)	Not detected	25.9 ± 8.8	3.9 ± 0.7	1.8 ± 0.2
P2 (mAU × s)	Not detected	Not detected	31.27 ± 4.09	Not detected

3.7. Quenching of radicals in the inhibition of laccase catalysis by humic acid

As described in the previous sections, the presence of HA inhibited the degradation of pollutant substances catalyzed by laccase, HRP, and Cc. Enzymatic inhibition by HA has been reported by other authors (Zavarzina *et al*. 2004; Bielińska *et al*. 2018; Ruggiero and Radogna 1985), but the inhibition mechanism is still unclear. The potential of HA to quench radicals due to its antioxidant properties has been reported (Aeschbacher *et al*. 2012) and is often measured through $ABTS^{\bullet+}$ decolorization assays (Klein *et al*. 2018). Quenching of $ABTS^{\bullet+}$ would cause an apparent effect of inhibition in ABTS oxidation assays, which are measured by monitoring the formation of $ABTS^{\bullet+}$, and may also inhibit the radical-chain reactions described in Figure 1.4 responsible for the degradation of MO and anthracene by decreasing the concentration of $ABTS^{\bullet+}$ present in the media (Efimova *et al*. 2012).

The radical quenching potential of HA was investigated through assays with laccase.

3.7.1. Quenching of ABTS radicals

To test the hypothesis that HA reacts with $ABTS^{\bullet+}$, two types of assays were designed: (1) oxidizing ABTS with laccase and posteriorly blocking the enzyme with azide, and (2) using $ABTS^{\bullet+}$ previously produced by oxidation with persulfate. In both methods, the reduction of $ABTS^{\bullet+}$ by HA was assessed by the addition of HA to a reactional media containing $ABTS^{\bullet+}$ in acetate buffer (100 mM, pH 5.0) and following the decrease of $ABTS^{\bullet+}$ concentration indicated by the absorbance at 420 nm.

Figure 3.43 shows results obtained by the azide method in which the enzyme was inhibited with azide when the absorbance at 420 nm reached approximately 0.5, corresponding to 14 µM $ABTS^{\bullet+}$. No ABTS oxidation was observed after the addition of 0.1 mM of sodium azide to the reactional mixture, indicating that laccase activity was completely blocked. After HA addition it was observed an absorbance decrease indicating a decrease in $ABTS^{\bullet+}$ concentration in the media. The absorbance dropped at a faster rate in the first instants after HA addition, but the absorbance decrease rate progressively slowed down and stabilized (Figure 3.43). It is conceivable that the HA solution contains chemical species that react with ABTS radicals at different rates, causing the gradual decline of the effect of HA.

Greater concentrations of HA resulted in greater absorbance decreases regarding to the initial absorbance drop and the following slower decrease (Figure 3.43). When a 75 mg/L concentration of HA was added to the reaction media, the effect in the absorbance was very small, both with the azide-inhibited and the non-inhibited laccase (Figure 3.43.A). However, addition of HA 150 mg/L to the media with azide-inhibited enzyme caused a substantial absorbance drop, evident for some minutes, and comparable to the apparent blockade (no change or decrease of absorbance) of the enzyme in the absence of azide that also is observed in the first minutes after addition of HA (Figure 3.43.B).

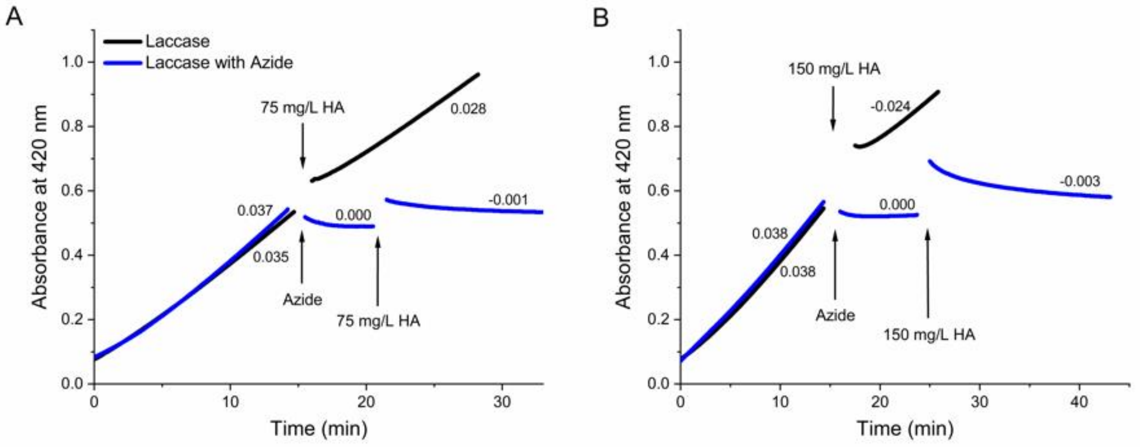

Figure 3.43 – Decay of $ABTS^{\bullet+}$ in the presence of 75 mg/L and 150 mg/L of humic acid. The initial concentration of ABTS was 500 µM. ABTS oxidation was catalyzed by laccase (1 µg/mL) until absorbance approximated 0.5 (14 µM) and then, the enzyme was blocked with azide (0.1 mM) before addition of humic acid. An equivalent assay with non-inhibited enzyme is shown. Assays were performed in acetate buffer (100 mM, pH 5.0) at 20 ºC. The observed ΔAbs/Δt (min^{-1}) are indicated for each reactional condition in the absence and after addition of humic acid.

Figure 3.44 shows results obtained with ABTS radical pre-formed with persulfate. In Control assays, $ABTS^{\bullet+}$ was monitored in aqueous solution at pH 5.0 for the same duration of the $ABTS^{\bullet+}$ quenching assays and no absorbance changes were observed (data not shown), indicating that no auto-decay occurred, in accordance with previous reports (Klein *et al*. 2018; Ozgen *et al*. 2006). Similar to the results obtained in the above assays with laccase-produced $ABTS^{\bullet+}$, the addition of HA caused a fast initial absorbance drop followed by a progressively slower absorbance decrease rate as shown in

Figure 3.44. The presence of a higher concentration of HA caused a greater drop in absorbance in the first moments after HA addition however, the rate of absorbance decrease diminished progressively in this assay as well until the decay observed stabilized at a similar rate (Figure 3.44).

These results indicate that HA can reduce back or quench the ABTS radical produced in the laccase (and HRP) reaction systems. This effect can justify the initial decrease of absorbance observed in the first seconds of the enzymatic assays. However, the ABTS-quenching effect of HA gradually wanes after the initial minutes, especially with low concentrations. On the contrary, the rate of absorbance increase on ABTS oxidation does not suffer significant changes after the first minutes post-addition of HA and remains almost constant through several minutes (see for example Figure 3.43, assays without azide). Thus, another mechanism in addition to $ABTS^{\bullet+}$ quenching is responsible for the sustained inhibition of laccase catalysis.

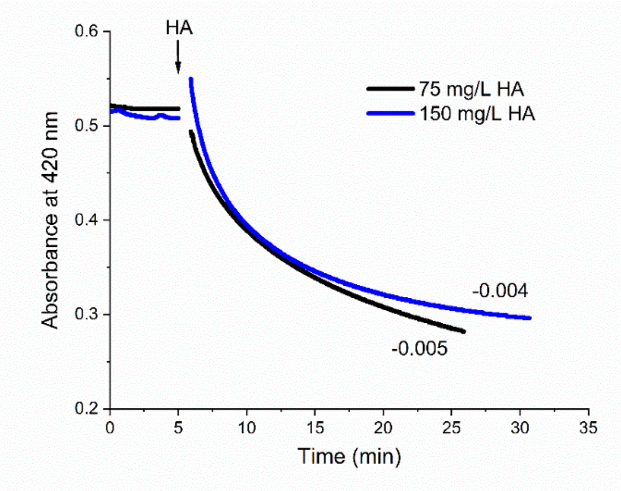

Figure 3.44 – Decay of $ABTS^{\bullet+}$ (14 µM) in the presence of 75 mg/L and 150 mg/L of humic acid. The $ABTS^{\bullet+}$ used was produced by oxidation of ABTS with persulfate. Assays were performed in acetate buffer (100 mM, pH 5.0) at 20 ºC. The steady ΔAbs/Δt (min^{-1}) observed several minutes after addition of humic acid is indicated in the plots.

3.7.2. Scavenging of methyl orange decolorization products

It was observed in Section 3.3 and 3.6 that HA also inhibited enzyme-catalyzed MO decolorization in the absence of ABTS which may be due to a reaction between HA and the decolorization products of MO. To test this hypothesis, HA was added to an aqueous solution (acetate buffer, 100 mM, pH 5.0) containing MO partially decolorized by laccase after laccase activity was completely blocked by azide. In these assays, a high concentration of laccase was used and azide 0.2 mM was necessary to block the enzyme activity.

As shown in Figure 3.45, the absorbance of the partially degraded MO solution after laccase activity was blocked with azide remained stable. Different concentrations of HA were added to the partially decolorized MO solution but no absorbance changes were observed, suggesting that HA does not react with products of MO transformation by laccase and, therefore, HA does not inhibit laccase-catalyzed decolorization of MO by reversing the dye degradation reactions.

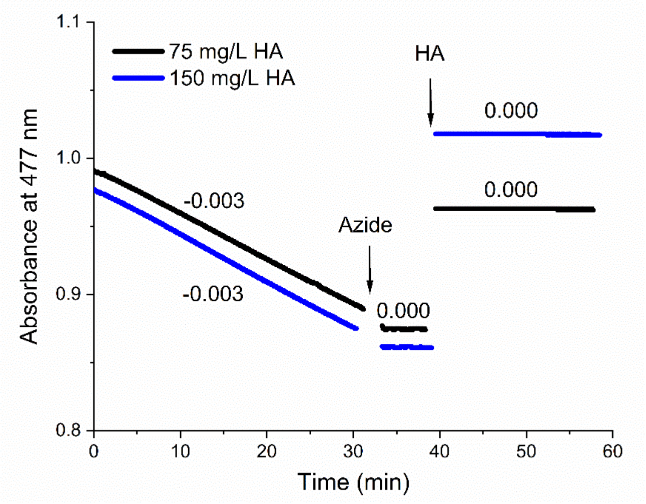

Figure 3.45 – Representative assay of methyl orange decolorization products in the presence of 75 mg/L and 150 mg/L of humic acid. The absorbance of methyl orange, initial concentration 10 mg/L (30.6 µM), in 100 mM acetate buffer pH 5.0, was followed at 477 nm, at 25 ºC. Laccase was used at a concentration of 300 µg/mL and blocked with 0.2 mM of azide.

3.8. Effect of lipid membranes in the peroxidase activity of heme proteins

The results presented in Section 3.6 showed interesting abilities of peroxidase and peroxidase-like hemeprotein to transform the model organic toxicants. The azo dye could be transformed by HRP at acid pH and by hemoglobin and Cc at both acid and neutral pH. Cc also oxidized the PAH anthracene without needing a mediator. Besides the biotechnological potential, these enzymatic activities might influence the toxicology of those compounds. Hemoglobin is a very abundant protein inside erythrocytes and Cc is concentrated in mitochondria. Importantly, Cc interaction with lipid membranes can increase its peroxidase activity (Lagoa *et al*. 2017; Muenzner *et al*. 2013).

Therefore, it is important to evaluate the potential peroxidase-inducing effect of lipid membranes representative of the compartments where hemoglobin and Cc are located in the cell. The lipids investigated in this work were PC and CL which were used to prepare two types of lipid vesicles, as described in Section 2.1.4, the SUVs of PC only and the SUVs of PC/CL, that were tested with both the proteins. SUVs of PC are representative of the cellular membranes in general and the PC/CL vesicles mimic the mitochondrial membranes.

3.8.1. Oxidation of ABTS and dye decolorization

The effect on the peroxidase activity of the heme proteins was initially assayed by measuring the rates of ABTS oxidation and MO decolorization in the presence of the lipid vesicles, at pH 7.0.

Preliminary results indicated that CL-containing SUVs enhanced the peroxidase activity of Cc. This effect was more evident in assays containing lower concentrations of Cc and ABTS thus it was decided to evaluate the effect of SUVs in heme proteins using lower concentrations of Cc (12.5 µg/mL, 1 µM) and ABTS (100 µM). The Sigma C2506 product of Cc was used in these studies. The results from hemoglobin assays showed no significant differences in peroxidase activity between assays containing PC or PC/CL SUVs and assays in the absence of lipid vesicles, regardless of the substrate used (Figure 3.46). These results indicated that PC and CL-containing SUVs have no effect on the peroxidase activity of hemoglobin.

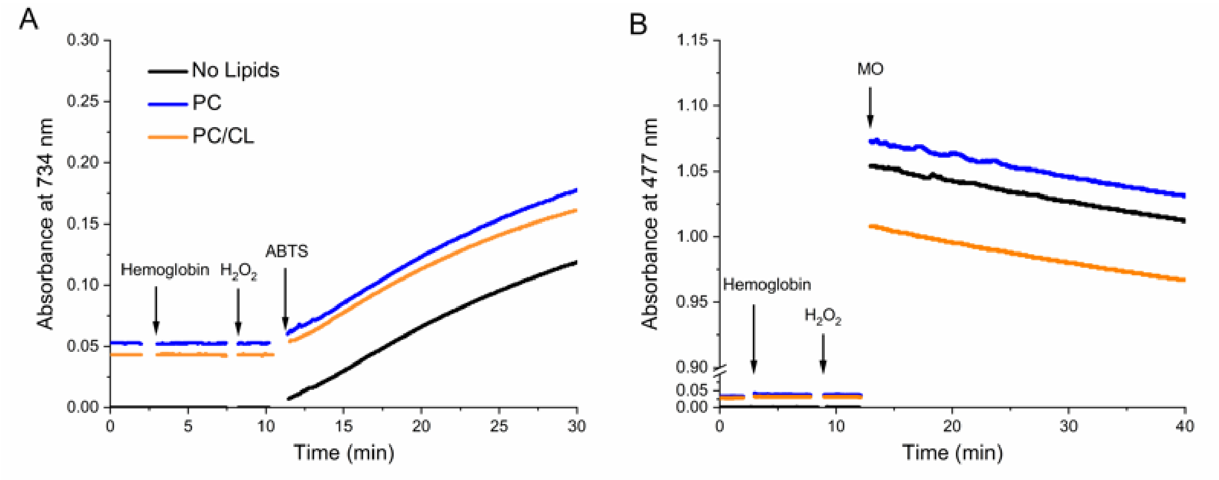

Figure 3.46 – Effect of phospholipid small unilamellar vesicles on (A) ABTS oxidation and (B) methyl orange decolorization by hemoglobin. Small unilamellar vesicles of phosphatidylcholine (PC) and PC/Cardiolipin (CL) were used at 200 µM. Assays were performed with 10 µg/mL of hemoglobin, 100 µM H_2O_2, and triggered with the addition of ABTS (100 µM) or methyl orange (30.6 µM), in phosphate buffer (20 mM, pH 7, supplemented with DTPA) at 25 ºC. The oxidation of ABTS was monitored at 734 nm and the decolorization of methyl orange was monitored at 477 nm. Control assays were performed in the absence of lipid vesicles.

Cc assays in the presence of PC SUVs did not show significant differences when compared to the control assays without lipids (Figure 3.47). However, the presence of CL-containing SUVs caused an increase in peroxidase activity of Cc in both ABTS oxidation and MO decolorization assays (Figure 3.47.A and B, respectively). Similar results were observed in assays containing higher Cc concentrations (50 µg/mL, 4 µM): no significant differences in peroxidase activity were observed between assays with and without PC SUVs, but the CL-containing SUVs increased the peroxidase activity (results not shown). The same CL-containing SUVs were tested for nonspecific interactions with the substrates used (ABTS and MO), in the absence of proteins, and no absorbance changes were observed.

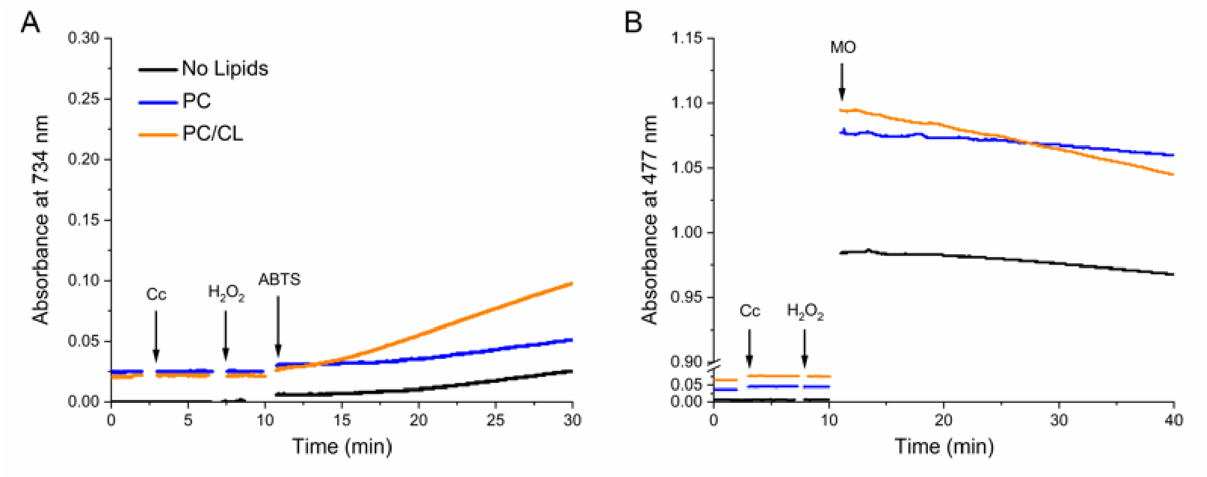

Figure 3.47 – Effect of phospholipid small unilamellar vesicles on (A) ABTS oxidation and (B) methyl orange decolorization by Cc. Small unilamellar vesicles of phosphatidylcholine (PC) and PC/Cardiolipin (CL) were used at 200 µM. Assays were performed with 12.5 µg/mL of Cc, 100 µM H_2O_2, and triggered with the addition of ABTS (100 µM) or methyl orange (30.6 µM), in phosphate buffer (20 mM, pH 7, supplemented with DTPA) at 25 ºC. The oxidation of ABTS was monitored at 734 nm and the decolorization of methyl orange was monitored at 477 nm. Control assays were performed in the absence of lipid vesicles.

The results obtained confirmed that CL enhances the peroxidase activity of Cc, whereas PC causes no effect. CL is an anionic phospholipid present in the inner mitochondrial membrane that associates to Cc through electrostatic and hydrophobic interactions and anchors the protein to the membrane (Díaz-Quintana *et al.* 2020). These interactions also promote structural changes in Cc which affect the coordination of the hemic Fe and consequently the redox properties of the protein and its function. The binding of Cc to CL-containing membranes has been reported to cause a negative shift in the redox potential of the protein and stimulate its peroxidase activity (Basova *et al.* 2007). The increase in ABTS oxidation and MO decolorization rates observed in the results with Cc (Figure 3.47) falls into accordance with the reported changes in redox proprieties caused by the structural alterations induced by CL.

3.8.2. Degradation of benzo[b]fluoranthene

Since the ability of Cc to oxidize a 3-ring PAH (anthracene) was already established in Section 3.6, it was decided to investigate the capacity of free and CL-bound Cc to transform a larger and more recalcitrant PAH, the 5-ring BbF (Table 3.1). BbF and benzo(k)fluoranthene are among the PAHs more resistant to laccase systems (Majcherczyk et al. 1998). Only CL-containing SUVs were tested since CL SUVs showed no effect in the peroxidase activity in ABTS oxidation and MO decolorization assays. The incubation assays with BbF were performed and analyzed as with anthracene, except that a Cc concentration of 1 µM was used (Section 2.7.1).

The enzymatic assays showed that Cc (without lipids) transformed approximately 9.1 ± 4.5% of the initial BbF and small peaks representing reaction products were observed at 2.84, 3.06, 4.05, 5.83, 6.08, 9.11, and 9.42 minutes in the chromatograms obtained (Figure 3.48). The formation of these reaction products was observed through small but consistent increases in the area of chromatographic peaks that were also detectable in the controls. In the incubation assays with CL-bound Cc, it was observed a higher transformation of BbF in comparison to free Cc. The assays resulted in 21.4 ± 5.7% transformation of BbF, a novel reaction product was observed at 9.87 minutes, and the peaks at 2.84, 3.06, 4.05 and 9.11 minutes possessed larger areas than observed with free Cc (Figure 3.48).

The results presented in this section reinforce that free and CL-bound Cc might participate in the metabolism of azo dyes and PAHs. In addition, the present results give support to the use of activators able to increase the peroxidase activity of Cc towards organic pollutants in technological applications.

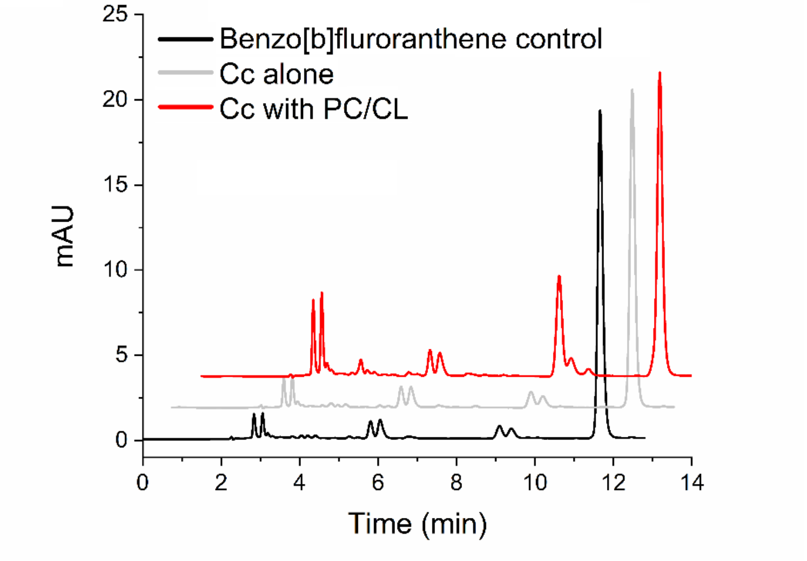

Figure 3.48 – HPLC chromatograms of BbF and degradation products generated by Cc in the absence and in the presence of CL-containing small unilamellar vesicles. Chromatograms are shown for a BbF control (1 mg/L) in the absence of Cc, BbF with Cc 12.5 µg/mL, and H_2O_2 100 µM with or without CL vesicles (200 µM). Incubation assays were carried in 20 mM phosphate buffer pH 7.0, in the absence of light, for 24h at 20 °C. The chromatograms are displaced in the vertical and horizontal axis for better observation. The chromatograms shown are representative results of triplicate assays for each reaction condition.

3.9. Studies of transformation of other PAHs and chlorpyrifos

The results presented in Sections 3.3, 3.4, and 3.6 showed the ability of laccase, HRP, and Cc, with or without ABTS, to catalyze the degradation of the dye MO and the PAH anthracene. The studies in the previous section also demonstrated the ability of Cc to directly oxidize BbF, at neutral pH and increased in the presence of mitochondria-mimicking lipid membranes. Therefore, it was important to investigate the capacity of the proteins to catalyze the transformation of other organic pollutants for bioremediation purposes. Additionally, the pollutants in this section are also relevant in human toxicology thus, the ability of Cc to transform these compounds is also important from a toxicology perspective.

3.9.1. Transformation of benzo[a]pyrene

Studies of BaP transformation were performed through incubation assays as before with other PAHs and described in Section 2.7.1. Incubation assays were carried for laccase and HRP with and without the addition of ABTS to the reactional media. Assays with Cc were carried only without ABTS since the results obtained in the previous degradation studies (Section 3.6) showed that ABTS did not provide any advantages for Cc. At the end of the 24h incubations, reactional media was extracted with hexane and the remaining BaP and generated products were analyzed.

Figure 3.49 shows the chromatograms of the hexane extracts of BaP incubation assays. No significant BaP transformation was observed in laccase incubations without ABTS but, with ABTS (50 µM), it was observed a transformation of 58 ± 19% of initial BaP and one major reaction product (considering the area) was detected at t_R 8.3 minutes (Figure 3.49.A).

In HRP incubations (Figure 3.49.B), it was observed a transformation of approximately 21 ± 18% and 21 ± 15% of initial BaP for assays without ABTS and with 50 µM of ABTS, respectively. In incubations containing ABTS, a reaction product was detected at t_R 8.3 minutes, while in incubations without ABTS reaction products were not observed. The absence of reactional products peaks does not support the idea that HRP (without ABTS) transformed BaP significantly that is evidenced by the decrease of the area of the peak corresponding to BaP in Figure 3.49.B. In addition, it was observed in Section 3.6 that, in the absence of ABTS, HRP was not able to significantly transform anthracene which is a more biodegradable PAH than BaP (Collins *et al*. 1996; Baldantoni *et al*. 2017). However, it is possible that HRP incubations without ABTS transformed BaP but produced different reactional products that do not absorb or absorb weakly at 266 nm or that are more hydrophilic and less soluble in the hexane extractant, hindering the hexane extraction.

Cc incubation assays showed a transformation of approximately 70 ± 4% of initial BaP and produced two major reaction products detected at t_R 5.47 and 5.69 minutes (Figure 3.49.C). The formation of other reaction products was observed by area increases of peaks that were also present in the chromatograms of the controls, for example at t_R 6.55 and 9.0 minutes.

Previous studies with the laccase-ABTS system in degradation of BaP, in acetate buffer, showed the formation of 6-benzo[a]pyrenyl acetate, in addition to BaP 1,6-, 3,6-, and 6,12-quinones as minor products (Cañas *et al*. 2007). The MW and logP of 6-benzo(a)pyrenyl acetate are 310 and 6, respectively, with a hydrophobicity similar to BaP, so if this compound is formed as a reaction product in the present work with laccase (Figure 3.49.A), the chromatographic peak of this BaP derivate cannot be differentiated from the peak of BaP. The logPs of the above-mentioned BaP quinones are between 3.9 and 4.3, and their MW is 282.3. Based on these logP values, the chromatographic peak observed in the chromatograms at t_R 8.2 probably corresponds to the BaP quinones reported by Cañas *et al.* (2007). The present work indicates that the same quinones are generated by the HRP-ABTS system (Figure 3.49.B).

Regarding Cc (Figure 3.49.C), other reaction products were observed in the chromatograms at t_R 9.0 minutes and at shorter t_R (approximately 5.5 to 6.5 minutes). The metabolism of BaP by cytochrome P450 monooxygenase has been well studied and BaP epoxides were reported as metabolites (Miller and Ramos 2001). The MW and logP of BaP 4,5-, 7,8-, and 9,10-oxides are 269.3 and 4.7. These log P values suggest that the chromatographic peak observed at t_R 9.0 minutes possibly corresponds to these BaP-oxides. Other chromatographic peaks are observed at the shorter t_Rs corresponding to reactional products with lower log P. BaP 7,8-diol-9,10-epoxide is a carcinogenic compound that is produced through metabolic activation in BaP metabolism, as mentioned in the Introduction. This compound possesses a log P of 2.9, so it is possible that one of the chromatographic peaks observed at short t_Rs corresponds to BaP 7,8-diol-9,10-epoxide.

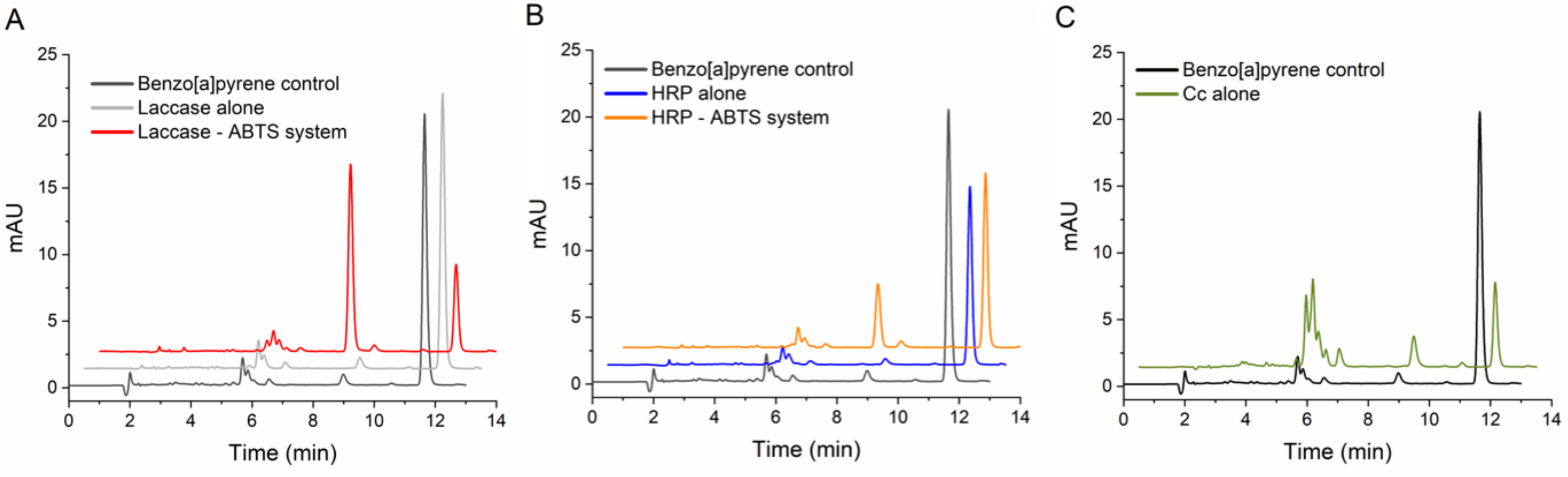

Figure 3.49 – HPLC chromatograms of BaP and degradation products generated by laccase, HRP, and Cc systems. Chromatograms are shown for (A) BaP with laccase 100 µg/mL with and without ABTS 50 µM, (B) BaP with HRP 0.2 µg/mL in the presence of H_2O_2 100 µM with and without ABTS 50 µM (C) and BaP with Cc 100 µg/mL with H_2O_2 100 µM without ABTS. A chromatogram corresponding to a BaP (1 mg/L) control incubation in the absence of protein is shown in the three panels. Incubation assays were carried in 100 mM acetate buffer pH 5.0, for 24h, in the absence of light, at 20 ºC. The chromatograms are displaced in the vertical and horizontal axis for better observation. The chromatograms shown are representative results of triplicate assays for each reaction condition.

3.9.2. Transformation of chlorpyrifos

Based on the successful degradation of PAHs observed before, it was decided to test the same enzymatic systems with the organophosphate pesticide chlorpyrifos through incubation assays with the same reactional conditions used in PAHs assays (Section 2.7.1).

The results of the transformation studies of chlorpyrifos are resumed in Table 3.9. The assays with the three proteins did not result in significant decrease in the concentration of chlorpyrifos and no formation of reactional products was observed (chromatograms not shown). The presence of ABTS in the laccase and HRP incubations also did not result in transformation of chlorpyrifos, showing that ABTS was unable to mediate the catalytic activity of the enzymes in the transformation of chlorpyrifos unlike what had been observed with MO, anthracene, and BaP.

The ability of laccases to transform chlorpyrifos is still debatable. A recent work with laccase from Trametes versicolor showed data pointing the degradation of the pesticide in soil (Das et al. 2020). However, the transformation of chlorpyrifos by laccase-mediator systems was previously studied by Jin *et al.* (2016) and reported significant transformation with the use of vanillin and syringaldehyde as mediators, but the laccase-ABTS system did not transform chlorpyrifos (Jin *et al*. 2016), similar to the results observed in the present work. Less expectable, HRP in conditions that afforded evident transformation of MO and PAHs was not able to transform the pesticide, nor Cc that previously presented an activity different of laccase and HRP against anthracene and BaP.

Table 3.9 – Results from transformation assays of chlorpyrifos by laccase, HRP, and Cc. Assays with 25 mg/L of chlorpyrifos were carried for laccase 100 µg/mL without ABTS and with ABTS 50 µM, HRP 0.2 µg/mL in the presence of H_2O_2 100 µM without ABTS and with ABTS 50 µM, and for Cc 100 µg/mL with H_2O_2 100 µM without ABTS. All assays were carried in 100 mM acetate buffer pH 5.0, in the absence of light, at 20 ºC. After 24 h incubation, the remaining chlorpyrifos concentration was compared to controls without protein, which were taken as 0% transformation. Results from triplicate assays are shown as Mean ± SE.

	Laccase		HRP		Cc
ABTS (µM)	0	50	0	50	0
Transformation (%)	16.3 ± 13.1	8.8 ± 7.2	5.5 ± 13.1	5.2 ± 13.9	-2.9 ± 10.9

3.9.3. Transformation of different PAHs by cytochrome c

Environmental occurrence and human exposition to PAHs usually occur as complex mixtures rather than single compounds (Lee 2010). Investigating the transformation of mixtures of PAHs allows to better test the biotechnological potential of enzymes and their toxicological role by representing more completely a contaminated environment or human exposition to the toxicants.

The previous studies indicated clearly that Cc can degrade extensively anthracene, BbF, and BaP in single solutions. In a final study, the capacity of Cc to transform PAHs in a complex mixture was challenged through 24h incubation assays, at pH 5.0 and 7.0, as described in Section 2.7.1.

The mixture of PAHs tested was designed considering published data on exposition of firefighters to these toxicants. Samples from skin surface of firefighters after a training session indicated the presence of BbF, benzo(k)fluoranthene, BaP, and BaA as the main PAHs (Stec *et al*. 2018). Urine analyses of firefighters after work shifts to characterize their total internal dose of PAHs revealed that 1-hydroxynaphthalene and 1-hydroxyacenaphthene were the predominant metabolites excreted in urine (Oliveira *et al*. 2017). On this basis, the PAHs mixture to test Cc was composed of BbF (20 mg/L), BaP (5 mg/L), BaA (5 mg/L), and naphthalene (0.5 mg/L).

Representative chromatograms of the hexane extracts of the assays with the mixture of PAHs are presented in Figure 3.50.A and B for the Cc incubations at pH 5.0 and 7.0, respectively. The peak at t_R 4.8 minutes corresponds to naphthalene, the peak at 9.8 minutes corresponds to BaA and the peak at 12.1 minutes corresponds to BaP plus BbF (similar t_R), as evidenced by the control assays shown in Figure 3.50.A and B. Transformation of PAHs was observed in Cc incubations both at pH 5.0 and pH 7.0 as evidenced by the decrease of the peak area of the initial PAHs and by the formation of several novel peaks of small areas at lower t_Rs. In general, higher Cc-catalyzed transformation of the PAHs was observed at pH 7.0 than at pH 5.0. At pH 7.0 it was observed a decrease in area of the peaks corresponding to naphthalene, BaA, and to BaP+BbF of 3 ± 6%, 22 ± 4%, and 23 ± 5%, respectively, in comparison to the control assays, while at pH 5.0 it was observed a decrease of 7 ± 6%, 10 ± 5%, and 12 ± 6% respectively.

These results show that Cc was able to transform the PAHs present in the mixture in high concentrations. The higher catalytical efficiency of Cc observed at neutral pH reinforces the hypothesis that Cc may participate in the metabolism of organic toxicants in the cells. Naphthalene was the compound that registered the lowest transformation values however, the relatively lower concentration of naphthalene in comparison to the other PAHs may be the cause for the lower transformation of naphthalene. Furthermore, it is possible that the initial naphthalene was more transformed than the results suggest because the transformation of the larger PAHs could have generated naphthalene or reaction products with similar t_Rs which would mask the peak decrease of naphthalene. Previous naphthalene degradation studies reported metabolites like 1,2- 1,4- and 1,7- naphthalenediol and 1,4-naphthoquinone that have low logP ranging from 1.7 and 2.2 (Cho *et al*. 2006) and, therefore, have lower hexane solubility. This would reduce extraction efficiency and explain the lack of chromatographic peaks of naphthalene transformation products.

Table 3.10 summarizes the t_Rs of the identified and unidentified chromatographic peaks observed in all assays of Cc-catalyzed transformation of PAHs. Transformation studies of the mixture of PAHs and of BbF produced chromatographic peaks with the same t_Rs (2.85 and 3.05-3.06 minutes). Additionally, the chromatograms of the transformation of the mixture of PAHs present a peak at 9.2 minutes, a similar t_R of a chromatographic peak observed in BbF and BaP transformation studies (9.11 and 9.0, respectively), suggesting that these peaks observed in the transformation of the mixture of PAHs correspond to reactional products of BaP, BbF or both.

The transformation studies carried for both individual PAHs and the mixture of PAHs resulted in the production of several chromatographic peaks however, the products to which they correspond remain unidentified and not quantified. Following studies for the identification of the generated oxidation products are of great interest to characterize the transformation pathways of the enzymatic systems investigated in the present work.

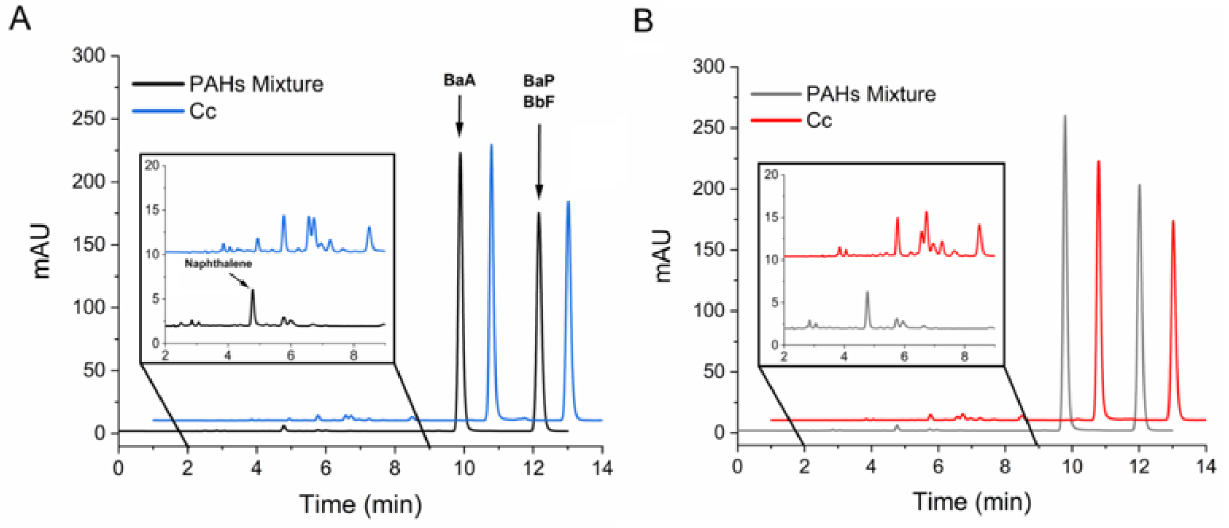

Figure 3.50 – HPLC chromatograms of a mixture of PAHs and degradation products generated by Cc. Chromatograms are shown for the PAH mixture incubated with and without Cc 100 µg/mL, in the presence of H_2O_2 100 µM, at pH 5.0 (A) and pH 7.0 (B). Incubations were carried in (A) 100 mM acetate buffer pH 5.0 and (B) 100 mM phosphate buffer pH 7.0, in the absence of light, at 20 ºC. A magnification of the chromatograms in the interval from 2 to 9 min is shown in the insets at each panel. The chromatograms (including in the magnification) are displaced in the vertical and horizontal axis for better observation. The chromatograms shown are representative results of triplicate assays for each reaction condition.

Table 3.10 – Summary of the retention times of the chromatographic peaks observed after incubations of polycyclic aromatic hydrocarbons with cytochrome *c*. The figures in the present work showing the chromatograms corresponding to incubations of each compound are indicated in the first column.

Parent compound	Retention Time (min)	Observations
Anthracene (Figure 3.20 in Section 3.4)	4.56	9,10-anthraquinone
	4.8	P1
	5.6	Peak with small area only observed in Cc assays without ABTS
	6.7	P2
	6.8	Anthracene
Benzo[b]fluoranthene (Figure 3.48 in Section 3.8)	2.84	Peaks with small areas observed in all assays, but with larger areas in Cc assays containing SUVs
	3.06	
	4.05	
	5.83	Peaks with small areas observed in controls and assays both with and without SUVs
	6.08	
	9.11	
	9.42	
	9.87	Peaks only observed in Cc assays containing SUVs
	11.7	BbF
Benzo[a]pyrene (Figure 3.49 in the present section)	5.47	Peak with small area observed in assays with Cc, but not with laccase nor HRP
	5.69	Peaks with small areas, observed in controls, but with larger areas in Cc assays
	5.87	
	6.11	
	6.55	
	9.0	
	10.56	Peak with small area, observed in controls and enzymatic assays, but with larger areas in Cc assays
	11.65	BaP
Mixture of PAHs: Naphthalene, benz[a]anthracene, benzo[a]pyrene and benzo[b]fluoranthene (Figure 3.50 in the present section)	2.85	Peaks observed in Cc assays at pH 5.0
	3.06	
	3.95	
	4.77	Naphthalene
	5.6	Peaks observed in Cc assays at pH 5.0 and 7.0
	5.7	
	7.5	
	8.9	
	9.2	
	9.8	BaA
	10.7	Peaks observed in Cc assays at pH 5.0
	10.8	
	12.1	BaP and BbF

4.

Conclusions

Pollution is a growing global transboundary problem that has been aggravated by the expanding industrialization and urbanization combined with inadequate waste management. The introduction of hazardous compounds in increasing amounts and chemical complexity alongside the continuous human exposure to them caused pollution to become the largest environmental cause of disease and premature death.

Some enzymes have the ability to efficiently transform organic pollutants into less toxic compounds. Enzymes play an important role in the detoxification of the organic pollutants to which humans are exposed on a daily basis. Furthermore, enzymatic remediation represents an alternative for environmental decontamination processes.

In this work, the capacity of laccase from *Tramates versicolor*, HRP, hemoglobin, and Cc to transform environmentally concerning pollutants was investigated to better understand the mechanisms and the potential role of hemoglobin and Cc in human metabolism and to explore their potential for the development of novel biocatalyst-based remediation technologies.

Enzymatic activity assessed through ABTS oxidation assays demonstrated that HRP and laccase exhibit high catalytic activity at acid pH, but not at neutral-alkaline pHs, while Cc showed lower enzymatic activity at acid pH but maintained activity at neutral pH.

Having in mind bioremediation applications, the use of enzyme-ABTS systems for the transformation of organic pollutants was investigated. Important for process optimization, low concentrations of ABTS (in the µM range) were enough to substantially promote laccase-catalyzed degradation of MO and PAHs. On the other hand, HRP, hemoglobin, and Cc efficiently decolorized MO without requiring ABTS and its presence did not improve the catalysis. It was also observed that the decrease of MO concentration in the media and H_2O_2 exhaustion limit the MO decolorization by the hemeproteins proteins. Nevertheless, a relatively low concentration of H_2O_2 was used in all the assays of peroxidase and peroxidase-like proteins to avoid auto-oxidation/inactivation processes (and physiologically irrelevant conditions). Hemoglobin also demonstrated the capacity to decolorize MO without requiring mediators, but its catalytic capacity rapidly decreased as the protein inactivated.

HRP was unable to oxidize anthracene without mediators but, in the presence of ABTS, it efficiently catalyzed the oxidation of anthracene and BaP, reinforcing the capacity of ABTS to mediate enzymatic PAH transformation and the bioremediation potential of HRP. Contrarily, Cc showed an evident capacity to transform PAHs without requiring mediators. The major reactional product (based on the peak area) from anthracene oxidation by laccase- and HRP-ABTS systems, and also by Cc alone, was 9, 10-anthraquinone.

Using ABTS in BaP oxidation, the same major product (based on the peak area) was observed with laccase- and HRP-ABTS systems while Cc transformed BaP in diverse products of oxidation however, none of them included the product obtained with the enzyme-ABTS systems.

The ability of the laccase- and HRP-ABTS systems and of Cc was further tested with the organophosphate pesticide chlorpyrifos however, despite the potential demonstrated with MO and PAHs, the enzymatic systems were unable to transform chlorpyrifos. The transformation capacity of Cc was further challenged against a mixture of PAHs and it was observed that Cc was capable of catalyzing the transformation of 4 different PAHs simultaneously without requiring mediators. The transformation of the PAHs catalyzed by Cc was more evident at pH 7.0 than at pH 5.0.

The bioremediation potential of these systems was additionally investigated in the presence of HA. The results showed an inhibitory effect in the degradation of MO and anthracene by laccase, HRP, and Cc. Further assays revealed that ABTS oxidation by laccase and HRP was also inhibited, and one of the mechanisms behind the decrease in ABTS oxidation was identified as quenching of the ABTS radical by HA. However, the quenching observed does not completely justify the inhibition observed in pollutant transformation by laccase- and HRP-ABTS systems. Therefore, additional mechanisms exist behind the inhibitory effect of HA. Further investigation of these inhibition mechanisms of HA is required and it could be beneficial to minimize this effect in remediation processes.

The other aim of the present work was to investigate the potential role of hemoglobin and Cc in the metabolism of organic toxicants. Upon investigating the influence of lipid vesicles in the peroxidase activity of these hemeproteins, it was observed that CL increased the peroxidase activity of Cc, enhancing azo dye decolorization and PAH transformation. The ability of Cc to transform organic toxicants (in the presence of H_2O_2), at physiological pH, alongside the increased peroxidase activity observed in the presence of CL-containing membranes, suggests that Cc can participate in the metabolism of organic toxicants, especially in the mitochondria.

The same studies were performed for hemoglobin however lipid vesicles produced no significant effect on the peroxidase activity of hemoglobin. Nevertheless, hemoglobin showed an ability to decolorize MO comparable to HRP and partly retained it at neutral pH, suggesting a potential role in the *in vivo* transformation of azo dyes and other environmental toxicants. In this line, during the period of this work, it was reported the ability of hemoglobin to catalyze the oxidation of BaP (Keum et al. 2021).

In future works, bioremediation studies could be followed through the optimization of reactional conditions to augment the catalytic efficiency of the proteins. Cc showed potential for bioremediation that could be further explored through the induction of peroxidase activity caused by the lipid-protein interaction observed.

The present work lends evidences supporting the hypothesis that Cc participates in the metabolism of organic toxicants. It also reinforces the potential of HRP for bioremediation applications which is capable of transforming organic pollutants without requiring mediators in some cases, althought the use of mediators can enhance the applicability of the enzyme to other compounds. It is also reported the bioremediation potential of Cc which was shown able to transform organic pollutants at different pHs and without requiring mediators. Anthracene degradation by laccase- and HRP-ABTS systems and Cc resulted in the formation of the same reactional product, 9, 10-anthraquinone, however, BaP degradation by Cc generated diverse reactional products that deserve further studies.

References

AAT Bioquest, Inc. 2021. "Acetate Buffer (PH 3.6 to 5.6) Preparation." 2021. https://www.aatbio.com/resources/buffer-preparations-and-recipes/acetate-buffer-ph-3-6-to-5-6.

AAT Bioquest, Inc. 2020. "Phosphate Buffer (PH 5.8 to 7.4) Preparation." 2020. https://www.aatbio.com/resources/buffer-preparations-and-recipes/phosphate-buffer-ph-5-8-to-7-4.

Abdel-Hamid, Ahmed M., Jose O. Solbiati, and Isaac K.O. Cann. 2013. "Insights into Lignin Degradation and Its Potential Industrial Applications." In *Advances in Applied Microbiology*, edited by Sima Sariaslani and Geoffrey M. Gadd, 82:1–28. Illinois: Elsevier. https://doi.org/10.1016/B978-0-12-407679-2.00001-6.

Abdel-Shafy, Hussein I., and Mona S.M. Mansour. 2016. "A Review on Polycyclic Aromatic Hydrocarbons: Source, Environmental Impact, Effect on Human Health and Remediation." *Egyptian Journal of Petroleum* 25 (1): 107–23. https://doi.org/10.1016/j.ejpe.2015.03.011.

Acevedo, F., L. Pizzul, M.dP. Castillo, M.E. González, M. Cea, L. Gianfreda, and M.C. Diez. 2010. "Degradation of Polycyclic Aromatic Hydrocarbons by Free and Nanoclay-Immobilized Manganese Peroxidase from Anthracophyllum Discolor." *Chemosphere* 80 (3): 271–78. https://doi.org/10.1016/j.chemosphere.2010.04.022.

Adeniji, Abiodun Olagoke, Omobola Oluranti Okoh, and Anthony Ifeanyi Okoh. 2018. "Analytical Methods for Polycyclic Aromatic Hydrocarbons and Their Global Trend of Distribution in Water and Sediment: A Review." *Recent Insights in Petroleum Science and Engineering*. https://doi.org/10.5772/intechopen.71163.

Adeola, Adedapo O., and Patricia B. C. Forbes. 2021. "Advances in Water Treatment Technologies for Removal of Polycyclic Aromatic Hydrocarbons: Existing Concepts, Emerging Trends, and Future Prospects." *Water Environment Research* 93 (3): 343–59. https://doi.org/10.1002/wer.1420.

Aeschbacher, Michael, Cornelia Graf, René P. Schwarzenbach, and Michael Sander. 2012. "Antioxidant Proprieties of Humic Acid." *Environmental Science and Technology* 46: 4916–25.

Agrawal, Archana, S. Kumari, and K. K. Sahu. 2009. "Iron and Copper Recovery/Removal from Industrial Wastes: A Review." *Industrial and Engineering Chemistry Research* 48 (13): 6145–61. https://doi.org/10.1021/ie900135u.

Ahmed, Ahmed Thabet, Munif A. Othman, Vasudeo D. Sarwade, and Gawai R. Kachru. 2012. "Degradation of Anthracene by Alkaliphilic Bacteria Bacillus Badius." *Environment and Pollution* 1 (2): 97–104. https://doi.org/10.5539/ep.v1n2p97.

Akbar, Hameed, Divine Mensah Sedzro, Mazhar Khan, Sm Faysal Bellah, and S M Saker Billah. 2018. "Structure , Function and Applications of a Classic Enzyme : Horseradish." *Journal of Chemical, Environmental and Biological Engineering* 2 (2): 52–59. https://doi.org/10.11648/j.jcebe.20180202.13.

Alcalde, Miguel. 2007. "Laccases: Biological Functions, Molecular Structure and Industrial Applications." In *Industrial Enzymes*, edited by J. Polaina and A.P. MacCabe, 461–76. Dordrecht: Springer, Netherlands. https://doi.org/10.1007/1-4020-5377-0_26.

Alcalde, Miguel, Thomas Bulter, and Frances H. Arnold. 2002. "Colorimetric Assays for Biodegradation of Polycyclic Aromatic Hydrocarbons by Fungal Laccases." *Journal of Biomolecular Screening* 7 (6): 547–53. https://doi.org/10.1177/1087057102238629.

Allison, Steven D. 2006. “Soil Minerals and Humic Acids Alter Enzyme Stability: Implications for Ecosystem Processes.” *Biogeochemistry* 81 (3): 361–73. https://doi.org/10.1007/s10533-006-9046-2.

Almansa, Eva, Andreas Kandelbauer, Luciana Pereira, Artur Cavaco-Paulo, and Georg M. Guebitz. 2004. “Influence of Structure on Dye Degradation with Laccase Mediator Systems.” *Biocatalysis and Biotransformation* 22 (5–6): 315–24. https://doi.org/10.1080/10242420400024508.

Ambatkar, Mugdha, and Usha Mukundan. 2015. “Enzymatic Decolourisation of Methyl Orange and Bismarck Brown Using Crude Peroxidase from Armoracia Rusticana.” *Applied Water Science* 5 (4): 397–406. https://doi.org/10.1007/s13201-014-0197-3.

Arca-Ramos, A., G. Eibes, G. Feijoo, J.M. Lema, and M.T. Moreira. 2015. “Coupling Extraction and Enzyme Catalysis for the Removal of Anthracene Present in Polluted Soils.” *Biochemical Engineering Journal* 93: 289–93. https://doi.org/10.1016/j.bej.2014.10.015.

Arregui, Leticia, Marcela Ayala, Ximena Gómez-Gil, Guadalupe Gutiérrez-Soto, Carlos Eduardo Hernández-Luna, Mayra Herrera de los Santos, Laura Levin, et al. 2019. “Laccases: Structure, Function, and Potential Application in Water Bioremediation.” *Microbial Cell Factories* 18 (1): 200. https://doi.org/10.1186/s12934-019-1248-0.

Ashraf, Muhammad Aqeel. 2017. “Persistent Organic Pollutants (POPs): A Global Issue, a Global Challenge.” *Environmental Science and Pollution Research* 24 (5): 4223–27. https://doi.org/10.1007/s11356-015-5225-9.

Atalla, M. Mabrouk, H. Kheiralla Zeinab, R. Hamed Eman, A. Youssry Amani, and A. Abd El Aty Abeer. 2013. “Characterization and Kinetic Properties of the Purified Trematosphaeria Mangrovei Laccase Enzyme.” *Saudi Journal of Biological Sciences* 20 (4): 373–81. https://doi.org/10.1016/j.sjbs.2013.04.001.

Ayala, Marcela. 2010. “Biocatalysis Based on Heme Peroxidases.” In *Biocatalysis Based on Heme Peroxidases: Peroxidases as Potential Industrial Biocatalysts*, edited by Eduardo Torres and Marcela Ayala, 1–358. Berlin, Heidelberg: Springer Berlin Heidelberg. https://doi.org/10.1007/978-3-642-12627-7.

Azevedo, Ana M., Verónica C. Martins, Duarte M.F. Prazeres, Vojislav Vojinović, Joaquim M.S. Cabral, and Luís P. Fonseca. 2003. “Horseradish Peroxidase: A Valuable Tool in Biotechnology.” *Biotechnology Annual Review* 9 (03): 199–247. https://doi.org/10.1016/S1387-2656(03)09003-3.

Baali, Ayoub, and Ahmed Yahyaoui. 2020. “Polycyclic Aromatic Hydrocarbons (PAHs) and Their Influence to Some Aquatic Species.” In *Biochemical Toxicology - Heavy Metals and Nanomaterials*, edited by Muharrem Ince, Olcay Kaplan, and Gabrijel Ondrasek. IntechOpen. https://doi.org/10.5772/intechopen.86213.

Babu, A. Giridhar, Shahi I. Reja, Nadeem Akhtar, Mehar Sultana, Prashant S. Deore, and Farukh I. Ali. 2019. “Bioremediation of Polycyclic Aromatic Hydrocarbons (PAHs): Current Practices and Outlook.” In *Microbial Metabolism of Xenobiotic Compounds*, edited by Pankaj Kumar Arora, 1st ed., 189–216. Singapore: Springer. https://doi.org/10.1007/978-981-13-7462-3_9.

Baldantoni, Daniela, Raffaella Morelli, Alessandro Bellino, Maria Vittoria Prati, Anna Alfani, and Flavia De Nicola. 2017. “Anthracene and Benzo(a)Pyrene Degradation in Soil Is Favoured by Compost Amendment: Perspectives for a Bioremediation Approach.” *Journal of Hazardous Materials* 339: 395–400. https://doi.org/10.1016/j.jhazmat.2017.06.043.

Baldrian, Petr. 2006. “Fungal Laccases-Occurrence and Properties.” *FEMS Microbiology Reviews* 30 (2): 215–42. https://doi.org/10.1111/j.1574-4976.2005.00010.x.

Bansal, Neelam, and Shamsher S. Kanwar. 2013. “Peroxidase(s) in Environment Protection.” *The Scientific World Journal* 2013: 1–9. https://doi.org/10.1155/2013/714639.

Barayeu, Uladzimir, Mike Lange, Lucía Méndez, Jürgen Arnhold, Oleg I. Shadyro, Maria Fedorova, and Jörg Flemmig. 2019. “Cytochrome c Autocatalyzed Carbonylation in the Presence of Hydrogen Peroxide and Cardiolipins.” *Journal of Biological Chemistry* 294 (6): 1816–30. https://doi.org/10.1074/jbc.RA118.004110.

Basova, Liana V., Igor V. Kurnikov, Lei Wang, Vladimir B. Ritov, Natalia A. Belikova, Irina I. Vlasova, Andy A. Pacheco, et al. 2007. “Cardiolipin Switch in Mitochondria: Shutting off the Reduction of Cytochrome c and Turning on the Peroxidase Activity.” *Biochemistry* 46 (11): 3423–34. https://doi.org/10.1021/bi061854k.

Bennett, Gary F. 1995. *In Situ Bioremediation: When Does It Work? Journal of Hazardous Materials*.

Vol. 42. Washington, D.C.: National Academy Press. https://doi.org/10.1016/S0304-3894(95)90047-0.

Bibi, Nadia, Muhammad Hamayun, Sumera Afzal Khan, Amjad Iqbal, Badshah Islam, Farooq Shah, Muhammad Aaqil Khan, and In Jung Lee. 2018. “Anthracene Biodegradation Capacity of Newly Isolated Rhizospheric Bacteria Bacillus Cereus S13.” *PLoS ONE* 13 (8). https://doi.org/10.1371/journal.pone.0201620.

Bielińska, Elżbieta J., Barbara Futa, Aleksandra Ukalska-Jaruga, Jerzy Weber, Szymon Chmielewski, Sylwia Wesołowska, Agnieszka Mocek-Płóciniak, Krzysztof Patkowski, and Lilla Mielnik. 2018. “Mutual Relations between PAHs Derived from Atmospheric Deposition, Enzymatic Activity, and Humic Substances in Soils of Differently Urbanized Areas.” *Journal of Soils and Sediments* 18 (8): 2682–91. https://doi.org/10.1007/s11368-018-1937-z.

Bleam, William. 2017. *Natural Organic Matter*. *Soil and Environmental Chemistry*. https://doi.org/10.1016/b978-0-12-804178-9.00007-0.

Bourbonnais, Robert, and Michael G. Paice. 1990. “Oxidation of Non-Phenolic Substrates.” *FEBS Letters* 267 (1): 99–102. https://doi.org/10.1016/0014-5793(90)80298-W.

Bowman, B. T., and W. W. Sans. 1983. “Determination of Octanol-Water Partitioning Coefficients (Kow) of 61 Organophosphorus and Carbamate Insecticides and Their Relationship to Respective Water Solubility (s) Values.” *Journal of Environmental Science and Health, Part B* 18 (6): 667–83. https://doi.org/10.1080/03601238309372398.

Brigelius-Flohé, Regina, and Matilde Maiorino. 2013. “Glutathione Peroxidases.” *Biochimica et Biophysica Acta* 1830 (5): 3289–3303. https://doi.org/10.1016/j.bbagen.2012.11.020.

Buettner, Garry R. 2008. “DETAPAC (DTPA), Aqueous Stock Solution.” 2008. https://www.healthcare.uiowa.edu/corefacilities/esr/protocols/detapac/DETAPAC-Protocol.pdf.

Burke, Richard D., Spencer W. Todd, Eric Lumsden, Roger J. Mullins, Jacek Mamczarz, William P. Fawcett, Rao P. Gullapalli, William R. Randall, Edna F. R. Pereira, and Edson X. Albuquerque. 2017. “Developmental Neurotoxicity of the Organophosphorus Insecticide Chlorpyrifos: From Clinical Findings to Preclinical Models and Potential Mechanisms.” *Journal of Neurochemistry* 142 (3): 162–77. https://doi.org/10.1111/jnc.14077.

Cai, Huahua, Xin Liu, Jing Zou, Junyang Xiao, Baoling Yuan, Fei Li, and Qingfeng Cheng. 2018. “Multi-Wavelength Spectrophotometric Determination of Hydrogen Peroxide in Water with Peroxidase-Catalyzed Oxidation of ABTS.” *Chemosphere* 193: 833–39. https://doi.org/10.1016/j.chemosphere.2017.11.091.

Cañas, Ana I., Miguel Alcalde, Francisco Plou, María Jesús Martínez, Ángel T. Martínez, and Susana Camarero. 2007. “Transformation of Polycyclic Aromatic Hydrocarbons by Laccase Is Strongly Enhanced by Phenolic Compounds Present in Soil.” *Environmental Science and Technology* 41 (8): 2964–71. https://doi.org/10.1021/es062328j.

Cañas, Ana I., and Susana Camarero. 2010. “Laccases and Their Natural Mediators: Biotechnological Tools for Sustainable Eco-Friendly Processes.” *Biotechnology Advances* 28 (6): 694–705. https://doi.org/10.1016/j.biotechadv.2010.05.002.

Cano, Antonio, Olga Alcaraz, Manuel Acosta, and Marino B. Arnao. 2002. “On-Line Antioxidant Activity Determination: Comparison of Hydrophilic and Lipophilic Antioxidant Activity Using the ABTS•+ Assay.” *Redox Report* 7 (2): 103–9. https://doi.org/10.1179/135100002125000334.

Cantarella, Gaetano, Carlo Galli, and Patrizia Gentili. 2003. “Free Radical versus Electron-Transfer Routes of Oxidation of Hydrocarbons by Laccase/Mediator Systems.” *Journal of Molecular Catalysis B: Enzymatic* 22 (3–4): 135–44. https://doi.org/10.1016/S1381-1177(03)00014-6.

Castegnaro, M, G. Grimmer, O. Hutzinger, W. Karcher, H. Kunte, M. LaFontaine, E.B Sansone, G. Telling, and S.P. Tucker. 1983. “Laboratory Decontamination and Destruction of Carcinogens in Laboratory Wastes: Some Polycyclic Aromatic Hydrocarbons.” *International Agency for Research on Cancer* 49: 45.

Chang, Yunkang, Dandan Yang, Rui Li, Tao Wang, and Yimin Zhu. 2021. “Textile Dye Biodecolorization by Manganese Peroxidase: A Review.” *Molecules* 26 (15): 4403. https://doi.org/10.3390/molecules26154403.

Chernykh, A., N. Myasoedova, M. Kolomytseva, M. Ferraroni, F. Briganti, A. Scozzafava, and L. Golovleva. 2008. “Laccase Isoforms with Unusual Properties from the Basidiomycete Steccherinum Ochraceum Strain 1833.” *Journal of Applied Microbiology* 105 (6): 2065–75.

https://doi.org/10.1111/j.1365-2672.2008.03924.x.

Chianese, Simeone, Angelo Fenti, Pasquale Iovino, Dino Musmarra, and Stefano Salvestrini. 2020. "Sorption of Organic Pollutants by Humic Acids: A Review." *Molecules* 25 (4): 918. https://doi.org/10.3390/molecules25040918.

Cho, Taehyeon M., Randy L. Rose, and Ernest Hodgson. 2006. "In Vitro Metabolism of Naphthalene by Human Liver Microsomal Cytochrome P450 Enzymes." *Drug Metabolism and Disposition* 34 (1): 176–83. https://doi.org/10.1124/dmd.105.005785.

Choi, Kyoungju, Hyun Joo, Randy L. Rose, and Ernest Hodgson. 2006. "Metabolism of Chlorpyrifos and Chlorpyrifos Oxon by Human Hepatocytes." *Journal of Biochemical and Molecular Toxicology* 20 (6): 279–91. https://doi.org/10.1002/jbt.20145.

Christopher, Lew Paul, Bin Yao, and Yun Ji. 2014. "Lignin Biodegradation with Laccase-Mediator Systems." *Frontiers in Energy Research* 2: 1–13. https://doi.org/10.3389/fenrg.2014.00012.

Coates, Christopher J., and Heinz Decker. 2017. "Immunological Properties of Oxygen-Transport Proteins: Hemoglobin, Hemocyanin and Hemerythrin." *Cellular and Molecular Life Sciences* 74 (2): 293–317. https://doi.org/10.1007/s00018-016-2326-7.

Collin, Gerd, Hartmut Höke, and Helmut Greim. 2003. "Naphthalene and Hydronaphthalenes." *Ullmann's Encyclopedia of Industrial Chemistry* 23: 661–70. https://doi.org/10.1002/14356007.a17_001.pub2.

Collins, Patrick J., Michiel J.J. Kotterman, Jim A. Field, and Alan D.W. Dobson. 1996. "Oxidation of Anthracene and Benzo[a]Pyrene by Laccases from Trametes Versicolor." *Applied and Environmental Microbiology* 62 (12): 4563–67. https://doi.org/10.1128/aem.62.12.4563-4567.1996.

Cozzolino, A., and A. Piccolo. 2002. "Polymerization of Dissolved Humic Substances Catalyzed by Peroxidase. Effects of PH and Humic Composition." *Organic Geochemistry* 33 (3): 281–94. https://doi.org/10.1016/S0146-6380(01)00160-7.

Criquet, S., A.M Farnet, S. Tagger, and J. Le Petit. 2000. "Annual Variations of Phenoloxidase Activities in an Evergreen Oak Litter: Influence of Certain Biotic and Abiotic Factors." *Soil Biology and Biochemistry* 32 (11–12): 1505–13. https://doi.org/10.1016/S0038-0717(00)00027-4.

D'Acunzo, Francesca, and Carlo Galli. 2003. "First Evidence of Catalytic Mediation by Phenolic Compounds in the Laccase-Induced Oxidation of Lignin Models." *European Journal of Biochemistry* 270 (17): 3634–40. https://doi.org/10.1046/j.1432-1033.2003.03752.x.

Dalal, Sohel, and Munishwar Nath Gupta. 2007. "Treatment of Phenolic Wastewater by Horseradish Peroxidase Immobilized by Bioaffinity Layering." *Chemosphere* 67 (4): 741–47. https://doi.org/10.1016/j.chemosphere.2006.10.043.

Dar, Mohd Ashraf, Garima Kaushik, and Juan Fransisco Villarreal-Chiu. 2019. "Pollution Status and Bioremediation of Chlorpyrifos in Environmental Matrices by the Application of Bacterial Communities: A Review." *Journal of Environmental Management* 239: 124–36. https://doi.org/10.1016/j.jenvman.2019.03.048.

Das, Anamika, Vijay Jaswal, and K.N. Yogalakshmi. 2020. "Degradation of Chlorpyrifos in Soil Using Laccase Immobilized Iron Oxide Nanoparticles and Their Competent Role in Deterring the Mobility of Chlorpyrifos." *Chemosphere* 246: 125676. https://doi.org/10.1016/j.chemosphere.2019.125676.

Deere, Joseph, Edmond Magner, J. Gerard Wall, and B. Kieran Hodnett. 2003. "Oxidation of ABTS by Silicate-Immobilized Cytochrome c in Nonaqueous Solutions." *Biotechnology Progress* 19 (4): 1238–43. https://doi.org/10.1021/bp0340537.

Dev, Som, and Jodie L. Babitt. 2017. "Overview of Iron Metabolism in Health and Disease." *Hemodialysis International* 21 (Suppl 1): S6–20. https://doi.org/10.1111/hdi.12542.

Díaz-Quintana, Antonio, Gonzalo Pérez-Mejías, Alejandra Guerra-Castellano, Miguel A. De la Rosa, and Irene Díaz-Moreno. 2020. "Wheel and Deal in the Mitochondrial Inner Membranes: The Tale of Cytochrome c and Cardiolipin." *Oxidative Medicine and Cellular Longevity* 2020: 1–20. https://doi.org/10.1155/2020/6813405.

Diederix, Rutger E. M., Marcellus Ubbink, and Gerard W. Canters. 2002. "Peroxidase Activity as a Tool for Studying the Folding of c -Type Cytochromes." *Biochemistry* 41 (43): 13067–77. https://doi.org/10.1021/bi0260841.

Dong, Shiming, Shuguang Wang, Gernerique Stewart, Huey Min Hwang, Peter P. Fu, and Hongtao Yu. 2002. "Effect of Organic Solvents and Biologically Relevant Ions on Thelight-Induced DNA Cleavage by Pyrene and Its Amino and Hydroxy Derivatives." *International Journal of Molecular Sciences* 3 (9): 937–47. https://doi.org/10.3390/i3090937.

Eaton, David L., Robert B. Daroff, Herman Autrup, James Bridges, Patricia Buffler, Lucio G. Costa, Joseph Coyle, et al. 2008. "Review of the Toxicology of Chlorpyrifos With an Emphasis on Human Exposure and Neurodevelopment." *Critical Reviews in Toxicology* 38 (sup2): 1–125. https://doi.org/10.1080/10408440802272158.

Efimova, I. V., S. L. Khil'ko, and O. V. Smirnova. 2012. "Antioxidant Activity of Humic Acids in Radical-Chain Oxidation Processes." *Russian Journal of Applied Chemistry* 85 (9): 1351–54. https://doi.org/10.1134/S1070427212090091.

Eibes, G., T. Lú-Chau, G. Feijoo, M. T. Moreira, and J. M. Lema. 2005. "Complete Degradation of Anthracene by Manganese Peroxidase in Organic Solvent Mixtures." *Enzyme and Microbial Technology* 37 (4): 365–72. https://doi.org/10.1016/j.enzmictec.2004.02.010.

Eibes, Gemma, Tomas Cajthaml, Maria Teresa Moreira, Gumersindo Feijoo, and Juan M. Lema. 2006. "Enzymatic Degradation of Anthracene, Dibenzothiophene and Pyrene by Manganese Peroxidase in Media Containing Acetone." *Chemosphere* 64 (3): 408–14. https://doi.org/10.1016/j.chemosphere.2005.11.075.

Errede, B., G. P. Haight, and M. D. Kamen. 1976. "Oxidation of Ferrocytochrome c by Mitochondrial Cytochrome c Oxidase." *Proceedings of the National Academy of Sciences of the United States of America* 73 (1): 113–17. https://doi.org/10.1073/pnas.73.1.113.

EU. 1998. "Council Directive 98/83/EC of 3 November 1998 on the Quality of Water Intended for Human Consumption." 1998. https://eur-lex.europa.eu/legal-content/EN/TXT/?uri=celex:31998L0083.

Everse, Johannes. 2004. "Heme Proteins." Edited by William J Lennarz and M Daniel B T - Encyclopedia of Biological Chemistry Lane. *Encyclopedia of Biological Chemistry* 2: 354–61. https://doi.org/https://doi.org/10.1016/B0-12-443710-9/00304-5.

Fan, Jing, Yanhui Guo, Jianji Wang, and Maohong Fan. 2009. "Rapid Decolorization of Azo Dye Methyl Orange in Aqueous Solution by Nanoscale Zerovalent Iron Particles." *Journal of Hazardous Materials* 166 (2–3): 904–10. https://doi.org/10.1016/j.jhazmat.2008.11.091.

Field, J. A., E. De Jong, G. F. Costa, and J. A.M. De Bont. 1992. "Biodegradation of Polycyclic Aromatic Hydrocarbons by New Isolates of White Rot Fungi." *Applied and Environmental Microbiology* 58 (7): 2219–26. https://doi.org/10.1128/aem.58.7.2219-2226.1992.

Fowler, Lewis, Walter N. Trump, and Carl E. Vogler. 1968. "Vapor Pressure of Naphthalene: New Measurements between 40° and 180° C." *Journal of Chemical and Engineering Data* 13 (2): 209–10. https://doi.org/10.1021/je60037a020.

Gholami-Borujeni, Fathollah, Amir Hossein Mahvi, Simin Naseri, Mohammad Ali Faramarzi, Ramin Nabizadeh, and Mahmood Alimohammadi. 2011. "Application of Immobilized Horseradish Peroxidase for Removal and Detoxification of Azo Dye from Aqueous Solution." *Research Journal of Chemistry and Environment* 15 (2): 217–22.

Gianfreda, Liliana, Feng Xu, and Jean-Marc Bollag. 1999. "Laccases: A Useful Group of Oxidoreductive Enzymes." *Bioremediation Journal* 3 (1): 1–26. https://doi.org/10.1080/10889869991219163.

Gorinova, N., M. Nedkovska, and A. Atanassov. 2005. "Cytochrome P450 Monooxygenases as a Tool for Metabolizing of Herbicides in Plants." *Biotechnology and Biotechnological Equipment* 19: 105–15. https://doi.org/10.1080/13102818.2005.10817290.

Greaves, Alana K., and Robert J. Letcher. 2016. "A Review of Organophosphate Esters in the Environment from Biological Effects to Distribution and Fate." *Bulletin of Environmental Contamination and Toxicology* 98 (1): 2–7. https://doi.org/10.1007/s00128-016-1898-0.

Gündüz, Bayram. 2013. "Effects of Molarity and Solvents on the Optical Properties of the Solutions of Tris[4-(5-Dicyanomethylidenemethyl-2-Thienyl)Phenyl]Amine (TDCV-TPA) and Structural Properties of Its Film." *Optical Materials* 36 (2): 425–36. https://doi.org/10.1016/j.optmat.2013.10.005.

Guzik, Urszula, Katarzyna Hupert-Kocurek, and Danuta Wojcieszyńska. 2014. "Immobilization as a Strategy for Improving Enzyme Properties-Application to Oxidoreductases." *Molecules* 19 (7):

8995–9018. https://doi.org/10.3390/molecules19078995.

Hansch, C, A Leo, D H Hoekman, and American Chemical Society. 1995. *Exploring QSAR.: Hydrophobic, Electronic, and Steric Constants*. Edited by C Hansch, A Leo, and DH Hoekman. ACS Professional Reference Book. American Chemical Society. https://books.google.nl/books?id=_LzYAQAACAAJ.

Hart, J. Roger. 2011. "Ethylenediaminetetraacetic Acid and Related Chelating Agents." *Ullmann's Encyclopedia of Industrial Chemistry* 13: 573–78. https://doi.org/10.1002/14356007.a10_095.pub2.

Herwijnen, René Van, Dirk Springael, Pieter Slot, Harrie A.J. Govers, and John R. Parsons. 2003. "Degradation of Anthracene by Mycobacterium Sp. Strain LB501T Proceeds via a Novel Pathway, through o-Phthalic Acid." *Applied and Environmental Microbiology* 69 (1): 186–90. https://doi.org/10.1128/AEM.69.1.186-190.2003.

Hilgers, Roelant, Jean-Paul Vincken, Harry Gruppen, and Mirjam A. Kabel. 2018. "Laccase/Mediator Systems: Their Reactivity toward Phenolic Lignin Structures." *ACS Sustainable Chemistry & Engineering* 6 (2): 2037–46. https://doi.org/10.1021/acssuschemeng.7b03451.

Hofrichter, Martin. 2002. "Review: Lignin Conversion by Manganese Peroxidase (MnP)." *Enzyme and Microbial Technology* 30 (4): 454–66. https://doi.org/10.1016/S0141-0229(01)00528-2.

Hou, Meifang, Fangbai Li, Xinming Liu, Xugang Wang, and Hongfu Wan. 2007. "The Effect of Substituent Groups on the Reductive Degradation of Azo Dyes by Zerovalent Iron." *Journal of Hazardous Materials* 145 (1–2): 305–14. https://doi.org/10.1016/j.jhazmat.2006.11.019.

Husain, Maroof, and Qayyum Husain. 2007. "Applications of Redox Mediators in the Treatment of Organic Pollutants by Using Oxidoreductive Enzymes: A Review." *Critical Reviews in Environmental Science and Technology* 38 (1): 1–42. https://doi.org/10.1080/10643380701501213.

IARC. 2005. "IARC Monographs Volume 92 - Appendix - Chemical and Physical Data for Some Non-Heterocyclic Polycyclic Aromatic Hydrocarbons." *Water* 92: 774–814.

Ike, Priscila Tomie Leme, Willian Garcia Birolli, Danilo Martins dos Santos, André Luiz Meleiro Porto, and Dulce Helena Ferreira Souza. 2019. "Biodegradation of Anthracene and Different PAHs by a Yellow Laccase from Leucoagaricus Gongylophorus." *Environmental Science and Pollution Research* 26 (9): 8675–84. https://doi.org/10.1007/s11356-019-04197-z.

Ioannidou, Despoina, Laure Malherbe, Maxime Beauchamp, Nicolas Saby, Roseline Bonnard, and Julien Caudeville. 2018. "Characterization of Environmental Health Inequalities Due to Polyaromatic Hydrocarbon Exposure in France." *International Journal of Environmental Research and Public Health* 15 (12): 2680. https://doi.org/10.3390/ijerph15122680.

Islam, K.M.S., A Schumacher, and J.M. Gropp. 2005. "Humic Acid Substances in Animal Agriculture." *Pakistan Journal of Nutrition* 4 (3): 126–34. https://doi.org/10.3923/pjn.2005.126.134.

Janusz, Grzegorz, Anna Pawlik, Urszula Świderska-Burek, Jolanta Polak, Justyna Sulej, Anna Jarosz-Wilkołazka, and Andrzej Paszczyński. 2020. "Laccase Properties, Physiological Functions, and Evolution." *International Journal of Molecular Sciences* 21 (3): 966. https://doi.org/10.3390/ijms21030966.

Jin, Xiaoting, Xiangyang Yu, Guangyan Zhu, Zuntao Zheng, Fayun Feng, and Zhiyong Zhang. 2016. "Conditions Optimizing and Application of Laccase-Mediator System (LMS) for the Laccase-Catalyzed Pesticide Degradation." *Scientific Reports* 6 (35787): 1–7. https://doi.org/10.1038/srep35787.

Johannes, C., A. Majcherczyk, and A. Hüttermann. 1996. "Degradation of Anthracene by Laccase of Trametes Versicolor in the Presence of Different Mediator Compounds." *Applied Microbiology and Biotechnology* 46 (3): 313–17. https://doi.org/10.1007/s002530050823.

John, Elizabeth Mary, and Jisha Manakulam Shaike. 2015. "Chlorpyrifos: Pollution and Remediation." *Environmental Chemistry Letters* 13 (3): 269–91. https://doi.org/10.1007/s10311-015-0513-7.

Jones, K.C., and P. de Voogt. 1999. "Persistent Organic Pollutants (POPs): State of the Science." *Environmental Pollution* 100 (1–3): 209–21. https://doi.org/10.1016/S0269-7491(99)00098-6.

Kagalkar, Anuradha N., Rahul V. Khandare, and Sanjay P. Govindwar. 2015. "Textile Dye Degradation Potential of Plant Laccase Significantly Enhances upon Augmentation with Redox Mediators." *RSC Adv.* 5 (98): 80505–17. https://doi.org/10.1039/C5RA12454A.

Kapralov, Alexandr, Irina I. Vlasova, Weihong Feng, Akihiro Maeda, Karen Walson, Vladimir A.

Tyurin, Zhentai Huang, et al. 2009. “Peroxidase Activity of Hemoglobin·Haptoglobin Complexes.” *Journal of Biological Chemistry* 284 (44): 30395–407. https://doi.org/10.1074/jbc.M109.045567.

Karigar, Chandrakant S., and Shwetha S. Rao. 2011. “Role of Microbial Enzymes in the Bioremediation of Pollutants: A Review.” *Enzyme Research* 2011 (1): 1–11. https://doi.org/10.4061/2011/805187.

Keum, Haein, Juhee Kim, Yong Hoon Joo, Guyoung Kang, and Namhyun Chung. 2021. “Hemoglobin Peroxidase Reaction of Hemoglobin Efficiently Catalyzes Oxidation of Benzo[a]Pyrene.” *Chemosphere* 268: 128795. https://doi.org/10.1016/j.chemosphere.2020.128795.

Khan, Amjad A., Arshad H. Rahmani, Yousef H. Aldebasi, and Salah M. Aly. 2014. “Biochemical and Pathological Studies on Peroxidases –An Updated Review.” *Global Journal of Health Science* 6 (5): 87–98. https://doi.org/10.5539/gjhs.v6n5p87.

Kim, Ki-Hyun, Shamin Ara Jahan, Ehsanul Kabir, and Richard J.C. Brown. 2013. “A Review of Airborne Polycyclic Aromatic Hydrocarbons (PAHs) and Their Human Health Effects.” *Environment International* 60: 71–80. https://doi.org/10.1016/j.envint.2013.07.019.

Klein, Olga I., Natalia A. Kulikova, Ivan S. Filimonov, Olga V. Koroleva, and Andrey I. Konstantinov. 2018. “Long-Term Kinetics Study and Quantitative Characterization of the Antioxidant Capacities of Humic and Humic-like Substances.” *Journal of Soils and Sediments* 18 (4): 1355–64. https://doi.org/10.1007/s11368-016-1538-7.

Kohler, Amanda C., Blake A. Simmons, and Kenneth L. Sale. 2018. “Structure-Based Engineering of a Plant-Fungal Hybrid Peroxidase for Enhanced Temperature and PH Tolerance.” *Cell Chemical Biology* 25 (8): 974-983.e3. https://doi.org/10.1016/j.chembiol.2018.04.014.

Kondraganti, Sudha R., Pedro Fernandez-Saluguero, Frank J. Gonzalez, Kenneth S. Ramos, Weiwu Jiang, and Bhagavatula Moorthy. 2003. “Polycyclic Aromatic Hydrocarbon-Inducible DNA Adducts: Evidence by 32P-Postlabeling and Use of Knockout Mice for AH Receptor-Independent Mechanisms of Metabolic Activation in Vivo.” *International Journal of Cancer* 103 (1): 5–11. https://doi.org/10.1002/ijc.10784.

Kousba, A. A., L. G. Sultatos, T. S. Poet, and C. Timchalk. 2004. “Comparison of Chlorpyrifos-Oxon and Paraoxon Acetylcholinesterase Inhibition Dynamics: Potential Role of a Peripheral Binding Site.” *Toxicological Sciences* 80 (2): 239–48. https://doi.org/10.1093/toxsci/kfh163.

Kristensen, Peter, Caroline Whalley, Fernanda Néry, Nihat Zal, and Trine Christiansen. 2018. “European Waters Assessment of Status and Pressures 2018.” *EEA Report*. Copenhagen. https://doi.org/10.2800/303664.

Kumar, and Bharadvaja. 2019. “Enzymatic Bioremediation: A Smart Tool to Fight Environmental Pollutants.” In *Smart Bioremediation Technologies*, edited by Pankaj B T Bhatt, 99–118. Elsevier. https://doi.org/10.1016/B978-0-12-818307-6.00006-8.

Lagoa, Ricardo, Dorinda Marques-da-Silva, Mário Diniz, Maria Daglia, and Anupam Bishayee. 2020. “Molecular Mechanisms Linking Environmental Toxicants to Cancer Development: Significance for Protective Interventions with Polyphenols.” *Seminars in Cancer Biology*. https://doi.org/10.1016/j.semcancer.2020.02.002.

Lagoa, Ricardo, Alejandro K. Samhan-Arias, and Carlos Gutierrez-Merino. 2017. “Correlation between the Potency of Flavonoids for Cytochrome c Reduction and Inhibition of Cardiolipin-Induced Peroxidase Activity.” *BioFactors* 43 (3): 451–68. https://doi.org/10.1002/biof.1357.

Lamb, Stephen B., David C. Lamb, Steven L. Kelly, and David C. Stuckey. 1998. “Cytochrome P450 Immobilisation as a Route to Bioremediation/Biocatalysis.” *FEBS Letters* 431 (3): 343–46. https://doi.org/10.1016/S0014-5793(98)00771-6.

Lauer, Alexandra. 2010. “The Dual Photochemistry of Exploring the Competing Ultrafast Photoinduced Reactions of a Model Aromatic Endoperoxide.” Freien Universität Berlin.

Lee, Byeong-Kyu. 2010. “Sources, Distribution and Toxicity of Polyaromatic Hydrocarbons (PAHs) in Particulate Matter.” In *Air Pollution*, edited by Vanda Villanyi. IntechOpen. https://doi.org/10.5772/10045.

Lombi, E., and R.E. Hamon. 2005. “Remediation of Polluted Soils.” In *Encyclopedia of Soils in the Environment*, edited by D. S. Powlson, D. L. Sparks, M. J. Singer, K. M. Scow, C. Rosenzweig, D. Hillel, and J. L. Hatfield, 4:379–85. Oxford: Elsevier. https://doi.org/10.1016/B0-12-348530-4/00087-4.

Lopes, Wilson Araújo, Pedro Afonso, De Paula Pereira, and Hans Viertler. 2005. “Electrochemical

Reduction Potentials of 1-Nitropyrene, 9-Nitroanthracene, 6-Nitrochrysene and 3-Nitrofluoranthene and Their Correlation with Direct-Acting Mutagenicities.” *Journal of the Brazilian Chemical Society* 16 (6): 1099–1103.

Lyon, D.Y., and T.M. Vogel. 2011. “Bioaugmentation as a Strategy for the Treatment of Persistent Pollutants.” In *Comprehensive Biotechnology*, 2nd ed., 6:69–81. Lyon: Elsevier. https://doi.org/10.1016/B978-0-08-088504-9.00366-4.

Ma, Xiaofeng, Rui Sun, Jinghui Cheng, Jiaoyan Liu, Fei Gou, Haifeng Xiang, and Xiangge Zhou. 2016. “Fluorescence Aggregation-Caused Quenching versus Aggregation-Induced Emission: A Visual Teaching Technology for Undergraduate Chemistry Students.” *Journal of Chemical Education* 93 (2): 345–50. https://doi.org/10.1021/acs.jchemed.5b00483.

Maagd, P. Gert-Jan de, Dorien Th. E. M. ten Hulscher, Henny van den Heuvel, Antoon Opperhuizen, and Dick T.H.M. Sijm. 1998. “Physicochemical Properties of Polycyclic Aromatic Hydrocarbons: Aqueous Solubilities, n -Octanol/Water Partition Coefficients, and Henry’s Law Constants.” *Environmental Toxicology and Chemistry* 17 (2): 251–57. https://doi.org/10.1002/etc.5620170216.

Maiti, Subhabrata, Krishnendu Das, Sounak Dutta, and Prasanta Kumar Das. 2012. “Striking Improvement in Peroxidase Activity of Cytochrome c by Modulating Hydrophobicity of Surface-Functionalized Gold Nanoparticles within Cationic Reverse Micelles.” *Chemistry - A European Journal* 18 (47): 15021–30. https://doi.org/10.1002/chem.201202398.

Majcherczyk, Andrzej, Christian Johannes, and Aloys Hüttermann. 1998. “Oxidation of Polycyclic Aromatic Hydrocarbons (PAH) by Laccase of Trametes Versicolor.” *Enzyme and Microbial Technology* 22 (5): 335–41. https://doi.org/10.1016/S0141-0229(97)00199-3.

Mallick, Somnath. 2019. “A Review on Origin, Occurrence, and Biodegradation of Polycyclic Aromatic Hydrocarbon Acenaphthene.” *Applied Ecology and Environmental Sciences* 7 (6): 263–69. https://doi.org/10.12691/aees-7-6-8.

Manikandan, Palrasu, and Siddavaram Nagini. 2018. “Cytochrome P450 Structure, Function and Clinical Significance: A Review.” *Current Drug Targets* 19 (1): 38–54. https://doi.org/10.2174/1389450118666170125144557.

May, Willie E., Stanley P. Wasik, and David H. Freeman. 1978. “Determination of the Solubility Behavior of Some Polycyclic Aromatic Hydrocarbons in Water.” *Analytical Chemistry* 50 (7): 997–1000. https://doi.org/10.1021/ac50029a042.

Mikolasch, Annett, and Frieder Schauer. 2009. “Fungal Laccases as Tools for the Synthesis of New Hybrid Molecules and Biomaterials.” *Applied Microbiology and Biotechnology* 82 (4): 605–24. https://doi.org/10.1007/s00253-009-1869-z.

Miller, Kimberly P., and Kenneth S. Ramos. 2001. “Impact of Cellular Metabolism on the Biological Effects of Benzo[a]Pyrene and Related Hydrocarbons.” *Drug Metabolism Reviews* 33 (1): 1–35. https://doi.org/10.1081/DMR-100000138.

Min, Lee, and Xu Jian-xing. 2007. “Detoxifying Function of Cytochrome c against Oxygen Toxicity.” *Mitochondrion* 7 (1–2): 13–16. https://doi.org/10.1016/j.mito.2006.11.011.

Mojiri, Amin, John L. Zhou, Akiyoshi Ohashi, Noriatsu Ozaki, and Tomonori Kindaichi. 2019. “Comprehensive Review of Polycyclic Aromatic Hydrocarbons in Water Sources, Their Effects and Treatments.” *Science of The Total Environment* 696: 133971. https://doi.org/10.1016/j.scitotenv.2019.133971.

Moody, Joanna D., James P. Freeman, Daniel R. Doerge, and Carl E. Cerniglia. 2001. “Degradation of Phenanthrene and Anthracene by Cell Suspensions of Mycobacterium Sp. Strain PYR-1.” *Applied and Environmental Microbiology* 67 (4): 1476–83. https://doi.org/10.1128/AEM.67.4.1476-1483.2001.

Moorthy, Bhagavatula, Chun Chu, and Danielle J. Carlin. 2015. “Polycyclic Aromatic Hydrocarbons: From Metabolism to Lung Cancer.” *Toxicological Sciences* 145 (1): 5–15. https://doi.org/10.1093/toxsci/kfv040.

More, Sunil S., P. S. Renuka, K. Pruthvi, M. Swetha, S. Malini, and S. M. Veena. 2011. “Isolation, Purification, and Characterization of Fungal Laccase from Pleurotus Sp.” *Enzyme Research* 2011 (1): 1–7. https://doi.org/10.4061/2011/248735.

Morozova, O. V., G. P. Shumakovich, S. V. Shleev, and Ya I. Yaropolov. 2007. “Laccase-Mediator Systems and Their Applications: A Review.” *Applied Biochemistry and Microbiology* 43 (5):

523–35. https://doi.org/10.1134/S0003683807050055.

Morsi, Rana, Muhammad Bilal, Hafiz M.N. Iqbal, and S. Salman Ashraf. 2020. “Laccases and Peroxidases: The Smart, Greener and Futuristic Biocatalytic Tools to Mitigate Recalcitrant Emerging Pollutants.” *Science of The Total Environment* 714: 136572. https://doi.org/10.1016/j.scitotenv.2020.136572.

Mousavi, Seyyed Mojtaba, Seyyed Alireza Hashemi, Seyed Mohammad Iman Moezzi, Navid Ravan, Ahmad Gholami, Chin Wei Lai, Wei-Hung Chiang, Navid Omidifar, Khadije Yousefi, and Gity Behbudi. 2021. “Recent Advances in Enzymes for the Bioremediation of Pollutants.” Edited by Néstor Gutiérrez-Méndez. *Biochemistry Research International* 2021: 1–12. https://doi.org/10.1155/2021/5599204.

Muenzner, Julia, Jason R. Toffey, Yuning Hong, and Ekaterina V. Pletneva. 2013. “Becoming a Peroxidase: Cardiolipin-Induced Unfolding of Cytochrome C.” *The Journal of Physical Chemistry B* 117 (42): 12878–86. https://doi.org/10.1021/jp402104r.

Murugesan, Kumarasamy, Young Mo Kim, Jong Rok Jeon, and Yoon Seok Chang. 2009. “Effect of Metal Ions on Reactive Dye Decolorization by Laccase from Ganoderma Lucidum.” *Journal of Hazardous Materials* 168 (1): 523–29. https://doi.org/10.1016/j.jhazmat.2009.02.075.

Na, So-Young, and Yunho Lee. 2017. “Elimination of Trace Organic Contaminants during Enhanced Wastewater Treatment with Horseradish Peroxidase/Hydrogen Peroxide (HRP/H2O2) Catalytic Process.” *Catalysis Today* 282: 86–94. https://doi.org/10.1016/j.cattod.2016.03.049.

Nagai, M., T. Sato, H. Watanabe, K. Saito, M. Kawata, and H. Enei. 2002. “Purification and Characterization of an Extracellular Laccase from the Edible Mushroom Lentinula Edodes, and Decolorization of Chemically Different Dyes.” *Applied Microbiology and Biotechnology* 60 (3): 327–35. https://doi.org/10.1007/s00253-002-1109-2.

NCBI. 2020a. “PubChem Compound Summary for CID 931, Naphthalene.” National Center for Biotechnology Information. 2020. https://pubchem.ncbi.nlm.nih.gov/compound/Naphthalene.

NCBI. 2020b. “PubChem Compound Summary for CID 8418, Anthracene.” National Center for Biotechnology Information. 2020. https://pubchem.ncbi.nlm.nih.gov/compound/Anthracene.

NCBI. 2020c. “PubChem Compound Summary for CID 5954, Benz[a]Anthracene.” National Center for Biotechnology Information. 2020. https://pubchem.ncbi.nlm.nih.gov/compound/Benz_a_anthracene.

NCBI. 2020d. “Compound Summary for CID 9153, Benzo[b]Fluoranthene.” National Center for Biotechnology Information. 2020. https://pubchem.ncbi.nlm.nih.gov/compound/Benzo_b_fluoranthene.

NCBI. 2020e. “PubChem Compound Summary for CID 2336, Benzo[a]Pyrene.” National Center for Biotechnology Information. 2020. https://pubchem.ncbi.nlm.nih.gov/compound/Benzo_a_pyrene.

NCBI. 2020f. “PubChem Compound Summary for CID 2730, Chlorpyrifos.” National Center for Biotechnology Information. 2020. https://pubchem.ncbi.nlm.nih.gov/compound/Chlorpyrifos.

Oliveira, Marta, Klara Slezakova, Maria José Alves, Adília Fernandes, João Paulo Teixeira, Cristina Delerue-Matos, Maria do Carmo Pereira, and Simone Morais. 2017. “Polycyclic Aromatic Hydrocarbons at Fire Stations: Firefighters’ Exposure Monitoring and Biomonitoring, and Assessment of the Contribution to Total Internal Dose.” *Journal of Hazardous Materials* 323: 184–94. https://doi.org/10.1016/j.jhazmat.2016.03.012.

Ozgen, M, R. N. Reese, A. Z. Tulio Jr., J. C. Scheerens, and A. R. Miller. 2006. “Modified 2,2-Azino-Bis-3-Ethylbenzothiazoline-6-Sulfonic Acid (ABTS) Method to Measure Antioxidant Capacity of Selected Small Fruits and Comparison to Ferric Reducing Antioxidant Power (FRAP) and 2,2′-Diphenyl-1-Picrylhydrazyl (DPPH) Methods.” *Journal of Agricultural and Food Chemistry* 54 (4): 1151−1157. https://doi.org/10.1021/jf071046f.

Patel, Avani Bharatkumar, Shabnam Shaikh, Kunal R. Jain, Chirayu Desai, and Datta Madamwar. 2020. “Polycyclic Aromatic Hydrocarbons: Sources, Toxicity, and Remediation Approaches.” *Frontiers in Microbiology* 11 (562813). https://doi.org/10.3389/fmicb.2020.562813.

PatenaudeE, J, P Sauvageau, and C Sandorfy. 1962. “The Assignment of Bands in the Ultraviolet Spectrum of Benzo[a]Anthracene.” *Spectrochimica Acta* 18 (3): 241–57. https://doi.org/10.1016/S0371-1951(62)80129-5.

Patricia Twala, Pontsho, Alfred Mitema, Cindy Baburam, and Naser Aliye Feto. 2020. “Breakthroughs in the Discovery and Use of Different Peroxidase Isoforms of Microbial Origin.” *AIMS Microbiology* 6 (3): 330–49. https://doi.org/10.3934/microbiol.2020020.

Pokora, Wojciech, and Zbigniew Tukaj. 2010. “The Combined Effect of Anthracene and Cadmium on Photosynthetic Activity of Three Desmodesmus (Chlorophyta) Species.” *Ecotoxicology and Environmental Safety* 73 (6): 1207–13. https://doi.org/10.1016/j.ecoenv.2010.06.013.

Potthast, A., T. Rosenau, and K. Fischer. 2001. “Oxidation of Benzyl Alcohols by the Laccase-Mediator System (LMS) – a Comprehensive Kinetic Description.” *Holzforschung* 55 (1): 47–56. https://doi.org/10.1515/hfsg.2001.47.

Pukalchik, Maria, Kamila Kydralieva, Olga Yakimenko, Elena Fedoseeva, and Vera Terekhova. 2019. “Outlining the Potential Role of Humic Products in Modifying Biological Properties of the Soil-A Review.” *Frontiers in Environmental Science* 7 (80): 1–10. https://doi.org/10.3389/fenvs.2019.00080.

R. Lide, David. 2016. *“Physical Constants of Organic Compounds”. Handbook of Chemistry and Physics*. 96th ed. Boca Raton: CRC Press.

Radi, Rafael, Leonor Thomson, Homero Rubbo, and Eugenio Prodanov. 1991. “Cytochrome C-Catalyzed Oxidation of Organic Molecules by Hydrogen Peroxide.” *Archives of Biochemistry and Biophysics* 288 (1): 112–17. https://doi.org/10.1016/0003-9861(91)90171-E.

Rao, M. A., R. Scelza, R. Scotti, and L. Gianfreda. 2010. “Role of Enzymes in the Remediation of Polluted Environments.” In *Journal of Soil Science and Plant Nutrition,* 10:333–53. https://doi.org/10.4067/S0718-95162010000100008.

Rapacioli, M., F. Calvo, F. Spiegelman, C. Joblin, and D. J. Wales. 2005. “Stacked Clusters of Polycyclic Aromatic Hydrocarbon Molecules.” *Journal of Physical Chemistry A* 109 (11): 2487–97. https://doi.org/10.1021/jp046745z.

Re, R., N. Pellegrini, A. Proteggente, A. Pannala, M. Yang, and C. Rice-Evans. 1999. “Antioxidant Activity Applying an Improved ABTS Radical Cation Decolorization Assay.” *Free Radical Biology & Medicine* 26 (9–10): 1231–37. https://www.sciencedirect.com/science/article/abs/pii/S0891584998003153?via%3Dihub.

Reeder, Brandon J. 2010. “The Redox Activity of Hemoglobins: From Physiologic Functions to Pathologic Mechanisms.” *Antioxidants & Redox Signaling* 13 (7): 1087–1123. https://doi.org/10.1089/ars.2009.2974.

Reeder, Brandon J., Marie Grey, Radu-Lucian Silaghi-Dumitrescu, Dimitri A. Svistunenko, Leif Bülow, Chris E. Cooper, and Michael T. Wilson. 2008. “Tyrosine Residues as Redox Cofactors in Human Hemoglobin.” *Journal of Biological Chemistry* 283 (45): 30780–87. https://doi.org/10.1074/jbc.M804709200.

Rico, Andreu, Raquel Dafouz, Marco Vighi, José Luis Rodríguez-Gil, and Michiel A. Daam. 2021. “Use of Postregistration Monitoring Data to Evaluate the Ecotoxicological Risks of Pesticides to Surface Waters: A Case Study with Chlorpyrifos in the Iberian Peninsula.” *Environmental Toxicology and Chemistry* 40 (2): 500–512. https://doi.org/10.1002/etc.4927.

Riedl, K. M., and A. E. Hagerman. 2001. “Tannin-Protein Complexes as Radical Scavengers and Radical Sinks.” *Journal of Agricultural and Food Chemistry* 49 (10): 4917–23. https://doi.org/10.1021/jf010683h.

Ritter, L, K R Solomon, J Forget, M Stemeroff, and C O’leary. 1995. “A Review of Selected Persistent Organic Pollutants.” *International Programme on Chemical Safety (IPCS). PCS/95.39. Geneva: World Health Organization* 65: 66.

Rubio, Camila Peres, Josefa Hernández-Ruiz, Silvia Martinez-Subiela, Asta Tvarijonaviciute, Marino Bañón Arnao, and José Joaquín Ceron. 2016. “Validation of Three Automated Assays for Total Antioxidant Capacity Determination in Canine Serum Samples.” *Journal of Veterinary Diagnostic Investigation* 28 (6): 693–98. https://doi.org/10.1177/1040638716664939.

Ruggiero, P., and V.M. Radogna. 1985. “Inhibition of Soil Humus-Laccase Complexes by Some Phenoxyacetic and s-Triazine Herbicides.” *Soil Biology and Biochemistry* 17 (3): 309–12. https://doi.org/10.1016/0038-0717(85)90066-5.

Sakshi, S. K. Singh, and A. K. Haritash. 2019. “Polycyclic Aromatic Hydrocarbons: Soil Pollution and Remediation.” *International Journal of Environmental Science and Technology* 16 (10): 6489–6512. https://doi.org/10.1007/s13762-019-02414-3.

Samuel, Yalkowsky, Yan He, and Parijat Jain. 2010. *Handbook of Aqueous Solubility Data*. 2nd ed.

Boca Raton: CRC Press.

Sancho, Matias I., Maria C. Almandoz, Sonia E. Blanco, and Eduardo A. Castro. 2011. "Spectroscopic Study of Solvent Effects on the Electronic Absorption Spectra of Flavone and 7-Hydroxyflavone in Neat and Binary Solvent Mixtures." *International Journal of Molecular Sciences* 12 (12): 8895–8912. https://doi.org/10.3390/ijms12128895.

Scott, Susannah L., Wen Jang Chen, Andreja Bakac, and James H. Espenson. 1993. "Spectroscopic Parameters, Electrode Potentials, Acid Ionization Constants, and Electron Exchange Rates of the 2,2'-Azinobis(3-Ethylbenzothiazoline-6-Sulfonate) Radicals and Ions." *The Journal of Physical Chemistry* 97 (25): 6710–14. https://doi.org/10.1021/j100127a022.

Serban, Andrei, and Arie Nissenbaum. 1986. "Humic Acid Association with Peroxidase and Catalase." *Soil Biology and Biochemistry* 18 (1): 41–44. https://doi.org/10.1016/0038-0717(86)90101-X.

Sharma. 2021. "Bioremediation Techniques for Polluted Environment: Concept, Advantages, Limitations, and Prospects." In *Trace Metals in the Environment - New Approaches and Recent Advances*, edited by Mario Alfonso Murillo-Tovar, Hugo Saldarriaga-Noreña, and Agnieszka Saeid. IntechOpen. https://doi.org/10.5772/intechopen.90453.

Sharma, Arun Kumar Dangi, and Pratyoosh Shukla. 2018. "Contemporary Enzyme Based Technologies for Bioremediation: A Review." *Journal of Environmental Management* 210: 10–22. https://doi.org/10.1016/j.jenvman.2017.12.075.

Shin, K. S., and Y. J. Lee. 2000. "Purification and Characterization of a New Member of the Laccase Family from the White-Rot Basidiomycete Coriolus Hirsutus." *Archives of Biochemistry and Biophysics* 384 (1): 109–15. https://doi.org/10.1006/abbi.2000.2083.

Shraddha, Ravi Shekher, Simran Sehgal, Mohit Kamthania, and Ajay Kumar. 2011. "Laccase: Microbial Sources, Production, Purification, and Potential Biotechnological Applications." *Enzyme Research* 2011 (1): 1–11. https://doi.org/10.4061/2011/217861.

Sigma-Aldrich. n.d. "Cytochrome C7752." Accessed October 26, 2021. https://www.sigmaaldrich.com/catalog/product/sigma/c7752.

Speigth, J. 2011. "Chp. 13: Pharmaceuticals." In *Handbook of Industrial Hydrocarbon Processes*, 467–97. https://doi.org/10.1016/B978-0-7506-8632-7.10013-1.

Stamatelatou, K, C Pakou, and G Lyberatos. 2011. "Occurrence, Toxicity, and Biodegradation of Selected Emerging Priority Pollutants in Municipal Sewage Sludge." In , edited by Murray B T - Comprehensive Biotechnology (Second Edition) Moo-Young, 2nd ed., 473–84. Burlington: Academic Press. https://doi.org/https://doi.org/10.1016/B978-0-08-088504-9.00496-7.

Stark, Benjamin C., Meltem Urgun-Demirtas, and Krishna R. Pagilla. 2008. "Role of Hemoglobin in Improving Biodegradation of Aromatic Contaminants under Hypoxic Conditions." *Journal of Molecular Microbiology and Biotechnology* 15 (2–3): 181–89. https://doi.org/10.1159/000121329.

Stec, Anna A., Kathryn E. Dickens, Marielle Salden, Fiona E. Hewitt, Damian P. Watts, Philip E. Houldsworth, and Francis L. Martin. 2018. "Occupational Exposure to Polycyclic Aromatic Hydrocarbons and Elevated Cancer Incidence in Firefighters." *Scientific Reports* 8 (1): 2476. https://doi.org/10.1038/s41598-018-20616-6.

Swaathy, Sreethar, Varadharajan Kavitha, Arokiasamy Sahaya Pravin, Asit Baran Mandal, and Arumugam Gnanamani. 2014. "Microbial Surfactant Mediated Degradation of Anthracene in Aqueous Phase by Marine Bacillus Licheniformis MTCC 5514." *Biotechnology Reports* 4 (1): 161–70. https://doi.org/10.1016/j.btre.2014.10.004.

Swati, Ankita, and Subrata Hait. 2017. "Fate and Bioavailability of Heavy Metals during Vermicomposting of Various Organic Wastes—A Review." *Process Safety and Environmental Protection* 109: 30–45. https://doi.org/10.1016/j.psep.2017.03.031.

Tadesse, Mahelet Aweke, Alessandro D'Annibale, Carlo Galli, Patrizia Gentili, and Federica Sergi. 2008. "An Assessment of the Relative Contributions of Redox and Steric Issues to Laccase Specificity towards Putative Substrates." *Organic & Biomolecular Chemistry* 6 (5): 868. https://doi.org/10.1039/b716002j.

Thomas, Olivier, and Marine Brogat. 2017. "Organic Constituents." In *UV-Visible Spectrophotometry of Water and Wastewater*, edited by Olivier Thomas and Christopher B T - UV-Visible Spectrophotometry of Water and Wastewater (Second Edition) Burgess, 2nd ed., 73–138. Elsevier. https://doi.org/https://doi.org/10.1016/B978-0-444-63897-7.00003-2.

Tobiszewski, Marek, and Jacek Namieśnik. 2012. “PAH Diagnostic Ratios for the Identification of Pollution Emission Sources.” *Environmental Pollution* 162: 110–19. https://doi.org/10.1016/j.envpol.2011.10.025.

Ubaid ur Rahman, Hafiz, Waqas Asghar, Wahab Nazir, Mansur Abdullah Sandhu, Anwaar Ahmed, and Nauman Khalid. 2021. “A Comprehensive Review on Chlorpyrifos Toxicity with Special Reference to Endocrine Disruption: Evidence of Mechanisms, Exposures and Mitigation Strategies.” *Science of the Total Environment* 755: 142649. https://doi.org/10.1016/j.scitotenv.2020.142649.

Varma, Geetha, and Anil K. Misra. 2018. “Copper Contaminated Wastewater – An Evaluation of Bioremedial Options.” *Indoor and Built Environment* 27 (1): 84–95. https://doi.org/10.1177/1420326X16669397.

Veitch, Nigel C. 2004. “Horseradish Peroxidase: A Modern View of a Classic Enzyme.” *Phytochemistry* 65 (3): 249–59. https://doi.org/10.1016/j.phytochem.2003.10.022.

Vishwakarma, Gajendra Singh, Gargi Bhattacharjee, Nisarg Gohil, and Vijai Singh. 2020. “Current Status, Challenges and Future of Bioremediation.” In *Bioremediation of Pollutants*, edited by Vimal Chandra Pandey and Vijai Singh, 403–15. Elsevier. https://doi.org/10.1016/B978-0-12-819025-8.00020-X.

Vlasova, Irina. 2018. “Peroxidase Activity of Human Hemoproteins: Keeping the Fire under Control.” *Molecules* 23 (10): 2561. https://doi.org/10.3390/molecules23102561.

Vuorilehto, K. 2008. “Stable, Colourless and Water-Soluble Electron-Transfer Mediators Used in Enzyme Electrochemistry.” *Journal of Applied Electrochemistry* 38 (10): 1427–33. https://doi.org/10.1007/s10800-008-9587-2.

Wallace, C.J., and I. Clark-Lewis. 1992. “Functional Role of Heme Ligation in Cytochrome c. Effects of Replacement of Methionine 80 with Natural and Non-Natural Residues by Semisynthesis.” *Journal of Biological Chemistry* 267 (6): 3852–61. https://doi.org/10.1016/S0021-9258(19)50604-4.

Wang, Mengyun, Daiyao Wang, Shiyi Qiu, Junyang Xiao, Huahua Cai, and Jing Zou. 2019. “Multi-Wavelength Spectrophotometric Determination of Hydrogen Peroxide in Water by Oxidative Coloration of ABTS via Fenton Reaction.” *Environmental Science and Pollution Research* 26 (26): 27063–72. https://doi.org/10.1007/s11356-019-05884-7.

Wang, Sufang, Xiaopei Yu, Zhihua Lin, Shunqin Zhang, Liangyi Xue, Qinggang Xue, and Yongbo Bao. 2017. “Hemoglobins Likely Function as Peroxidase in Blood Clam Tegillarca Granosa Hemocytes.” *Journal of Immunology Research* 2017: 1–10. https://doi.org/10.1155/2017/7125084.

Wenning, Richard J., and Linda Martello. 2014. “POPs in Marine and Freshwater Environments.” In *Environmental Forensics for Persistent Organic Pollutants*, 357–90. Elsevier. https://doi.org/10.1016/B978-0-444-59424-2.00008-6.

Wu, Yi Rui, Zhu Hua Luo, and L. L.P. Vrijmoed. 2010. “Biodegradation of Anthracene and Benz[a]Anthracene by Two Fusarium Solani Strains Isolated from Mangrove Sediments.” *Bioresource Technology* 101 (24): 9666–72. https://doi.org/10.1016/j.biortech.2010.07.049.

Xu, Wenjing, Tomasa Barrientos, and Nancy C. Andrews. 2013. “Iron and Copper in Mitochondrial Diseases.” *Cell Metabolism* 17 (3): 319–28. https://doi.org/10.1016/j.cmet.2013.02.004.

Yap, Chiew Lin, Suyin Gan, and Hoon Kiat Ng. 2012. “Evaluation of Solubility of Polycyclic Aromatic Hydrocarbons in Ethyl Lactate/Water versus Ethanol/Water Mixtures for Contaminated Soil Remediation Applications.” *Journal of Environmental Sciences (China)* 24 (6): 1064–75. https://doi.org/10.1016/S1001-0742(11)60873-5.

Yaropolov, A. I., O. V. Skorobogat’ko, S. S. Vartanov, and S. D. Varfolomeyev. 1994. “Laccase.” *Applied Biochemistry and Biotechnology* 49 (3): 257–80. https://doi.org/10.1007/BF02783061.

Yashnik, Svetlana A., Zinfer R. Ismagilov, and Vladimir F. Anufrienko. 2005. “Catalytic Properties and Electronic Structure of Copper Ions in Cu-ZSM-5.” *Catalysis Today* 110 (3–4): 310–22. https://doi.org/10.1016/j.cattod.2005.09.029.

Ye, Jin Shao, Hua Yin, Jing Qiang, Hui Peng, Hua Ming Qin, Na Zhang, and Bao Yan He. 2011. “Biodegradation of Anthracene by Aspergillus Fumigatus.” *Journal of Hazardous Materials* 185 (1): 174–81. https://doi.org/10.1016/j.jhazmat.2010.09.015.

Zahmatkesh, M., H. Spanjers, M. J. Toran, P. Blánquez, and J. B. van Lier. 2016. “Bioremoval of Humic

Acid from Water by White Rot Fungi: Exploring the Removal Mechanisms." *AMB Express* 6 (1). https://doi.org/10.1186/s13568-016-0293-x.

Zatón, Ana María L, and Eduardo Ochoa de Aspuru. 1995. "Horseradish Peroxidase Inhibition by Thiouracils." *FEBS Letters* 374 (2): 192–94. https://doi.org/https://doi.org/10.1016/0014-5793(95)01088-V.

Zavarzina, A.G, A.A Leontievsky, L.A Golovleva, and S.Ya Trofimov. 2004. "Biotransformation of Soil Humic Acids by Blue Laccase of Panus Tigrinus 8/18: An in Vitro Study." *Soil Biology and Biochemistry* 36 (2): 359–69. https://doi.org/10.1016/j.soilbio.2003.10.010.

Zdarta, Jakub, Katarzyna Jankowska, Karolina Bachosz, Oliwia Degórska, Karolina Kaźmierczak, Luong N. Nguyen, Long D. Nghiem, and Teofil Jesionowski. 2021. "Enhanced Wastewater Treatment by Immobilized Enzymes." *Current Pollution Reports* 7 (2): 167–79. https://doi.org/10.1007/s40726-021-00183-7.

Zeinali, M., M. Vossoughi, and S. K. Ardestani. 2008. "Degradation of Phenanthrene and Anthracene by Nocardia Otitidiscaviarum Strain TSH1, a Moderately Thermophilic Bacterium." *Journal of Applied Microbiology* 105 (2): 398–406. https://doi.org/10.1111/j.1365-2672.2008.03753.x.

Zheng, Dong, Xiang Ai Yuan, Haibo Ma, Xiaoxiong Li, Xizhang Wang, Ziteng Liu, and Jing Ma. 2018. "Unexpected Solvent Effects on the UV/Vis Absorption Spectra of o-Cresol in Toluene and Benzene: In Contrast with Non-Aromatic Solvents." *Royal Society Open Science* 5 (3). https://doi.org/10.1098/rsos.171928.

Zhou, Wen, Zheng Bing Guan, Yu Jie Cai, Yu Chen, Ning Zhang, and Xiang Ru Liao. 2017. "Preparation and Characterization of Immobilized Spores with Laccase Activity from Bacillus Pumilus W3 on DEAE-Cellulose and Their Application in Dye Decolorization." *Brazilian Journal of Chemical Engineering* 34 (1): 41–52. https://doi.org/10.1590/0104-6632.20170341s20150492.

Zhu, Weihuang, Mengran Shi, Dan Yu, Chongxuan Liu, Tinglin Huang, and Fengchang Wu. 2016. "Characteristics and Kinetic Analysis of AQS Transformation and Microbial Goethite Reduction: Insight into 'Redox Mediator-Microbe-Iron Oxide' Interaction Process." *Scientific Reports* 6: 1–11. https://doi.org/10.1038/srep23718.

Zouboulis, Anastasios I., Xiao Li Chai, and Ioannis A. Katsoyiannis. 2004. "The Application of Bioflocculant for the Removal of Humic Acids from Stabilized Landfill Leachates." *Journal of Environmental Management* 70 (1): 35–41. https://doi.org/10.1016/j.jenvman.2003.10.003.

NOVA SCHOOL OF
SCIENCE & TECHNOLOGY

BIOTRANSFORMATION OF ENVIRONMENTAL TOXICANTS BY DIFFERENT ENZYMES

JOÃO RICARDO MARQUES LOPES

⟨2021⟩